PREPARATION AND CHARACTERIZATION OF EVA-WOOD FIBRE COMPOSITES

by

DORINE GENETH DIKOBE (B.Sc. Honours)

submitted in accordance with the requirements for the degree

MASTERS OF SCIENCE (M.Sc.)

in the

Department of Chemistry
Faculty of Natural and Agricultural Sciences

at the

UNIVERSITY OF THE FREE STATE (Qwa-Qwa campus)

SUPERVISOR: PROFESSOR AS LUYT

APRIL 2006

DECLARATION

I, the undersigned, hereby declare that the research in this thesis is my own original work, which has not partly or fully been submitted to any other University in order to obtain a degree.

DORINE GENETH DIKOBE

DEDICATIONS

Our hands are endowed with energy, our minds with power to reason,
And our hearts with power to feel,
We are placed upon the scene of nature abounding with raw materials
With which we can build to our heart's desire
-B.Z Bokser-

I was not delivered into this world in defeat, nor does failure run in my veins. I refuse to walk, to talk and to sleep with those who fail. I will not listen to those who weep and complain, for their disease is contagious. The house of failure is not my destiny. I will persist until I sUcceed.

I will never consider defeat and I will remove from my vocabulary words such as quit, cannot, unable, impossible, improbable, hopeless and unworkable, for they are words of fools. I will avoid despair. I will toil and I will endure. I will persist until I sUcceed.

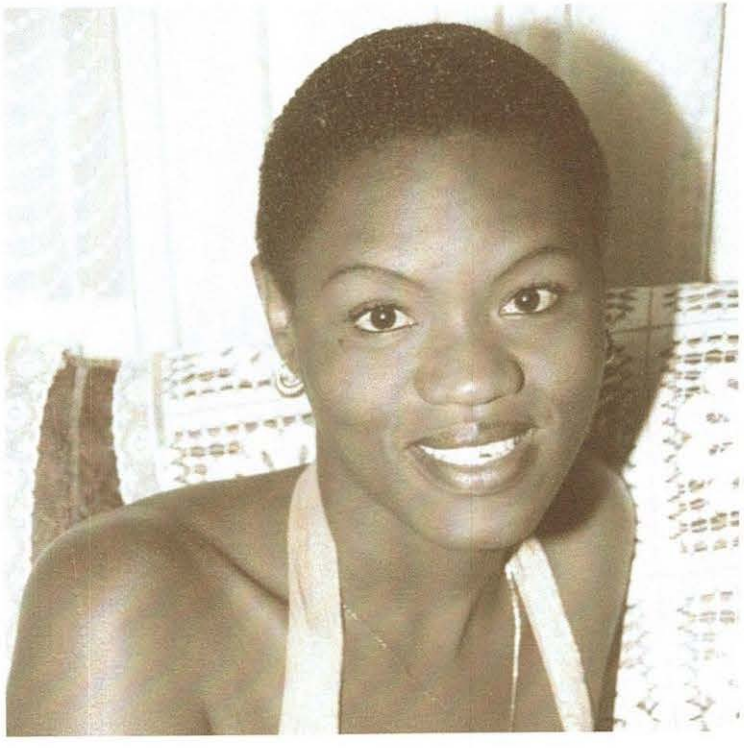

I will try and try again. Each obstacle will be considered as a mere detour to my goal and a challenge to my profession. I will persist and develop my skills as the mariner develops his, by learning to ride out of the wrath of each storm. I will persist until I sUcceed..

So long as there is breath in me, I will persist. For now, I know one of the greatest principles of sUccess... ..... If I persist long enough I will win.

This book is dedicated to my late mom, Kerileng Rose Dikobe.
For I know that there is no way that I can spell sUccess without U. I love U mom, always. Thank U, for everything.

ABSTRACT

Ethylene vinyl acetate copolymer (EVA) and wood fibre (WF) composites, compatibilized with ethylene-glycidyl methacrylate copolymer (EGMA) were investigated. The study is divided into two systems, i.e. EVA-WF (uncompatibilized composites) and EVA/EGMA-WF (compatibilized composites). The composites were prepared and their mechanical, morphological and thermal properties were investigated and compared. Their O_2 permeability and water absorption behavior were also studied.

Results showed that EVA-WF composites have poorer mechanical properties and an unacceptable physical appearance, while EVA/EGMA-WF composites showed improved properties. The reason for this is that the interfacial adhesion between EVA and WF is weak because of the difference in surface free energy of EVA and WF. This problem was overcome by the addition of EGMA to the EVA-WF mixture, which resulted in the formation of an EGMA-WF grafted product, and which provides an OH group that forms a hydrogen bond with –C=O on EVA, resulting in EVA/EGMA-WF composites with better properties, proving that EGMA can act as an effective compatibilizer for EVA and WF.

The effect of WF particle size and content, as well as the effect of the amount of EGMA used in the composite, were thoroughly investigated. The proposed interaction mechanism for EVA-WF, and the reaction and interaction mechanism for EVA/EGMA-WF composites, supported by IR, are presented.

TABLE OF CONTENTS

CHAPTER 1

Introduction

1.1 History of composites

One of the earliest known composite materials is adobe brick in which straw (a fibrous material) was mixed with mud or clay (an adhesive with strong compressive strength). The straw allowed the water in the clay to evaporate and uniformly distributed cracks in the clay, greatly improving the strength of this early building material. Another form of a composite material is construction material called plywood. Plywood uses natural materials (thin slabs of wood) held together by a strong adhesive, making the structure stronger than just the wood itself. In nature, bamboo is often cited as an example of a wood composite structure, combining cellulose fibres and lignin, with the lignin providing the adhesive to hold the fibres together. Reinforced concrete is a combination of two remarkable materials, concrete (a composite by itself) and steel, that takes advantage of the strengths of each material to overcome their individual limitations. Steel has very high tensile strength, while concrete has very high compressive strength; in combination they make a superior material for road and bridge construction [1].

By the broadest definition, a composite material is one in which two or more materials that are different, are combined to form a single structure with an identifiable interface. One of the materials acts as filler while the other one is called the matrix. Combination of the two gives the filler-matrix composites. The name and properties of that new structure are dependent upon the properties of the constituent materials as well as the properties of the interface. Thus, the term "composites" is used extremely broadly to describe many materials with many different properties targeted at an even larger number of applications. Composites changed our world; modern car components are made of composite materials, the entire body is made of fibreglass or carbon reinforced composite materials. Tyres are a composite of rubber and a reinforcing material such as steel and nylon [2].

The emergence of new, light-weight polymers from development laboratories offered a possible solution for a variety of uses, provided something could be done to increase the mechanical properties of plastics. By immersing fibres in a matrix of a lightweight, lower-strength material, a stronger material could be obtained, because the fibres stop the propagation of the cracks in the matrix. A polymer with insufficient strength or stiffness

could be reinforced with fibres to produce a stronger, stiffer, lighter-weight product. The polymer matrix provides an environment for the fibres to reside in their original form – single, independent needles – and protects them from scratches that might cause them to fracture under low stress. The fibrous filler adds strength to the more fragile polymer material by shouldering much of the stress that was transferred from the polymer to the fibre through their strong interfacial bonds. Products that result from this are called polymer-fibre composites [3].

1.2 Benefits of composites

Composites in general offer many advantages over other materials. Within aerospace and marine markets, where exceptional performance is required but weight is critical, composites continue to grow in importance. The advantages of composites may be summarized as:

- *Stronger and stiffer than metals on a density basis*
  For the same strength, composites are lighter than steel by 80% and Al by 60%.
- *High corrosion resistance*
  Composites are essentially inert in most corrosive environments. The non-reactive nature of many resins and reinforcements can be custom selected to resist degradation by many common materials and in corrosive environments.
- *Electrically insulating properties are inherent in most composites*
  Depending on the reinforcement selected, composites can be made conducting or selectively conducting as needed.
- *Tolerable thermal expansion properties*
  Composites can be compounded to closely match surrounding structures to minimize thermal stresses.
- *Outstanding durability*
  Well-designed composites exhibited apparent infinite life characteristics, even in extremely harsh environments.
- *Low investment in fabrication equipment*
  The inherent characteristics of composites allow production at a small fraction of the cost that would normally be required for non-composites [4, 5].

1.3 Applications of composites

Each year, composites find their way into hundreds of new applications, from golf clubs and tennis rackets to jet skis, aircraft, missiles and spacecraft. The earliest applications for composites were in the marine industry. Fibreglass boats were manufactured in the early 1940s to replace traditional wood or metal boats. The lightweight, strong fibreglass composites were not subject to rotting or rusting like their counterparts, and they were easy to maintain. All the electrical terminal boards on ships were replaced with fibreglass-melamine or asbestos-melamine composite boards with improved electrical insulation properties [6].

At the same time, composite cost trends are highly favourable, especially when the total cost of fabrication is considered. Processes that would normally need a lot of labour time and machinery to be completed when ordinary materials were used can be finished in a single trip when composites are used instead. For example, composite sheet molding compounds allow the formation of complete car skin panels in a single stroke of a press.

Kevlar, a synthetic reinforcement that was discovered in 1971, is used in the manufacturing of Kevlar-based polymers. Kevlar-reinforced polymers are used in applications such as bulletproof vests and helmets for law enforcement officers. A slight variation in the synthesis of Kevlar produced Nomex, which is a fire-resistant fibre that is used in the production of protective gear for firefighters [7, 8].

1.4 Natural fibre – polymer composites

Natural fibres, used to fill and reinforce polymers, represent one of the fastest-growing types of polymer additives. Natural fibre composites (NFC) are formulated from a blend of natural fibres, including cane fibres, bamboo, oat, kenaf, hemp, flax, jute and sisal, and wood fiber, and thermoplastic polymers such as polypropylene and polyester. Natural fibres offer several advantages over man-made fibres such as glass, carbon and aramid. The advantages are [9]:

- their renewable origin,
- world-wide availability,
- low production energy requirements,
- reduced equipment wear,
- environmentally friendly,
- biodegradability

Particularly attracting is the low density of natural fibres, in particular wood powder, which leads to the production of composites with high specific mechanical properties, and which can be used in the following applications [10]:

- Wood fibre composites are used in building industries such as decking, windows and door profiles, decorative trims and railings.
- Wood-polymer composites can be used as excellent floor materials and kitchen unit tops, because of increasing cost of pure wooden products; they exhibit the artistic appearance of wood and the processing capability of thermoplastics.
- The automotive industries use some of these products for interior paneling in cars.
- Wood-polymer composites had replaced traditional materials in musical instruments, such as guitars, violins, windpipes, and pianos, lowering costs and labour time. Wood-polymer composite instruments last longer and can also help with ease of playing and maintenance in some cases.

Natural fibres, however, do not usually perform satisfactorily as polymer reinforcement, owing to their high surface polarity. In a composite the efficiency of fibre reinforcement depends primarily on the capability to transfer the applied stress from the continuous phase (matrix) to the fibres. This is not achieved with natural fibres, owing to poor adhesion between the hydrophilic surface of the natural fibres and the essentially hydrophobic polymers which are commonly used as the matrix [11, 12].

The second drawback is the high moisture absorption of the natural fibres. Moisture absorption can result in swelling of the fibres, and concerns on the stability of the fibre composites cannot be ignored. The absorption of moisture by the fibres is minimized in the composite, due to encapsulation by the polymer. It is difficult to entirely eliminate the absorption of moisture without using expensive surface barriers on the composite surface. If necessary, the moisture absorption of the fibres can be dramatically reduced through chemical modification of some of the hydroxyl groups present in the fibre, but with some increase in the cost of the fibre. Good fibre-matrix bonding can also decrease the rate and amount of water absorbed by the composite [13].

With the use of a variety of fibres and matrices, a general notion of composites has emerged. The design of composite materials led scientists and engineers to turn their attention towards the interface between two phases. Because the mechanical properties of heterogeneous structures depend on the quality of interfaces between the components, it was crucial to develop additive substances favouring chemical bonds between the fibre and the

matrix. Composites thus favoured a new direction of materials research in which chemists had to play a major role.

1.5 Aim of the study

There is a considerable commercial interest in thermoplastic composites filled with wood fibre, due to potential opportunities of combining the attractive characteristics and properties of both components. The developed product has the appearance of wood and the processing capability of thermoplastics. Due to the relatively high bulk density and free flowing nature of wood, as well as its low cost and availability, the material can be considered as an easily attainable natural option and convenient for a wide range of applications.

This study is focused on using a natural fibre, wood fibre, as filler in an ethylene vinyl acetate copolymer (EVA). This research is based on the following major investigations:

- The effect of the wood fibre content on the properties of the composites.
- The effect of wood fibre particle size on the properties of the composites.
- The effect of a compatibilizer (EGMA) on the properties of the composites.

Thermal and mechanical properties, as well as morphology of the composites, were investigated by using analytical techniques such as differential scanning calorimetry (DSC), thermogravimetric analyses (TGA), tensile testing, polarized optical microscopy, permeability and surface free energy.

1.6 References

1. http://www.gogulftech.com/techform/default.htm#anchor1132163 (23 July 2005)
2. http://www.epp.goodrich.com/why.shtml (25 July 2005)
3. http://www.compositesatlantic.com/pdf/vol1_2.pdf (12 August 2005)
4. http://www.epp.goodrich.com/compositebenefits.shtml (12 August 2005)
5. http://www.rmi.org/sitepages/pid445.php (30 August 2005)
6. http://www.tms.org/pubs/journals/JOM/9602/Scala-9602.html#ToC6 (5 September 2005)
7. http://hrst.mit.edu/hrs/materials/public/composites/Composites_Overview.htm (28 July 2005)
8. http://www.wtec.org/loyola/polymers/c1_s2.htm (12 September 2005)

9. Georgopoulos ST, Tarantili PA, Avgerinos E, Andreopoulos AG, Koukios AG, *Polym. Degrad. Stabil.*, 90 (2005) 303
10. Selke SE, Wichman I, *Composites A*, 35 (2004) 321
11. Gassan J, Gutowski VS, *Comp. Sci. Technol.*, 60 (2000) 2857
12. Tserkia V, Zafeiropoulos NE, Simon F, Panayiotou C, *Composites A*, 36 (2005) 1110
13. Yang HS, Kim HJ, Park HJ, Lee BJ, Hwang TS, *Comp. Struct.*, 72 (2006) 429

CHAPTER 2 (Literature review)

The fibre industry is divided into natural fibres, those from plant, animal, or mineral sources, and man-made fibres called synthetic fibres. The history of composites was previously dominated by synthetic fibres. This is rapidly changing because of increasing environmental consciousness and demands of legislative authorities. The manufacture, use and removal of synthetic composite structures, usually made of glass, carbon or aramid fibres being reinforced with polymers such as epoxy, unsaturated polyester resins, polyurethanes or phenolics, are considered critically. The most important disadvantages of such composite materials is the problem of convenient removal after end-of-life time, as the components are closely interconnected, relatively stable and therefore difficult to separate and recycle [1].

Government regulations and growing environmental awareness throughout the world have triggered a paradigm shift towards designing materials compatible with the environment. The natural and wood fibres derived from annually renewable resources, as reinforcing fibres in both thermoplastic and thermoset matrix composites; provide positive environmental benefits with respect to ultimate disposability and raw material utilization [2].

After decades of high technology developments of artificial fibres like carbon, aramid and glass, it is remarkable that natural grown fibres have gained a renewed interest, especially as a glass fibre substitute in automotive industries. Fibres like jute, wood, flax, sisal or hemp are cheap, have better stiffness per unit weight and have a lower impact on the environment [3].

2.1 Synthetic fibres

Initially, transportation vehicles such as airplanes, helicopters, and boats were manufactured using heavy metals and pure wood. While metallic components, that had been used up to that point, certainly did the job in terms of mechanical properties, the heavy weight of such components was excessive, and this placed limits on their speed and increased fuel consumption. Heavy ships and airplanes use a lot of fuel to move. This era led to the synthesis of fibres such as glass, carbon, and nylon that were mixed with matrices to produce light-weight, strong non-brittle materials with high strength that were to replace heavy weight metals. Fibres improve the strength-to-weight ratio of base materials such as titanium and aluminium [4].

2.1.1 Metal and ceramic fibres

Metal and ceramic fibres are used in high-strength, high-temperature, lightweight composite materials for different applications. Desired properties can be designed by applying relevant conditions during synthesis and processing. Fibres of stainless steel or aluminium provide conductivity in plastic components for static-electricity dissipation or, with higher loadings, shielding from electromagnetic interference. Shielding is particularly important for housings of computers, copiers, and other business machines. Because only small levels of stainless-steel fibres are needed, base-resin properties remain relatively unchanged, and the composite has good collaboration [5].

Among the strongest materials are metal fibres formed by controlled solidification and cold drawing. Some non-metallic fibres such as aluminium oxide and silicon carbide are nearly as strong as metal fibres, but have a higher modulus of elasticity. Fibres in a metal matrix combine the strength of the fibre with the ductility or other characteristics of the matrix. Many combinations of properties are possible – for example, tungsten fibres in a copper matrix add the strength of the fibre to the conductivity of the matrix. Aluminium oxide and silicon carbide are among several fibres added to aluminium to produce high strength-to-weight ratio composites [5].

2.1.2 Glass fibres

Glass fibre is the most widely used reinforcement for plastic and rubber products. Glass fibres are also the finest, having the smallest diameter, of all fibres. Because glass fibres have a large surface area in proportion to volume, surface conditions of the fibre have a strong influence on its strength and behaviour. Most glass-reinforced products are made with E-glass (electrical glass), which has good electrical and mechanical properties and high heat resistance. E-glass is available as chopped fibre, milled fibre, continuous roving, woven roving, woven fabric, and reinforcing mat. The tensile strength, modulus and elongation of the fibres were high. Applications are in many industries, ranging from shower units and boat hulls to tanks, ducts, and automotive exterior panels. Fabrication of components, using both thermoplastic and thermoset matrix resins, is done by all conventional molding processes [6, 7].

For higher performance than that provided by E-glass, S-glass is used. It offers 30 % higher tensile strength and 18 % higher modulus than E-glass. S-glass is used in such applications as aircraft flooring, helicopter blades, and filament-wound pressure containers.

C-glass is a corrosion resistant type of glass, and is usually used as a surfacing veil cloth on outer surfaces of laminates, or against tool surfaces to protect the laminate from corrosion [7].

2.1.3 Carbon fibres

Carbon fibres, sometimes called graphite fibres, offer the widest range of stiffness of any material - from about 5 million to as high as 100 million psi. Most commonly used carbon fibre materials are those fibres in the midrange, having moduli in the 30 to 40 million-psi range, because they have the most useful balance of properties [8].

Used alone or as a part of a hybrid reinforcement with glass or aramid, carbon adds considerable strength and stiffness to engineering resins. In chopped form, molding procedures of carbon-reinforced composites is essentially the same as those used for glass-reinforced compounds. In tape form, often with an epoxy resin, the fibres are usually laid up as laminates, with the continuous fibres at various angles to one another. In between chopped and continuous fibres are the recently introduced long-fibre-reinforced composites, which are available with either carbon or glass-fibre reinforcement. In these compounds, the carbon fibres provide strength values between those of the chopped and continuous-fibre-reinforced composites [8].

Because of their light weight and high strength and stiffness, carbon-reinforced composites are used in aircraft components. Their high-temperature properties qualify them for applications such as pump packing, bearings, and brake components. Sports equipment of carbon materials includes skis, racquets, golf club shafts, and lightweight bicycle parts [5, 8].

2.1.4 Aramid fibres

These aromatic polyamides are characterized by excellent environmental and thermal stability, static and dynamic fatigue resistance and impact resistance. They also have a high specific tensile strength. Aramid-reinforced thermoplastic composites have excellent wear resistance and near-isotropic properties, characteristics not available with glass or carbon reinforced composites. Aramid fibre, trade named Kevlar, is available in several grades and property levels for specific applications. The grade designated simply as Kevlar is made specifically to reinforce tyres, hoses and belting, such as V-belts and conveyor belts [9].

Kevlar 29 is similar to the basic Kevlar in properties, but is designated specifically for use in ropes and cables, protective apparel, and as the substrate for coated fabrics. In short fibre or pulp form, Kevlar 29 can be a substitute for asbestos in friction products or gaskets.

Fabrics of Kevlar 29 can be made into bullet-resistant vests. Clothing made from Kevlar 29 can be as heat resistant as that made from asbestos [10]. Kevlar 49 has half the elongation and twice the modulus of Kevlar 29. Applications are principally in reinforcing plastic compounds used in lightweight aircraft, boat hulls and sports equipment. Composites containing Kevlar are also used as interior panels and secondary structural parts, such as fairings and doors on commercial aircraft. Kevlar 149 is a highly crystalline aramid that has a modulus of elasticity 40 % greater than that of Kevlar 49 and a specific modulus nearly equal to that of high-tenacity graphite fibres. It is used to reinforce composites for aircraft components [10].

Nomex aramid fibre is characterized by excellent high-temperature durability with low shrinkage. It does not melt and therefore retains a high percentage of its initial strength at elevated temperatures. It is available as continuous filament fibre, staple, and tow. Nomex is used in military and civilian protective apparel, dry gas filtration, rubber reinforcement, and industrial fabrics. Nomex aramid fibres are also available as a paper for use in high-temperature electrical insulation and in resilient, corrosion proof honeycomb core for aerospace and other transportation applications [10].

2.1.5 Thermoplastic fibres

Thermoplastic fibres are also used to reinforce composite materials. Two such families are Compet and Spectra fibres. Thermoplastic fibres are particularly effective where high-shear processing would degrade conventional glass-fibre reinforcement, thereby reducing performance of the composite [11].

Compet fibres of nylon and polyester provide excellent impact resistance, surface appearance, and abrasion and corrosion resistance. They were developed to provide a degree of toughness and impact strength in brittle thermoset matrices [11]. Spectra fibres are lightweight, high-strength, extended-chain polyethylene fibres and have two grades. One is a 1,200-denier fibre designed for high strength under intermittent loading conditions, and is used in sports equipment, ballistic fabrics, and medical products. The other is a 650-denier fibre for high strength under continuous load, and it is applied in sailcloth, high-tension ropes, and cables that must withstand flex-fatigue conditions [11].

2.2 Natural fibres

Natural fibres are composed of various organic materials, primarily cellulose, hemicelluloses and lignin, therefore their thermal treatment leads to a variety of physical and chemical changes. Thermal degradation of those fibres leads to production of odour and colours, and moreover to deterioration of their mechanical properties. It also results in the generation of gaseous products, when processing takes place at temperatures above 200 °C, which can create high porosity, low density and reduced mechanical properties [12].

For the improvement of thermal stability, attempts have been made to blend or graft the fibres with thermoplastic materials. The moisture content of these fibres can vary in the range of 5 to 10 %. During processing of composites with thermoplastic matrices, the moisture content can lead to poor processing and porous products. Treatment of natural fibres with hydrophobic chemicals or modification with monomers can reduce the moisture gain [12].

Natural fibres are largely divided into two categories depending on their origin: plant-based and animal-based. In general, plant-based natural fibres are lignocellulosic in nature and are composed of cellulose, hemicelluloses and lignin, whereas animal-based fibres are of proteins. A large number of papers reported on bio composites based upon these plant-based natural fibres. However, use of animal-based natural fibres like silk and wool in a bio composite material has been rarely reported [13-17].

2.2.1 Animal based natural fibres

Silk fibres spun out from silkworm cocoons consist of fibroin in the inner layer and sericin in the outer layer, all protein-based. The chemical compositions are, in general, silk fibroin, sericin, and waxes. Silk fibres are biodegradable and highly crystalline with well-aligned structure. They also have higher tensile strength than glass fibre or synthetic organic fibres. Their other properties are good elasticity and excellent resilience. The densities are in the range of 1320–1400 $kg.m^{-3}$ with sericin, and 1300–1380 $kg.m^{-3}$ without sericin [18, 19].

2.2.2 Plant-based natural fibres

Plant-based natural fibres like flax, jute, sisal and kenaf have been more frequently utilized and studied so far, due to their natural abundance, cost effectiveness, world annual production and a wide range of properties depending on the plant source. Other resources includes wood, straw, stalks, reeds, bamboo, cotton, hemp, papyrus, grasses, water plants, and a wide variety of waste agro-mass including recycled paper, and paper products. The popularity of these fibres is because of their renewable origin. Other factors are that they are light-weight, biodegradable, and have moderate strengths and moduli. Besides their light weight, plant fibres prevent tool wear during processing and show damage-tolerant material behaviour [20-23].

2.3 Animal based natural fibre – polymer composites

The effect of short fibre content on the mechanical and thermal properties of novel silk-poly (butylene succinate) (PBS) biocomposites were investigated by and Lee and co-workers [24]. In this study, silk fibre poly(butylene succinate) biocomposites were fabricated with varying fibre contents by a compression molding method, and their mechanical and thermal properties were studied in terms of tensile and flexural properties, thermal stability, thermal expansion, dynamic mechanical properties, and microscopic observations. The results demonstrate that chopped silk fibres play an important role as reinforcement for improving the mechanical properties of PBS, although raw silk fibres were used without any surface modification normally used to enhance the interfacial adhesion between the natural fibre and the matrix. The tensile and flexural properties of the PBS matrix resin were markedly improved when increasing the short fibre content in the composites, showing a maximum value at a fibre loading of 50 wt%. The thermomechanical stability of the PBS resin was also greatly improved by incorporating reinforcing short silk fibres in the composite matrix, showing much lower linear coefficient of thermal expansion and higher storage modulus than the PBS control. This work suggests that the use of animal-based natural silk fibre as reinforcement in a natural fibre composite system has the potential of effectively improving the properties and performance of biodegradable polymer matrix resins [24].

2.4 Plant based natural fibre – polymer composites

The utilization of plant based natural fibre as reinforcement for the thermoplastic composites is growing, not only for ecological concern but also for a wide range of applications. Currently 400 million pounds of natural fibre reinforced thermoplastic composites are produced annually, and the figure is expected to double in few years to come. This growth is attributed to an increasing interest in the construction and motor industries. There is about a 60 and 50 % increase in the demand for natural filler composites in the building and motor industries, respectively. In the building industries these composites are used mainly in decking, trim, fencing, flooring, furnishers, windows and door profiles [25].

The rest of this chapter will focus on previous work done on natural fibre polymer composites. Research done on composites, made mainly from natural plant fibres such as jute, wood fibre, flax, and hemp, is revised. Polypropylene (PP), ethylene propylene (EP), high density polyethylene HDPE, and low density polyethylene (LDPE) are amongst different polymer matrices used.

The major problem, incompatibility, between the hydrophilic (polar) character of natural fibres and hydrophobic (non-polar) polymer matrix was investigated by various researchers. Due to this problem, many efforts were focused on physical and chemical methods to optimize or influence the quality of the fibre–matrix interface. Physical modification was done by considering the particle size of the filler, proper alignment, and the length of the filler. Chemical methods such as change in the surface free energy, impregnation, coatings, coupling agents and graft co-polymerization were also studied [25].

2.4.1 Physical modification

The effect of particle size and content of the filler on oil palm wood powder reinforced epoxidised natural rubber composites was investigated by Ismail *et al.* [26]. In this study it was found that the maximum torque increased with increasing fibre content, and that the composite with the smallest particle size showed the highest torque values. Addition of wood powder to the matrix increased tear strength, modulus and elongation at break. Small particle sizes gave better mechanical properties compared to large particle sizes [26].

Zaini *et al.* [27] reported the effect of filler content and size on the mechanical properties of polypropylene – oil palm wood powder composites. They found that the

composites filled with large sized filler showed a high modulus, tensile and impact strength, particularly at high filler content [27].

Kumar and Singh [28] studied three types of composites that were prepared by melt mixing of ethylene–propylene (EP) copolymer and (i) 3 % NaOH treated jute fiber, (ii) 17.5 % NaOH treated jute fiber and (iii) commercial microcrystalline cellulose powder using maleated EP copolymer as compatibilizer. The obtained composites were characterized by Fourier transform infrared spectroscopy (FTIR), thermal gravimetric analysis (TGA) and microscopic measurements. The durability of the composites was evaluated under polychromatic irradiation ($\lambda \geq 290$ nm) and composting conditions for different time intervals. It was found that the treatments on the natural fibre influenced the service life of the end product. Composites made from microcrystalline cellulose showed better mechanical properties as well as photo-resistance. The specimen containing 3 % NaOH treated fiber exhibited the lowest photo-resistance and biosusceptibility. Composites were less durable under both abiotic and biotic conditions in comparison to the neat polymer matrix [28].

The effect of alkalization and fibre alignment on the mechanical and thermal properties of kenaf and hemp fibre composites using a polyester resin matrix was investigated by Aziz *et al.* [29]. In this study, long and random hemp and kenaf fibres were used in the as-received condition and alkalized with a 0.06 M NaOH solution. They were combined with polyester resin and hot-pressed to form natural fibre composites. The mechanical properties of the composites were measured to observe the effect of fibre alignment and alkalization. A general trend was observed whereby alkalized and long fibre composites gave higher flexural modulus and flexural strength compared to composites made from as-received fibres. Alkalized long kenaf–polyester composites possessed superior mechanical properties to alkalized long hemp–polyester composites. Scanning electron microscopy micrographs of the treated hemp and kenaf fibres showed the absence of surface impurities which were present on the untreated fibres. Apparent density measurements on hemp and kenaf fibres did not show a significant change after alkalization with 0.06 M NaOH. Differential scanning calorimetry (DSC) analysis indicated the presence of moisture which leads to undesired mechanical properties. Dynamic mechanical thermal analysis (DMA) results showed that treated fibre composites had greater interfacial bond strength and adhesion between the matrix resin and the fibre, and much better impact properties compared to the untreated fibre composites [29].

The effect of processing conditions on the fibre length distribution and the dependence of the composite mechanical properties on fibre content were investigated. Composites of

aliphatic polyester (Bionolle) with natural flax fibres were prepared by batch mixing. The tensile modulus changed with fibre content. The strength of the Bionolle-flax composites decreased with fibre loading, showing that there was no adhesion between the matrix and fibres. With the aim to improve fibre–matrix adhesion, chemically modified flax fibres were also tested as reinforcing agents. A 30 % strength increase was observed when natural fibres were substituted by fibres containing acetate groups. No significant strength changes were observed in composites containing fibres with valerate groups or polyethylene glycol chains grafted on the surface [30].

Jacob *et al.* [31] studied the effects of concentration and modification of fibre surface on sisal/oil palm hybrid fibre reinforced rubber composites. Natural rubber was reinforced with untreated sisal and oil palm fibres chopped to different fibre lengths. Composites were prepared using fibres treated with varying concentrations of sodium hydroxide solution and for different time intervals. The processability characteristics and mechanical properties of these composites were investigated as a function of fibre loading, ratio and treatment. Fibre breakage analysis revealed that the extent of breaking was low. The mechanical properties of the composites in the longitudinal direction were superior to those in the transverse direction. Addition of sisal and oil palm fibres led to an increase in tensile and tear strength, and increased modulus. The extent of adhesion between the fibre and rubber matrix was found to increase on alkali treatment of the fibres. The alkali treated fibre composites exhibited better tensile properties than the untreated composites. Processing characteristics were found to be independent of fibre loading and modification of the fibre surface. Swelling studies revealed that the composites containing bonding agents and alkali treated fibres showed higher crosslink density and better adhesion. The study also indicated that the presence of short fibres restricted the entry of solvent [31].

Brahmakumar *et al.* [32] used coconut fibre as reinforcement in low-density polyethylene. The effect of the natural waxy surface layer of the fibre on fibre-matrix interfacial bonding and composite properties was studied by a single fibre pull-out test and evaluation of the tensile properties of oriented discontinuous fibre composites. The natural waxy surface layer of coconut fibre provided a strong interfacial bonding between the fibre and the polyethylene matrix. Removal of the waxy layer resulted in weak interfacial bonding, a 40 % decrease in composite tensile strength and a 60 % modulus decrease. The waxy layer, due to its polymeric nature, showed a stronger effect on fibre-matrix bonding than the grafted layer of a C_{15} long alkyl chain molecule onto the wax-free fibre [32].

The morphological features of the fibre along with its surface compatibility with the matrix favoured oriented flow of relatively long fibres (20 mm) along with the molten matrix during extrusion, in contrast to a fibre length limit of 6 mm that was observed for sisal and pineapple fibres under identical extrusion conditions. The longitudinal tensile strength and modulus of a coconut fibre composite improves by about 300 % and 700 % respectively [32].

2.4.2 Chemical modification

Cellulose fibres are highly polar due to the presence of hydroxyl groups, which are readily available for the formation of hydrogen bonds in the interface of reinforced systems. However, plant fibres are covered with pectin and waxy substances, thus hindering the hydroxyl groups from reacting with polar matrices, which gives rise to reduced adhesion. On the other hand, this polar structure is the reason for the very hydrophilic behaviour of the fibres. That means that such fibres are swelling strongly in an aqueous environment. For high adhesion forces it is necessary to have polar functional groups, but swelling processes should be prevented. Intense chemical treatment such as surface treatment, addition of compatibilizer, etc. is therefore required for fibre cleaning and preparation for interfacial bonding. The use of coupling agents like silanes serve not only as an adhesion promoter, but also to hydrophobize the fibre surface to prevent swelling processes. Silane coupling agents may alter the hydrophilic properties of the interface. More specifically, the amino-functional silanes, such as epoxies and urethane-silanes, are used as primers for reactive polymers [33].

In order to study the durability of composites containing lignocellulosic fibres, their degradation and weathering characteristics must be thoroughly evaluated. Sapieha *et al.* [34] investigated the thermal degradation of polyethylene-cellulose composites during processing, and found that oxidation during processing resulted in enhanced adhesion between polymer and cellulose fibres [34].

Maldas and Kokta [35] studied the mechanical properties of polystyrene-cellulose-mica composites under different conditions of boiling water and subzero temperatures. Silane and isocyanate treatment of fibres were found to enhance the stability of fibres under these conditions.

Several researchers reported improvement in mechanical properties of cellulose fibre when alkalized at different NaOH concentrations. Bisanda and Ansell [36] applied a concentration of 0.5 M NaOH on sisal fibres, while Sreekala and co-workers [37], and

Geethamma and co-workers [38], used 5 % NaOH to remove surface impurities on oil palm fibres and short coir fibres, respectively.

Mwaikambo and Ansell [39] treated hemp, jute, sisal and kapok fibres with various concentrations of NaOH and found 6 % to be the optimum concentration in terms of cleaning the fibre bundle surfaces, yet retaining a high index of crystallinity [39].

The mechanical behaviour of high density polyethylene (HDPE) reinforced with continuous henequen fibres *Agave fourcroydes* was studied by Franco and Gonza´lez [40]. Fibre-matrix adhesion was promoted by fibre surface modifications using an alkaline treatment and a matrix pre-impregnation together with a silane coupling agent. The use of the silane coupling agent to promote chemical interaction, improved the degree of fibre-matrix adhesion. However, it was found that the resulting strength and stiffness of the composite depended on the amount of silane deposited on the fibre. A maximum value for the tensile strength was obtained for a certain silane concentration, but when using higher concentrations, the tensile strength did not increase. Using the silane concentration that resulted in higher tensile strength values, the flexural and shear properties were also studied. The elastic modulus of the composite did not improve with the fibre surface modification. The elastic modulus in the longitudinal fibre direction, obtained from the tensile and flexural measurements, were compared with values calculated using the rule of mixtures. It was observed that the increase in stiffness from the use of henequen fibres was approximately 80 % of the calculated values. The increase in the mechanical properties ranged between 3 and 43 % for the longitudinal tensile and flexural properties, whereas in the transverse direction to the fibre, the increase was greater than 50 % with respect to the properties of the composite made with untreated fibres. In the case of shear strength, the increase was of the order of 50 % [40].

Mohanty *et al.* [41] investigated the effect of process engineering on the performance of natural fibre reinforced cellulose acetate bio composites. Eco-friendly bio composites were fabricated from chopped hemp fibre and a cellulose ester biodegradable plastic through two process engineering approaches: powder impregnation through compression molding (process I) and extrusion followed by injection molding (process II). Cellulose ester, e.g. cellulose acetate (CA), plasticized with 30 wt. % citrate plasticizer (CAP), was used as the matrix polymer for bio composite fabrication. Intimate mixing, due to shear forces experienced in process II, produced bio composites of superior strength compared to their counterparts made in process I. Bio composites fabricated through process II, containing 30 wt.% hemp natural fibre, showed an improvement in storage modulus of 150 % over the pure matrix polymer,

and SEM analysis of impact fractured surfaces proved that the bio composites made through process I showed poor adhesion and lack of fibre dispersion as compared to process II. This is due to sufficient shear forces for the intimate mixing of the powdered polymer, liquid plasticizer and fibres. The coefficient of thermal expansion of the bio composite decreased from that of the CAP polymer by 60 %, whereas the heat deflection temperature improved by 30 % compared to the virgin bio plastic, indicating superior thermal behaviour of the bio composite. Plasticized cellulose acetate proved to be a much better matrix than the non-polar polypropylene (PP) for hemp fibre reinforcements, because of the better interaction of the polar cellulose ester with the polar natural fibre. Fabricated through process II and with the same content of hemp (30 wt.%), the hemp fibre based CAP bio composite exhibited flexural strength of 78 MPa and a modulus of elasticity of 5.6 GPa as compared to 55 MPa and 3.7 GPa for the corresponding PP-HF based composite. The incorporation of a high content of natural fibre, say up to 50 wt.% or more, in the bio composite system along with suitable surface treatments of natural fibres and the use of coupling agents during composite fabrication, was found to generate superior performance bio composites [41].

Gassan *et al.* [42] studied the possibilities for improving the mechanical properties of jute-epoxy composites by alkali treatment of fibres. In their study, the mechanical properties of tossa jute fibres were optimized by using a NaOH-treatment process with different alkali concentrations and shrinkages. Shrinkage of the fibres during treatment had the most significant effect on the fibre structure and, as a result, the fibre's mechanical properties such as tensile strength, modulus and toughness were improved. Alkali treatment under isometric conditions (20 min at 20°C in 25 % NaOH solution) led to an increase in jute yarn tensile strength and modulus of about 120 % and 150 %, respectively. The rougher surface morphology after treatment did not improve the adhesion between the fibres and matrix in epoxy composites. Nevertheless, a general increase of up to 60 % was measured for the fibres-dominated strength and stiffness of unidirectional composites with respect to fibres direction by using NaOH-treated jute fibres (isometric conditions). Young's modulus of composites with both untreated and isometric alkali treated jute fibres was linearly dependent on fibre content [42].

None of the above studies looked at the natural and artificial weathering of polymer-cellulose fibre composites, but Sharkh and Hamid [43] investigated the degradation and stabilization of polypropylene-date palm cellulose fibre composites under artificial and natural weathering conditions. It was concluded that PP- palm cellulose fibre composites are found to be much more stable than PP under the severe natural weathering conditions and in

accelerated weathering trials. In addition, compatibilized samples are generally less stable than uncompatibilized ones as a result of the lower stability of the maleated polypropylene. Two stabilizers, Irgastab and Tinuvin, were found to be efficient stabilizers for PP-cellulose fibre composites. In addition to the enhanced stability imparted by the presence of the fibre in the composites, enhanced interfacial adhesion resulting from oxidation of the polymer matrix can be a source of retention of mechanical strength [43].

Georgopoulos *et al.* [44] studied the perspectives of using lignocelluloses fibrous plant residues as fillers of thermoplastic polymers. The lignocellulosic materials used in this study were both untreated and pre-treated residues from eucalyptus wood, ground corncob, and brewery's spent grain. Polymer matrices of low-density polyethylene (LDPE) and PVC plastisol were used, to prepare composite specimens with different amounts of lignocellulose fillers were used. These specimens were tested for their mechanical properties, and additional assessment was made via measurements of their surface hardness and observations by stereoscopic optical microscopy. The results of this study show that loading of LDPE with natural fibres led to a decrease in tensile strength of the pure polymer. On the other hand, Young's modulus increased due to the higher stiffness of the fibres. Although the properties of some blends are acceptable for some applications, further improvement will be necessary, mainly by optimizing fibre polymer interface characteristics [44].

The steady state shear flow for simple blends of HDPE and wood composites was studied with capillary rheometry by Li *et al.* [45]. Two kinds of composites were investigated, i.e. maple and pine composites at different wood contents. It was observed that the shear flow of wood composites was characterized by a varying level of wall slip, and the viscosity depended on both wood content and species. The extensional flow of the wood composites showed that the extensional viscosity depended strongly on wood content but less on wood species. Strain thinning behaviour was observed for composites of 40 % maple and 60 % pine, respectively, while strain hardening was recorded with 40 % of pine or 60 % of maple [45].

Treatments and properties of polypropylene/wood flour (WF) composites were studied by Ichazi *et al.* [46]. The filler was treated with sodium hydroxide at different immersion times and with vinil-tri-(2-metoxietoxi-) silane. Propylene, fuctionalized with maleic anhydride (maleated polypropylene, MAPP), was used as compatibilizer. The results showed that the chemical treatment made on WF as well as the use of MAPP as compatibilizer improved the tensile properties of the composites. PP produced an increase in modulus, although it caused a decrease in the elongation at break and impact strength. The morphology of the composites was improved by treating the wood flour. Functionalized PP

and the use of silane improved the adhesion and the dispersion of the particles, and displayed lower rate of water absorption compared to untreated wood flour composites. This proved that the use of these compounds improves the filler polymer interaction [46]. Alkaline treatment of the wood flour improved the particle dispersion and not their adhesion to the polymer matrix, due to a higher availability of the OH group in the particle surface, which in turn favours the water absorption and hence the composite swelling. The addition of the filler and the treatment thereof, caused an increase in the crystallization temperature that would imply a shorter molding time, which in turn meant energy saving while processing these materials. The treatment and the use of MAPP did not have any effect on the melting index of the composites, thereby making them suitable for processing by conventional methods.

The effectiveness of a maleated polypropylene (MAPP) as a coupling agent in wood fibre-polypropylene composites made by non-woven web technology was evaluated by Krzysik and Youngquist [47]. The composite panels were made with 70 or 85 % wood fibre, with the MAPP being incorporated in the panels at a level of 1 or 3 % by spraying an emulsified form on the wood fibres. Both levels of MAPP significantly increased bending, tensile strength and moduli, and dynamic modulus. At the 70 % wood fibre level, impact energy was increased significantly in panels with 3 % MAPP. At the 85 % wood fibre level, both 1 and 3 % MAPP significantly increased impact energy. The MAPP also led to small improvements in water resistance for composites containing 85 % wood fibre. The effectiveness of MAPP is believed to be the result of efficient incorporation at the wood-polypropylene interface, thus providing effective coupling of the polar wood component to the non-polar polymer matrix [47].

Wood flour (WF) reinforced linear low-density polyethylene (LLDPE) composites were prepared by Kuan *et al* [48]. For the improvement of physical properties, a water-crosslinking technique was used. Composites were compounded in a twin-screw extruder, treated with a coupling agent (vinyltrimethoxysilane, VTMOS), and then moisture-crosslinked in hot water. It was seen that the composite after water-crosslinking treatment exhibited better mechanical properties than the non-crosslinked one because of the improved chemical bonding between the wood fibre and the polyolefin matrix. As the wood fibre content reaches 30 wt %, and after water-crosslinking for 4 h, tensile strength and flexural strength are increased by 87 % (14.7 – 27.5 MPa) and 137.5 % (11.2 – 26.6 MPa) with respect to that of non-crosslinked ones. Thermal analysis of water-crosslinked composites indicate that the thermal degradation temperature and the heat deflection temperature of the composite

increase with increasing water-crosslinking time. The heat deflection temperature of the composite was increased from 55.7 to 88.5 °C [48].

The mechanical properties of compression-molded polystyrenes filled with sawdust wood residue of softwood and hardwood species were investigated by Maldas *et al.* [49]. The tensile modulus, tensile strength, elongation and energy at the yield point were reported. The suitability of sawdust wood residue as a filler for thermoplastics was tested using two different mesh sizes (20 and 60), as well as by varying the weight percentage of fibres from 10 to 40 %. Moreover, to improve the compatibility of the wood fibres with the polymer matrices, different treatments (e.g. graft copolymerization) and coupling agents (e.g. silanes and isocyanates at various concentrations) were used. The extent of the improvement in mechanical properties depended on the fibre loading, the particle size of the fibre, the concentration and chemical structure of the coupling agents, and on whether special treatments (e.g. coating or grafting of the fibre) were used. The mechanical properties of the composites were improved up to 30 % in the case of fibres having a mesh size 60 and when up to 3 % of isocyanates were used [49].

The mechanical properties and dimensional stability of composites consisting of hardwood aspen pulp in polystyrene were evaluated under various ageing conditions, including variation of the testing temperature (from +25 °C to −40 °C), exposure to boiling water, and heating in an oven at +105 °C. The influence of coupling agent, e.g. 3 % poly[methylene(polyphenyl isocyanate)], as well as treatments such as coating and grafting, on the properties of the composite materials were studied by Kokta and Maldas [49]. The treated composites showed superior mechanical properties and better dimensional stability compared with non-treated fibre-filled composites. Moreover, the mechanical properties, particularly of treated composites, were enhanced compared to those studied under ordinary conditions. Dimensional stability under the same conditions also supported this observation. The greater resistance of the treated composites under different conditions suggested the existence of an efficient interfacial area between the fibre and the polymer matrices [49].

The effect of coupling agents on the physical properties of wood-polymer composites was studied by Elvy *et al.* [50]. Wood-polymer composites based on two Australian commercial timbers, radiata pine *(pinus radiata)*, a soft wood and fast growing plantation timber, and black *(eucalyptus puliaris),* a hard wood which is also a plantation amber, were prepared using the vinyl monomer, methyl methacrylate (MMA). It was established that poly (methyl methacrylate) does not form bonds with the hydroxyl groups of the cellulose fibres, but simply bulks the void spaces within the wood structure. Coupling agents were known to

increase adhesion of wood fibre to the polymer matrix. In this study wood samples were pretreated with the coupling agent, vinyltriacetoxysilane, before impregnation with MMA in order to evaluate the effects of the silane coupling agent on the physical properties of the wood-polymer composites.

These composites were prepared using a catalyst-accelerator method and the polymerization process was initiated at room temperature. This method involved the impregnation of wood samples using MMA containing benzoyl peroxide (1 %), lauroyl peroxide (0.5 %) and 0.5 % of the the accelerator N,N-dimethylaniline. In contrast to the conventional catalyst-heat method, the method requires no heating in the initiation process and thus results in virtually no loss of monomer. In general, there were improvements in dimensional stabilities (positive effects in both anti-shrink and anti-absorption efficiencies), compressive strength and hardness of silane treated wood-polymer composites. The morphology of the composites was examined using scanning electron microscopy (SEM) and improved adhesion was evident for composites treated with the coupling agent [50].

The resistance of polymer-wood composites to chemical corrosion was studied by Spindler *et al.* [51]. The resistance to chemical attack of polymer composites based on ash, birch, elm and maple was evaluated for a representative range of corrosive reagents. The behaviour of these composites was compared with that of the untreated parent timbers, and with teak and iroko which have a high natural resistance to corrosion. The chemical resistance of composites was generally 2–5 times greater than that of the untreated timbers.

Wood-plastic composite (WPC) formation was studied by Mubarak *et al.* [52] with *simul*/styrene system at various compositions of styrene with methanol as the swelling solvent. The effect of additives, e.g. multifunctional monomers (MFM) and oligomers used in very low quantity (1 % v/v) on the polymer loading and tensile strength of the WPC was investigated. High tensile strength values were observed. Inorganic co-additives like lithium (Li^{+}), copper (Cu^{2+}), acid (H^{+}) and urea (U) used in combinations with additives (MFM or oligomers) influenced the tensile strength results in these systems. Co-additive Cu^{2+} used in this system acted as a preservative and protective agent for WPC [52].

Mechanical properties and decay resistance of wood–polymer composites, prepared from fast growing species in Turkey, were investigated by Yildiz *et al.* [53]. Wood–polymer composites were made from maritime pine (*Pinus pinaster Ait.*) and poplar (*Populus x. euramericana cv. I-214*) wood. Three different monomers, styrene, methyl methacrylate (MMA) and a styrene/methyl methacrylate (ST/MMA) mixture were used in the preparation of wood–polymer composites (WPCs). Full-loading, half-loading and quarter-loading were

used as polymer content levels. Untreated pine and pine–polymer composite samples were tested for compression strength parallel to the grain and static bending strength. WPC mechanical properties increased compared to untreated wood. The polymer had a greater effect on the strengths of the ST/MMA treated pine than on the ST and MMA treated pine samples. Increasing the mechanical properties should improve the structural competitiveness of WPC made from fast growing low-density woods. Weight losses due to fungal attack for pine and poplar–polymer composites were also determined. Although polymers at full and half loading levels helped decreasing weight losses due to both fungi for each wood species, weight losses were still found to be higher [53].

The influence of liquefied wood (LW), melt index (MI) and polymer on the mechanical properties and creep behavior of liquefied wood–polymer composites (LWPC) was investigated by Doh *et al* [54]. Polymer and LW showed significant effects on the flexural strength properties. The increase of flexural strength by the addition of 10 % LW is related to an increase in stiffness of LWPC. A high MI value helped to blend both liquefied wood and the polymer during the compounding process, thereby providing good dispersion of the polymer. The maximum Young's modulus and tensile strength values were also observed for PP with high MI with and without LW. The effects of polymer, MI, and LW on Young's modulus were significant. The impact strengths for HDPE and LDPE were high, due to high flexibility. With the increased stress concentration as a result of the poor bonding between LW and polymer, the impact strength of LWPC decreased, compared to that of the virgin polymer. The instantaneous and maximum creep deflections at the 40 % stress level were significantly higher than those at the 20 % stress level. MI provided a significant effect on the creep. The addition of 10 % LW showed no significant effect on the creep [54].

Water absorption of natural cellulose wood fibre-polypropylene composites and its influence on their mechanical properties were studied by Espert *et al.* [55]. Water absorption by natural fibre-PP composites was proved to be influenced by the fibre content, the type of matrix and mainly by the temperature. Mechanical properties were dramatically affected by the water absorption. Water-saturated samples presented poor mechanical properties such as lower values of Young's modulus and stress at maximum load. For samples with low fibre content, water acted in some way as a plasticizer leading to slightly higher values of strain, although this effect disappeared with the increase in temperature or fibre content. The use of a post-industrial polypropylene with a low percentage of EVA in its composition, in some cases led to improved resistance to water absorption. It was believed that EVA can further improve the compatibility between the fibres and matrix. EVA is a copolymer of ethylene,

which permits the adhesion to the PP matrix, and vinyl acetate, which could bond due to its acetate groups to the hydroxyl groups on the fibres.

Physical properties, i.e. the thickness swelling and water absorption, and mechanical properties, i.e. tensile strength and Izod impact strength, of lignocellulosic filler reinforced polyolefin bio-composites were investigated by Yang and co- workers [56]. The polyolefin was used as the matrix polymer and rice-husk flour as the reinforcing filler. Wood flour was also used as reinforcing filler, and commercial particleboard, medium-density fibreboard and solid woods (red pine and birch) were also included in this study in order to obtain comparative water absorption behaviour measurements. The physical and mechanical properties of the bio composites as a function of filler loading and filler type, as well as with respect to the thermoplastic polymer itself, were determined. During this study, it was observed that the thickness swelling and water absorption of the bio composites slightly increased as the filler loading increased, but to a negligible extent as compared to the wood-based composites (particleboard and fibreboard) and the solid woods (red pine and birch). The compatibilizing agents had a positive effect on the thickness swelling and water absorption of these bio composites. The mechanical properties of the composites decreased as the filler loading increased. This was due to the poor interfacial bonding between the filler and the polymer matrix. This caused the tensile strength and Izod impact strength of the composites to be reduced, and this poor interfacial bonding resulted in an increase in the number of micro voids, causing increased water absorption. With the addition of the compatibilizing agent, the interfacial bonding between the filler and the matrix polymer was greatly improved, resulting in improved dimensional stabilities and water absorption behaviour [56].

Joseph *et al.* [57] investigated water absorption and UV degradation of sisal fibre-polypropylene composites. Compatibilization was found to reduce the water absorption of the composites due to stronger adhesion between fibre and matrix materials. The tensile strength of the composites decreased with increasing UV irradiation time. Degradation was found to be caused by photo-oxidation and subsequent chain scission.

The incorporation of recycled materials originating from renewable sources into cement cores is a feasible alternative that has gained ground in civil construction. Stancato *et al.* [58] investigated the matrix of a vegetable waste composite with polymer-modified cement. Several mixtures composed of cement, treated vegetable residue, wood from the Pinus caribaea species, latex type polymer, styrene–butadiene rubber (SBR) and an adequate water ratio for the mixtures were studied. The composite mechanical behaviour, workability,

and water absorption by capillarity were investigated. Some of the essential properties, such as workability, mechanical strength, and durability were substantially altered by the addition of polymers. The effect of reduced capillary pores, resulting from the action of the polymer, contributed to a decrease in the permeability of the material, preventing the penetration of aggressive agents due to the phenomenon of water transport. The composite containing vegetable residues and SBR-modified core presented the best mechanical behavior, and an increase in the polymer content resulted in greater water retention in the fresh mixture and a significant reduction in porosity.

2.4.3 Irradiation modification

Gassan *et al.* [59] investigated the effects of corona discharge and UV treatment on the properties of jute fibre – epoxy composites, and it was found that corona discharge treated jute fibres exhibited a significant increase in the polar component of the surface free energy with increasing corona energy. Unfortunately, the oxidation of the fibres' surface always led to a decrease in fibre tensile strength. The UV treatment of jute yarn led to higher polarity (up to 200 % increase) with increased treatment time and constant bulb-substrate distance. Furthermore, the treatment distance had a significant effect on the polarity as well as on the firmness of the yarn. To improve the mechanical properties of jute-epoxy composites by the use of UV-oxidation of fibres, a balance between the increased polarity of the fibres' surface and the decrease in fibre strength is necessary. Under optimum treatment conditions an increase in the composite flexural strength of about 30 % was achieved.

Preservation of beech and spruce wood by allyl alcohol-based copolymers was investigated by S'olpan and GuEven [60]. In this study, allyl alcohol (AA), acrylonitrile (AN), methyl methacrylate (MMA) monomers and monomer mixtures AA+AN, AA+MMA were used to preserve and consolidate beech and spruce. After impregnation, copolymerisation and polymerisation were accomplished by gamma irradiation. The fine structure of wood-polymer composites was investigated by scanning electron microscopy (SEM). It was observed that the copolymer obtained from the AA+MMA monomer mixture showed the optimum compatibility. The compressional strength and Brinell hardness numbers determined for untreated and treated wood samples indicated that the mechanical strength of wood-copolymer composites increased. The mechanical strength of the wood samples containing the AA+MMA copolymer was higher than the others. The water uptake capacity

of wood-copolymer composites decreased by more than 50 % relative to the original samples, and biodegradation did not take place [60].

The influence of gamma irradiation on the thermal stability of blends of PP with previously treated sisal fibre was investigated by Albano *et al.* [61]. In this work, the thermal degradation of PP blends with previously treated sisal fibre (10mm), and irradiated to 10, 25, 50, 60 and 70 KGy, was studied. Sisal fibre was treated by: a) addition of an alkylating agent; 1% by weight, b) chemical treatment with NaOH at different times, 1/2 and 1 hour, and (c) the addition of functionalized PP, 5 % by weight. After treatment, a mixture of PP and 20 % sisal fibre was prepared. Different integral methods were used to evaluate the activation energy. The blend previously treated with NaOH for 1 hour showed the largest value of 60kJ.mol^{-1} for irradiation doses below 40 kGy. At higher irradiation doses, decay in the activation energy was experienced. When the fibre was treated for 30 minutes with NaOH, the activation energy decreased from 55 kJ. mol^{-1} to values below 45 kJ. mol^{-1}, when subjected to high irradiation doses of > 50 kGy. When sisal is treated with NaOH for a longer time, impurities and lignin are better removed, resulting in higher surface roughness and a better polymer to fibre interaction, which in turn makes the blend more stable at low irradiation doses. When the sisal fibres were instead treated with silane, the activation of the thermal degradation decreases at higher irradiation doses until the opposite occurs at 50 kGy, implying that this irradiation induces the production of the PP-filler bridges. With composites containing a compatibilizer, similar results were found with the opposite occurring at 70 kGy. From these results it can be concluded that the 1 hour NaOH treatment resulted in more thermally stable composites [61].

Wood fibre–polypropylene composites, irradiated with an electron beam, were studied by Czvikovszky [62]. It was found that treating wood fibre and polypropylene (PP) with an electron beam increased the compatibility between the filler and the matrix. Electron beam treatment is a productive method of creating active sites on both the matrix polymer and the fibrous reinforcement. Wood fibre and PP bound together by a reactive additive resulted in a composite which not only had a high modulus of elasticity, but also a significantly higher flexural and tensile strength and improved thermal tolerance over the conventional wood fibre-PP blends, and over the PP itself. Compatibilization is possible because of the long living free radicals and thermally active peroxy groups that are accumulated on the cellulose, as well as on the lignin after radiation treatment. The polypropylene is an excellent matrix for radiation initiated graft-copolymerization because of the formation of similar free radicals and

peroxy groups. These chemically reactive species can serve as bonding sites for suitably selected reactive additives, capable of high-speed polymerization chain-reactions.

2.5 Ethylene vinyl acetate copolymers

EVA is copolymer of ethylene and vinyl acetate, typically formed via free radical polymerization. EVA generally contains 1–50 wt.% of a vinyl acetate (VA) comonomer along the carbon chain backbone, and has the structural formula in Figure 2.1.

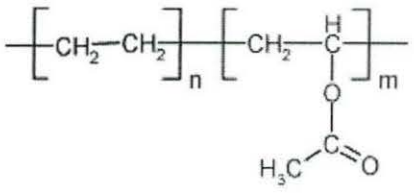

Figure 2.1 Structural presentation of EVA

Properties of EVA depend on the VA content. Generally the following properties are common among most EVA: density of 0.95 g cm^{-3}, tensile strength of 10 MPa, elongation at break of 900 %, and water absorption of 0.13 %. Advantages of using EVA are excellent heat strength, flexibility and low temperature performance. EVA is a widely used material, particularly as a zero-halogen material in the cable industry. It is frequently formulated with large quantities of inorganic filler material, such as aluminum trihydroxide (ATH) [63].

Since nanoclay incorporation is also believed to assist the formation of a protective layer, researchers studied the decomposition behaviour of EVA nanocomposite using nanofillers. According to Hull *et al.* [64], incorporation of clay reduced the rate of decomposition significantly. Thermal degradation of EVA occurred in two stages; in the first stage acetic acid is lost and in the second crosslinking takes place. There is significant improvement in flame retardancy, even though clay is not completely dispersed.

Rahul *et al.* [65] studied the shear and extensional rheology of EVA – layered silicate nanocomposites. Nanocomposites of EVA with 28 wt. % vinyl acetate content (EVA28) was prepared by melt intercalation with different loadings of organically modified bentonite clay. The microstructure and morphology of the nanocomposites were examined by X-ray diffraction (XRD) and transmission electron microscopy (TEM). XRD and TEM indicated that EVA28 nanocomposites had predominantly exfoliated morphologies. The dynamic and

steady shear rheological properties of the nanocomposites showed remarkable differences in comparison to that of pure EVA28 copolymer. Linear viscoelastic parameters were enhanced at all frequencies investigated, and indicated the presence of a percolated network structure. Steady shear measurements revealed that the elasticity of EVA28 nanocomposites were dependent on the silicate loading at high shear stresses. Uniaxial extensional viscosities were found to increase with silicate loading, and in general exhibited strain hardening behaviour. Beyond a critical strain, nanocomposite extensional viscosities were almost identical with that of the unfilled EVA28, suggesting that at high strains, silicates have little effect on the extensional viscosities.

Extrusion molding of both polymer-layered silicate nanocomposites and microcomposites based on the EVA copolymer with either 12 wt. % (EVA12) or 19 wt. % (EVA19) vinyl acetate content was examined by Zanetti *et al.* [66]. The study has demonstrated that the creation of nanocomposites by extrusion of EVA depends on both the type of silicate and the type of silicate modification. During thermal degradation, their deacylation is accelerated and may occur at temperatures lower than those for the pure polymer or an EVA microcomposite due to catalysis by the strongly acid sites created by thermal decomposition of the silicate modifier. These sites are active when there is an intimate contact between the polymer and the silicate. A slowing down of the volatilisation of the deacylated polymer in nitrogen was observed, due to the effect of the silicate layers in the polymer matrix. In air, the nanocomposite presented a significant delay of weight loss that may be derived from the barrier effect due to diffusion of both the volatile thermo-oxidation products to the gas phase and oxygen from the gas phase to the polymer.

Malunka *et al.* [67] prepared and studied the properties of EVA-sisal fibre composites. The results showed that polymer-fibre grafting occurred in all the samples, whether prepared in the absence or presence of DCP. It was found out that an increase in sisal content caused a decrease in crystallinity and lamellar thickness. The composite stiffness was increased by the incorporation of sisal in the matrix. The influence of crosslinking depended on the amount of sisal fibre used. For 0 and 10 % sisal content the tensile modulus decreased with increasing DCP content. For 20 and 30 % sisal, the tensile modulus increased with increasing DCP content due to grafting between the polymer matrix and the filler. Elongation at break increased in the presence of DCP and decreased in the presence of sisal. Stress at break was negatively affected by the addition of DCP, while more that 10 % sisal fibre had a positive effect on stress at break.

2.6 Ethylene-glycidyl methacrylate copolymer (EGMA)

As mentioned in the previous pages, the problem of compatibility between the matrix and the filler, experienced due to the difference in their polarity, can be overcome by the addition of comptatibilizers. Compatibilizers such as silane, maleic anhydride grafted polypropylene (MAPP), dicumyl peroxide (DCP), etc have been previously used [67].

Ethylene-glycidyl methacrylate copolymer (EGMA) was investigated by Chiou *et al.* [68] as a reactive compatibilizer for immiscible and incompatible blends of polypropylene (PP) and a liquid crystalline polymer (LCP). The epoxy functional groups of the EGMA co-polymer can react with the carboxylic acid and/or hydroxyl end-groups of the liquid co-polyester. The *in situ-formed* EGMA-g-LCP co-polymer tended to reside along the interface of the PP-LCP and reduced the interfacial tension during melt processing. The compatibilized PP/LCP blends showed finer dispersed LCP domains, and tended to shift the LCP fibrous structure near the skin region of the uncompatibilized blends into the droplet domains. The PP crystallinity in the compatibilized PP/LCP blends was lower than that of the corresponding uncompatibilized blends, due to interference in the PP crystallization by the *in situ-formed* EGMA-g-LCP copolymers. The lower PP crystallinity of the compatibilized blends was reflected in a substantial reduction in stiffness (in terms of the tensile modulus). However, the improved adhesion of the compatibilized blends resulted in an improvement in the toughness (interims of the tensile elongation and impact strength).

The paper by Yordanov and Minkova [69] presents differential scanning calorimetry and electron microscopy of the fractionated crystallization and polydispersity of the dispersed PA6 phase in compatibilized LDPE/PA6 75/25 w/w blends. The compatibilizers used were (i) acrylic acid functionalized polyethylene (EAA), (ii) ethylene–glycidyl methacrylate copolymer (EGMA), and (iii) polystyrene–poly(ethylene–butylene)–polystyrene triblock copolymer (SEBS-g-MA). It was reported that the compatibilizer SEBS-g-MA had the strongest reduction effect on the size of the PA-6 droplets. Its implementation provided the best fractionated crystallization. Fractionated crystallization was not observed for the blend compatibilized with EGMA. The results show that the degree of compatibilization could be evaluated qualitatively by the progress of the fractional crystallization. Thus, the three compatibilizers were rated according to their effectiveness as follows: SEBSg-MA > EAA > EGMA. The measurement of the micro-hardness of the compatibilized blends confirmed that the compatibilizing activity of SEBS-g-MA and EAA was stronger than that of EGMA.

Thermoplastic elastomers containing poly(ethylene terephthalate) (PET) in 50 wt.%, compatibilizer (glycidyl methacrylate grafted rubber or glycidyl methacrylate containing co-polymer) in 30 wt.%, and various rubbers (20 wt.%) were produced by melt blending with and without dynamic curing (dicumyl peroxide initiated), and were studied by Papke and Karger-Kocsis [70]. The tensile testing and dynamic mechanical thermal properties (DMTA) of the systems, along with their phase morphology (SEM), were determined. It was found that the blend compatibility with PET was strongly improved when a high acrylonitrile-containing nitrile rubber (NBR) and an ethylene-glycidyl methacrylate copolymer (EGMA) or a GMA grafted ethylene/propylene rubber (EPR-g-GMA) were used as rubber and/or compatibilizer in the blend recipes. The effect of dynamic curing on the tensile and DMTA properties of the blends was negligible. Fractured surfaces showed the development of a co-continuous phase structure which was in accordance with observations from the DMTA spectra.

Polymer blends of poly(butylene terephthalate) (PBT) and polypropylene (PP) compatibilized by ethylene-co-glycidyl methacrylate (EG) copolymers were studied by Tsail and Chang [71]. The EG copolymer was demonstrated to be an effective *in situ* reactive compatibilizer for immiscible and incompatible PBT/PP blends. The epoxy groups of the EG copolymer could have a covalent reaction with the PBT terminal carboxylic acid and/or the terminal hydroxyl groups at their interface to form various EG-g-PBT copolymers. These *in situ* formed grafted co-polymers tended to reside along the interface to reduce the interfacial tension in the melt and result in finer domains. Again, the interfacial adhesion was increased and resulted in better mechanical properties. The presence of as little as 50 ppm catalyst was able to further improve the compatibility of the compatibilized blends.

Pluta *et al.* [72] studied the immiscible blends of recycled poly(ethylene terephthalate) (R-PET) and high-density polyethylene (R-PE), in weight compositions of 75:25 and 25:75, were compatibilized with selected compatibilizers: maleated styrene-ethylene/butylene-styrene block copolymer (SEBS-*g*-MA) and ethylene-glycidyl methacrylate copolymer (EGMA). The efficiency of compatibilization was investigated as a function of the compatibilizer content. The rheological properties, phase structure, thermal, and viscoelastic behaviour for compatibilized and binary blends were studied. The results, discussed in terms of phase morphology and interfacial adhesion among components, showed that the addition of the compatibilizer to R-PET-rich blends and R-PE-rich blends increased the melt viscosity of these systems above the level characteristic for the respective binary blends. The dispersion of the minor phase improved with increasing compatibilizer content, and the largest effects were

observed for blends compatibilized with EGMA. Calorimetric studies indicated that the presence of a compatibilizer had a slight affect on the crystallization behaviour of the blends.

2.7 References

1. http://www.epp.goodrich.com/why.shtml (25 July 2005)
2. Felix JM, Gatenholm P, *J. Appl. Polym. Sci.*, 42 (1991) 609
3. Bataille P, Richard L, Sapieha S, *Polym.Comp.*, 10 (1989)103
4. http://hrst.mit.edu/hrs/materials/public/composites/Composites_Overview.htm (28 July 2005)
5. http://www.machinedesign.com/BDE/materials/bdemat3/bdemat3_1.htm (28 July 2005)
6. http://www.hexcel.com/Products/Fabrics/Fiberglass (2 August 2005)
7. http://www.compositesone.com/basics.html (2 August 2005)
8. http://www.chem.wisc.edu/~newtrad/CurrRef/BDGTopic/BDGtext/html (2 September 2005)
9. http://www.teijin-aramid.com/ENG/aramid_fiber.htm (2 September 2005)
10 http://www.teijin-aramid.com/ENG/aramid_fiber.htm (2 September 2005)
11. http://www.machinedesign.com/BDE/materials/bdemat3/bdemat3_6.html (10 September 2005)
12. Amash A, Zugenmaier P, *Polym. Bull.*, 40 (1998) 25
13. Selke SE, Wichman I, *Composites A*, 35 (2004) 321
14. Li B, He J, *Polym. Degrad. Stabil.*, 83 (2004) 241
15. Joseph PV, Rabello MS, Mattoso LHC, Joseph K, Thomas S, *Comp. Sci. Technol.,* 62 (10-12) (2002)1357
16. Woodhams RT, Thomas G, Rogers DK, *Polym. Eng. Sci.*, 24 (1984) 1160
17. Alvarez VA, Vazquez A, *Polym. Degrad. Stabil.,* 84 (2004) 13
18. Craven JP, Cripps R, Viney C, *Composites A,* 31 (2000) 653
19. Zhang Y-Q, *Biotechnol. Adv.,* 20 (2002) 91
20. Joyly C, Kofman M, Gauthier R, *J. Macromol. Sci A*, 33(12) (1996) 1981
21. Zadorecki P, Michell AJ, *Polym. Comp.*, 10 (1989) 69
22. Beshay B, Hoa SV, *Sci. Eng. Comp. Mater.,* 2 (1992) 86
23. Ismail H, Jaffri RM, *Polym. Test.*, 18 (1999) 381

24. Lee SM, Cho D, Park WH, Lee SG, Han SO, Drzal LT, *Comp. Sci. Technol.*, 65 (2005) 647
25. Bledzki AK, Gassan J, *Prog. Polym. Sci.*, 24 (1999) 221
26. Ismail H, Rozman HD, Jaffri RM, Mohd Ishak ZD, *Eur. Polym. J.*, 33(10-12) (1997) 1627
27. Zaini MJ, Fuad MYA, Ismail Z, Mansor MS, Mustaf J, *Polym. Int.*, 40 (1996) 51
28. Kumar AP, Singh RP, Sarwade DB, *Mater. Chem. Phys.*, 92 (2005) 458
29. Aziz SH, Ansell MP, *Comp. Sci. Technol.*, 64 (2004) 1219
30. Baiardo M, Zini E, Scandola M, *Composites A*, 35 (2004) 703
31. Jacob M, Thomas S, Varughese K, *Comp. Sci. Technol.*, 64 (2004) 955
32. Brahmakumar M, Pavithran C, Pillai RM, *Comp. Sci. Technol.*, 65 (2005) 563
33. Gassan J, Gutowski VS, *Comp. Sci. Technol.*, 60 (2000) 2857
34 Sapieha S, Pupo JF, Schreiber HP, *J. Appl. Polym. Sci.*, 37(1) (1989) 233
35. Maldas D, Kokta BV, *Polym. Degrad. Stabil.*, 1 (1991) 9
36. Bisanda E, Ansell M, *J. Mater. Sci.*, 27 (1992) 1690
37. Sreekala M, Kumaran M, Thomas S, *J. Appl. Polym. Sci.*, 66 (1997) 821
38. Geethamma V, Joseph R, Thomas S, *J. Appl. Polym. Sci.*, 55 (1995) 583
39. Mwaikambo L, Ansell M, *J. Appl. Polym. Sci.*, 84(12) (2002) 2222
40. Franco PJH, Gonzalez AV, *Composites A*, 35 (2004) 339
41. Mohanty AK, Wibowo A, Misra M, Drzal LT, *Composites A*, 35 (2004) 363
42 Gassan J, Bledzki AK, *Comp. Sci. Technol.*, 59 (1999) 1303
43. Abu-Sharkh BF, Hamid H, *Polym. Degrad. Stabil.*, 85 (2004) 967
44. Georgopoulosa ST, Tarantili PA, Avgerinos E, Andreopoulos AG, Koukios AG, *Polym. Degrad. Stabil.*, 90 (2005) 303
45. Li TQ, Wolcott MP, *Composites A*, 35 (2004) 303
46. Ichazo MN, Albano C, Gonzalez J, Perera R, Candal MV, *Comp. Struct.*, 54 (2001) 201
47. Krzysik AM, Youngquist YA, *Int. J. Adhes. Adhes.*, 11(4) (1991) 235
48. Kuan CF, Kuan HC, Ma CM, Huang CM, *Composites A*, (2005) (in Press)
49. Maldas D, Kokta BV, Raj RG, Daneault C, *Polymer*, 29(7) (1988) 1255
50. Elvy SB, Dennis GR, Teck L, *J. Mater. Process. Technol.*, 48 (1995) 365
51. Spindler MW, Pateman R, Hills PR, *Composites*, 4(6) (1973) 246
52. Mubarak AK, Ali KMI, *Int. J. Rad. Appl. Instrum. C. Rad. Phys. Chem.*, 40(6) (1992) 421

53. Yildiz UC, Yildiz S, Gezer ED, *Biores.Technol.*, 96 (2005) 1003
54. Doh GH, Kang IA, Lee SY, Kong YT, Jeong CS, Lim BS, *Comp. Struct.*, 68 (2005) 225
55. Espert A, Vilaplana F, Karlsson S, *Composites A*, 35 (2004) 1267
56. Yang HS, Kim HJ, Park HJ, Lee BJ, Hwang TS, *Comp. Struct.*, 72 (2006) 429
57. Joseph PV, Rabello MS, Mattoso LHC, Joseph K, Thomas S, *Comp. Sci. Technol.*, 62(10-12) (2002) 1357
58. Stancato AC, Burke AK, Beraldo AL, *Cement and Concrete Comp.*, 27 (2005) 599
59. Gassan J, Gutowski VS, *Comp. Sci. Technol.*, 60 (2000) 857
60. S' olpan D, GuÈ ven O, *Rad. Phys. Chem.*, 54 (1999) 583
61. Albano C, Reyes J, Ichazo M, Gonzalez J, Chipara MI, *Polym. Degrad. Stabil.*, 73 (2001) 225
62. Czvikovszky T, *Rad. Phys. Chem.*, 47(3) (1996) 425
63. Zanetti M, Camino G, Mulhaupt R. *Polym. Degrad. Stab.*, 74(3) (2001) 413
64. Hull TR, Price D, Liu Y, Wills CL, Brady J, *Polym. Degrad. Stab.*, 82 (2003) 365
65. Rahul K. Gupta V, Pasanovic Z, Bhattacharya SN, *J. Non-Newt. Fluid Mech.*, 128 (2005) 116
66. Zanetti M, Camino,G, Thomann R, Mulhaupt R, *Polymer*, 42 (2001) 4501
67. Malunka ME, Luyt AS, Krump H, *J. Appl. Polym. Sci.*, 100(2) (2006) 1607
68. Chiou YP, Chiou KC, Chang FC, *Polymer*, 37(18) (1996) 4099
69. Yordanov C, Minkova L, *Eur. Polym. J.*, 4(3) (2005) 527
70. Papke N, Kocsis JK, *Polymer*, 42 (2001) 1109
71. Tsai CH, Chang FC, *J. Appl. Polym. Sci.*, 61 (1996) 321
72. Pluta M , Bartczak Z, Pawlak A, Galeski A, Pracella M, *J. Appl. Polym. Sci.*, 82 (2001) 1423

CHAPTER 3 (Experimental)

3.1 Materials

3.1.1 Ethylene vinyl acetate co-polymer (EVA)

EVA with 9 % vinyl acetate (VA) content, a density of 0.93 g cm^{-3}, melting point of 95°C, tensile strength of 19 MPa and 750 % elongation at break, was supplied by Plastamid, Elsies River, South Africa.

3.1.2 Ethylene-glycidyl methacrylate copolymer (EGMA)

EGMA was used as a compatibilizer. It has a density of 0.93 g cm^{-3}, a melting point of 93°C, tensile strength of 12 MPa, elongation at break of 440 %, and was supplied by Plastamid, Elsies River, South Africa.

3.1.3 Wood fibre (WF)

Pine wood fibre, or pine saw dust, was obtained from FBW Taurus, Phuthaditjhaba, South Africa. It was supplied as light orange coloured powder with density 1.5 $g.cm^{-3}$. The particle sizes of the wood fibre studied ranged form 0-600 μm.

3.2 Methods

3.2.1 Preparation of the composites

WF was sieved into three different particle size groups (0-150 μm, 151-300 μm, and 301-600 μm) by using laboratory test sieves with pore sizes 600, 300 and 150 μm. For comparison sake, unsieved wood fibre was also used in this study. Without any modification or pre-treatment, wood fibre was dried by placing it in an oven at a temperature of 120°C for 24 hours. EVA was used as received.

Table 3.1 Compositions of uncompatibilized and compatibilized composites

w/w EVA/EGMA-WF	EVA / g	EGMA / g	WF / g
100/0/0	36.80	0	0
95/0/5	35.01	0	2.97
85/0/15	31.32	0	8.91
75/0/25	27.62	0	14.85
65/0/35	23.92	0	20.79
55/0/45	20.25	0	26.73
5 % EGMA compatibilized			
90/5/5	33.15	1.81	2.97
80/5/15	29.46	1.81	8.91
70/5/25	25.78	1.81	14.85
60/5/35	22.09	1.81	20.79
50/5/45	18.42	1.81	26.73
95/5/0	35.01	1.81	0
10 % EGMA compatibilized			
85/10/5	31.30	3.61	2.97
75/10/15	27.62	3.61	8.91
65/10/25	23.91	3.61	14.85
55/10/35	20.25	3.61	20.79
45/10/45	16.46	3.61	26.73
90/10/0	33.14	3.61	0

The composites were prepared to give a total mass of ± 37 g after addition of EVA, wood fibre and EGMA (in the case of compatibilized composites). Compositions of the composites are represented in Table 3.1. Mixing of the samples was done in a 55 cm^3 Brabender mixer at a temperature of 130°C and a mixing speed of 30 min^{-1} for 15 min. The samples were then melt pressed at 120°C and 100 bar for 5 minutes. Pressed composites were allowed to cool for 10 minutes before handling in order to avoid air penetration.

3.2.2 Differential scanning calorimetry (DSC)

The melting and crystallization behaviour of the EVA-WF composites was investigated by using a Perkin-Elmer DSC 7 thermal analyzer under nitrogen flow. The instrument was calibrated by using the onset temperature of melting of indium and zinc standards, and the melting enthalpy of indium. Composites samples of mass ± 7 mg were used. The program, applied to all samples was, heating from 25 to 150°C at 20°C min^{-1} (holding the sample for 1 minute at 25°C before heating), followed by cooling to 25°C at the same rate. The sample was then reheated under the same conditions. The onset and peak temperatures of melting and crystallization, as well as the melting and crystallization enthalpies, were determined from the second heating and cooling curves, where ΔH_m, the melting enthalpy of the sample, was calculated from the main melting peak.

3.3.3 Thermogravimetry analysis (TGA)

Thermogravimetric analyses were carried out on a Pelkin-Elmer TGA 7 thermogravimetric analyzer. Polymer samples of mass ± 7 mg were heated from 25 to 600 °C at 20 °C min^{-1} under flowing nitrogen. The sample was held at 25 °C for 1 minute before heating.

3.3.4 Tensile testing

Tensile tests of EVA-WF composites were performed under ambient conditions on a Hounstifield H5KS tensile tester at a cross-head speed of 50 mm min^{-1}. Tensile test specimens were prepared using a dumbbell shaped hollow die punch. The sample measurements are illustrated below:

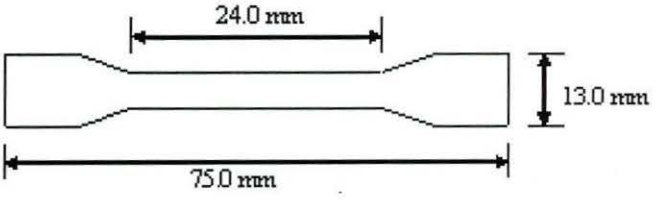

Eight samples per composite were used for each analysis. A statistics computer programme was used to eliminate out-of-range values, and the mean of the accepted values was reported. The tensile strength, Young's modulus, and elongation at break values were obtained from this testing.

3.2.5 Polarized optical microscopy (POR)

The morphology and number of voids in the EVA-WF composite were examined by means of a polarized optical microscope. A very thin film of the sample was placed on glass slides and polarized optical photos were taken at 100x and 400x magnifications, using a CETI polarized optical microscope made in Belgium. The photos were taken with a Ceist DCM digital camera.

3.2.6 Water permeability

The samples were cut into 30 x 20 cm^3 sheets. First, the samples were dried at 70°C overnight to reach a constant weight. The samples were then immersed into a static distilled water bath at room temperature to observe the absorption of water. Mass uptake of the samples was measured periodically by removing them from the water bath. The samples were wiped with tissue paper to remove the surface water, and weighed. Water uptake of EVA-WF composites at time t was calculated using the equation below:

$$\% \text{ Uptake} = \frac{M_t - M_o}{M_o} \times 100$$

Where M_t is the mass of the sample at time t and M_o is the mass of the sample at t = 0. Samples were immersed in water for 72 hours and water uptake measurements were recorded at 24 hour intervals. The water uptake was plotted as a function of time.

3.2.7 Infrared spectroscopy (IR)

IR analyses were done on a Nicolet Magna 550 FTIR spectrophotometer. Samples were prepared by mixing the composite (± 3 mg) with dry KBr (± 300 mg). The mixture was pressed in a die under high pressure to prepare a pellet. The pellet was scanned in the region of 400-4000 cm^{-1} at a resolution of 4 cm^{-1}.

3.2.8 Permeability

Permeability measurements were done using a Sierra Smart-Trak mass flow meter in a setup illustrated in Figure 3.1. Oxygen was used for the determination of the gas permeability of the composites. Oxygen (from **1**) was fed to the system. The desired amount of oxygen was adjusted by using a rotameter (**2**) and allowed to pass through the sample placed in the

sample holder chamber (**3**). The amount of oxygen that passed through the sample was recorded by the digital flow meter (**4**). Different oxygen flow rates were used to construct the permeability graphs.

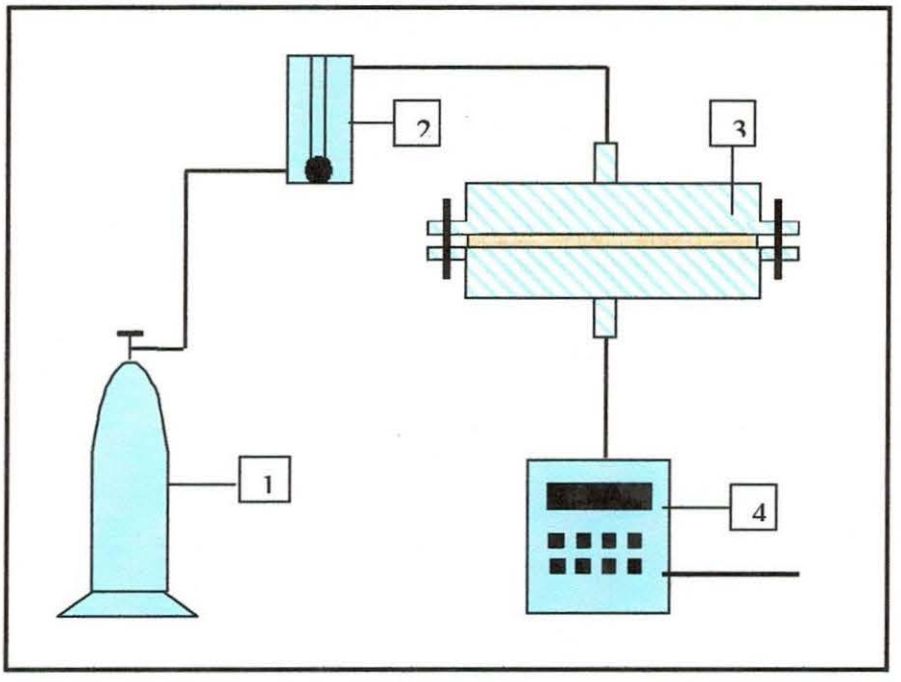

Figure 3.1 **Setup for permeability measurements (1 - O_2 gas bottle, 2-rotameter, 3 - sample holder chamber, 4-digital mass flow meter connected to a power socket)**

CHAPTER 4 (Results and discussion)

4.1 Polarized optical microscopy (POM)

The effect of a compatibilizer on the EVA-WF composites can be compared by looking at the photos vertically arranged in Figure 4.1. The degree of dispersion of the wood fibre in the matrix in the 95/0/5 w/w EVA/EGMA-WF (0-150 μm) composite (without compatibilizer) is restricted. The composite does not show homogeneity. WF particles appear to be on top rather than inside the matrix. This is due to the incompatibility between WF and EVA. Although EVA contains hydrophilic acetate groups that can bind to the hydrophilic cellulosic fibres, compatibility is not fully favourable because of the EVA polymer backbone which is hydrophobic and thus repels WF.

After addition of 5 % compatibilizer in the compounding step, the 90/5/5 w/w EVA/EGMA-WF (0-150 μm) composite shows a better dispersion of the wood fibre particles in the matrix. There is a better interaction between the polymer matrix and the wood fibre particles. The reason for this is that EGMA reacts with WF decreasing its surface energy and its hydrophylicity. This EGMA-WF grafted product interacts with EVA *via* the OH group, forming a hydrogen bond as the proposed mechanism suggests. EGMA also provides carbonyl group that may form a hydrogen bond with WF, which will further improve the interaction.

When 10 % of compatibilizer was used in the 85/10/5 w/w EVA/EGMA-WF (0-150 μm) composite, compatibility between the WF particles and the polymer is greatly improved. The wood fibre-polymer adhesion is better, and the surface of the composite is smooth in comparison to the uncompatibilized and 5 % compatibilized composites. This shows that the addition of more compatibilizer creates more active groups that can interact with WF. The same trend was observed when 301-600 μm particles were used as shown in Figure 4.1.

When 45 % of 0-150 and 301-600 μm wood fibre particles were used (Figure 4.2) for the 55/0/45 w/w EVA/EGMA-WF uncompatibilized composites, it can be seen that the difference in the filler and the matrix phases is not so pronounced. This is because of the co-continuous phase that is formed and the less clearly distinguishable difference between the filler and the matrix. The difference can be clearly seen when compatibilizer is added. The addition of 5 % and 10 % compatibilizer in respectively 0-150 μm – 50/5/45 and 0-150 μm – 45/10/45 w/w EVA/EGMA-WF composites show a better dispersion of the WF particles in the matrix.

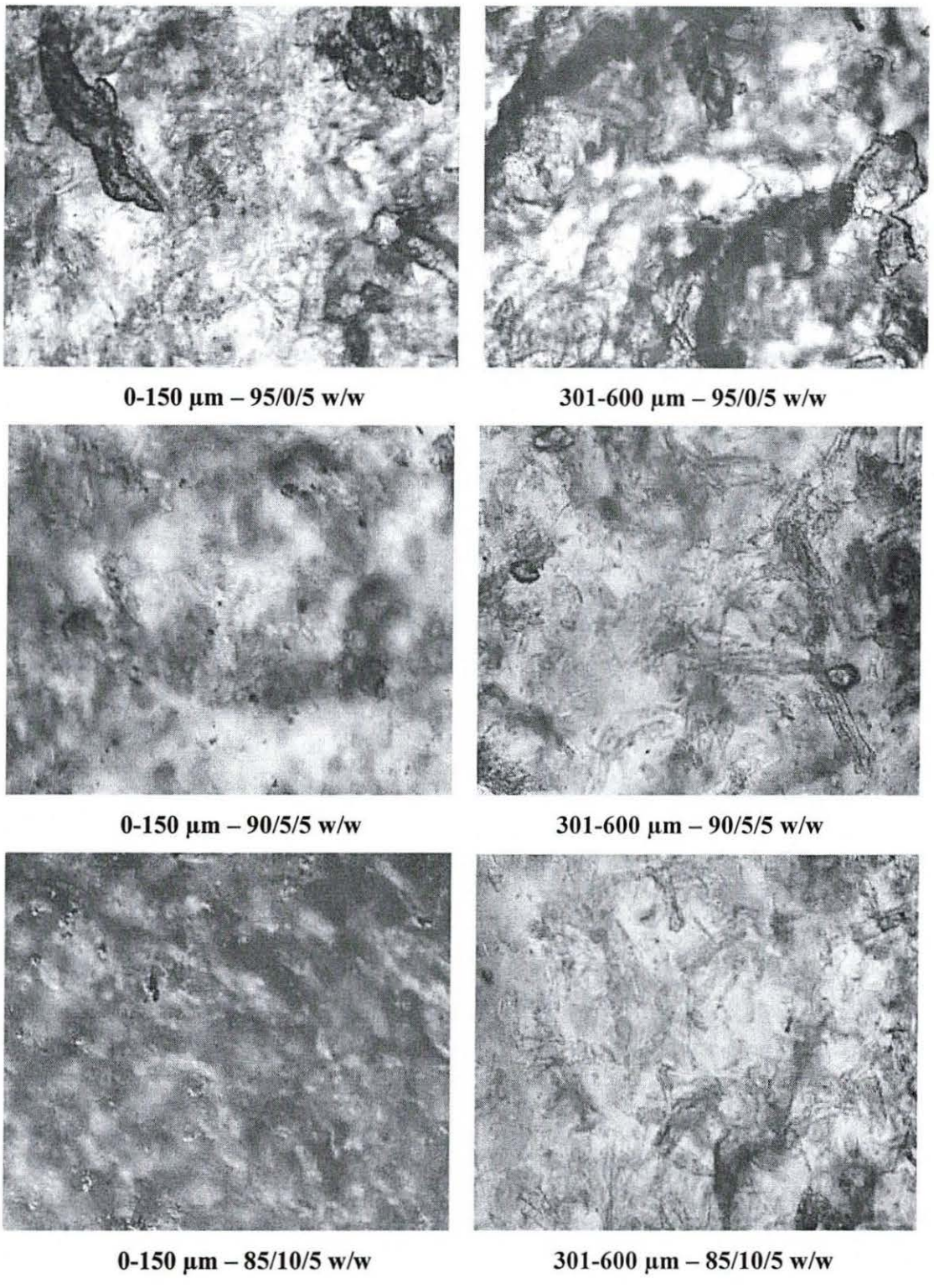

0-150 μm – 95/0/5 w/w

301-600 μm – 95/0/5 w/w

0-150 μm – 90/5/5 w/w

301-600 μm – 90/5/5 w/w

0-150 μm – 85/10/5 w/w

301-600 μm – 85/10/5 w/w

Figure 4.1 **POM micrographs (100x magnification) of EVA/EGMA-WF composites when 5 % of 0-150 μm and 301-600 μm WF particles are compared**

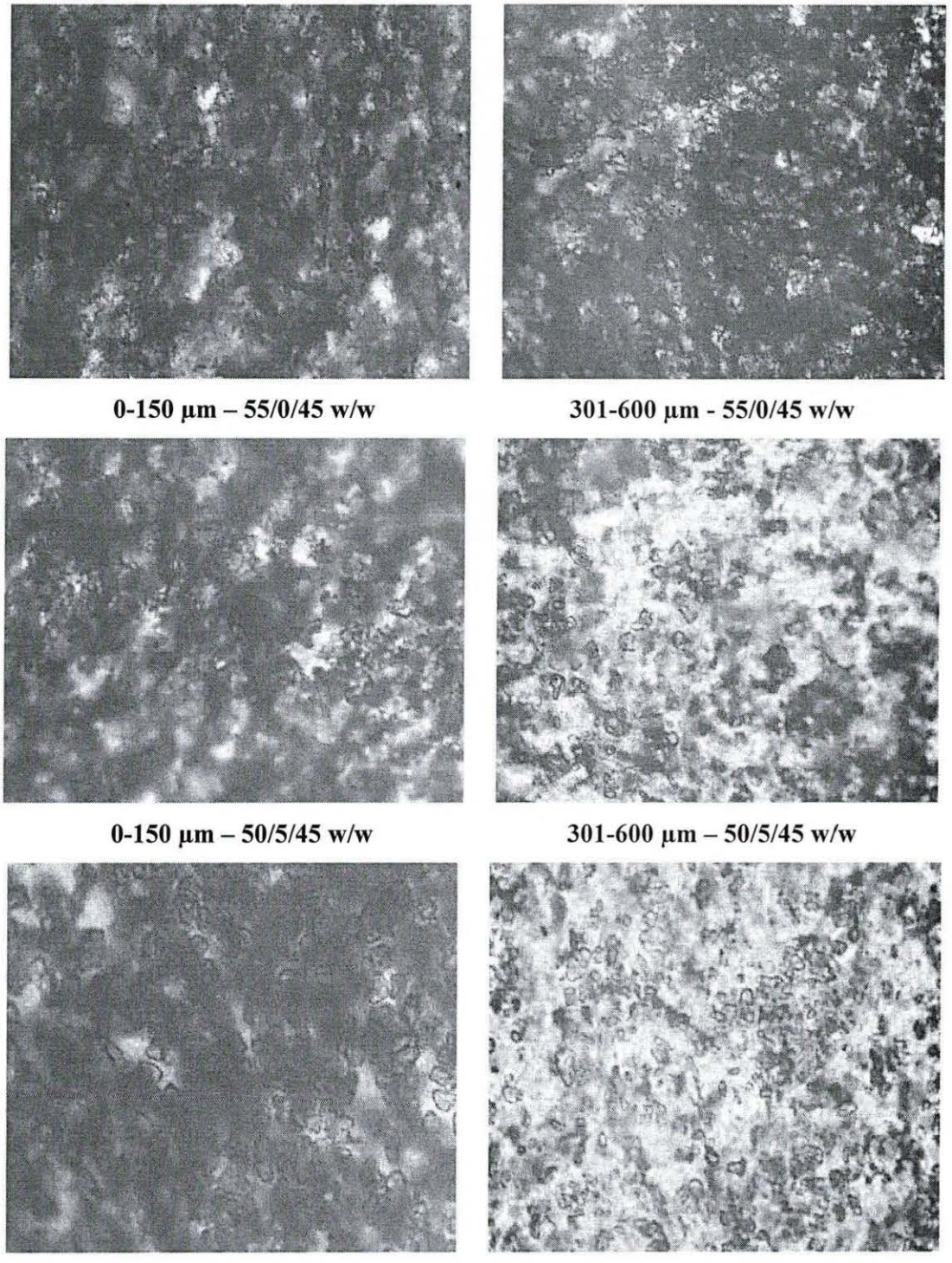

0-150 μm – 55/0/45 w/w **301-600 μm - 55/0/45 w/w**

0-150 μm – 50/5/45 w/w **301-600 μm – 50/5/45 w/w**

0-150 μm – 45/10/45 w/w **301-600 μm – 45/10/45 w/w**

Figure 4.2 **POM micrographs (100x magnification) of EVA/EGMA-WF composites when 45% of 0-150 μm and 301-600 μm WF particles are compared**

The roughness of the composites is decreased and the interaction between the wood fibre and EVA is greatly improved. The 10 % compatibilized composite shows better results than the 5 % compatibilized composite. This shows that even at higher filler loading EGMA is still able to act as a compatibilizer for EVA-WF composites as shown in Figure 4.2.

Salemane and Luyt [3] studied PP-WF composites and reported that the introduction of MAPP into the composite material causes the sample to be even smoother, so smooth that the matrix and filler in their case were indistinguishable in SEM photos.

Effect of particle size on the morphology of the EVA-WF composites can be seen by comparing the photos left and right in Figure 4.1. When 5 % of 0-150 μm and 301-600 μm wood fibre particles are used in the 95/0/5 w/w EVA/EGMA-WF composite, it is seen that there is better compatibility between the filler and the matrix when smaller WF particles are used. A better bonding quality between the two phases is experienced when smaller (0-150 μm) wood fibre particles are used compared to the larger (301-600 μm) particles. Salemane and Luyt [3] reported that the difference in wood fibre particle size has an effect on the morphological structures of the composites. For composites with smaller WF particles (< 38 μm), the surface is smoother than for samples containing larger particles (301-600 μm).

Addition of compatibilizer in the 90/5/5 w/w EVA/EGMA-WF (0-150 μm and 301-600 μm) composites improves adhesion between the two phases in comparison to the uncompatibilized composites, but it is still evident that the 0-150 μm particles interact better than 301-600 μm particles. The same trend is confirmed in the 10 % compatibilized composites.

4.2 Infrared spectroscopy (IR)

4.2.1 Uncompatibilized composites

Figure 4.4 shows the infra red spectra of pure EVA and EVA-WF composites. The pure EVA matrix shows absorbance peaks around 2850 and 2920 cm^{-1} that are associated with C-H asymmetric stretching. The peak representing the vibration of the -C=O ester of the carboxyl group appears at 1750 cm^{-1}.

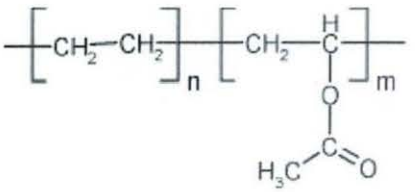

Figure 4.3 Structural representation of EVA

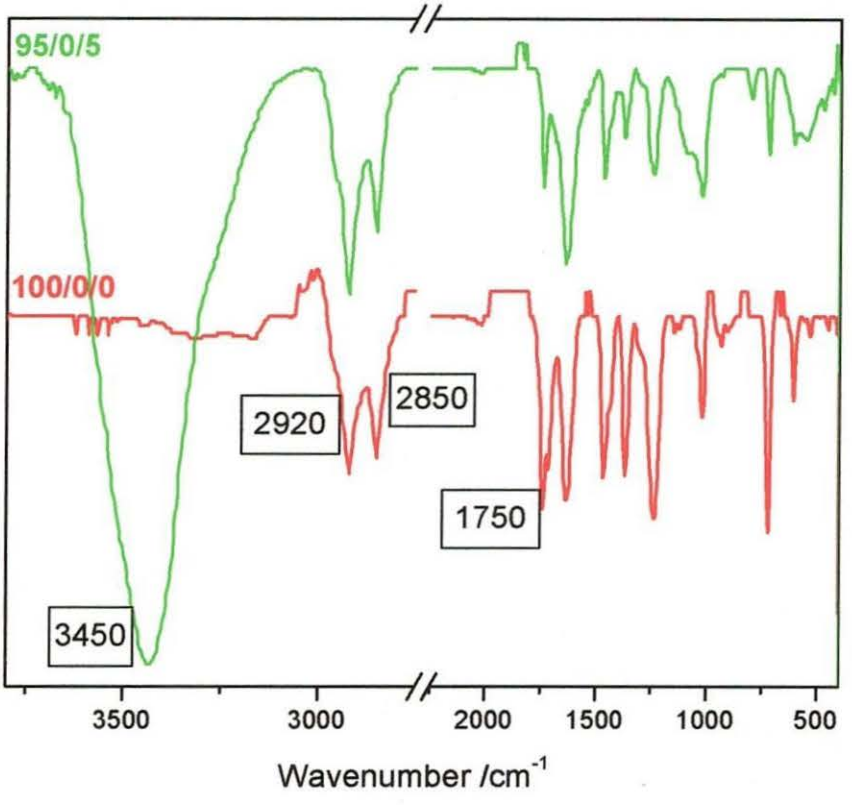

Figure 4.4 IR spectra of pure EVA and an EVA-WF composite

When 5 % WF is added to pure EVA with no compatibilizer, a large peak at 3450 cm^{-1} is seen, indicating the presence of OH groups. The other peaks that were seen in pure EVA are still present. The relative intensities of the peaks around 2850 and 2920 cm^{-1} increase, which indicates that the WF consists of C-H groups. The presence of the peak at 1750 cm^{-1} indicates that the –C=O is still maintained in the new composite as the proposed mechanism (Figure 4.5) suggests.

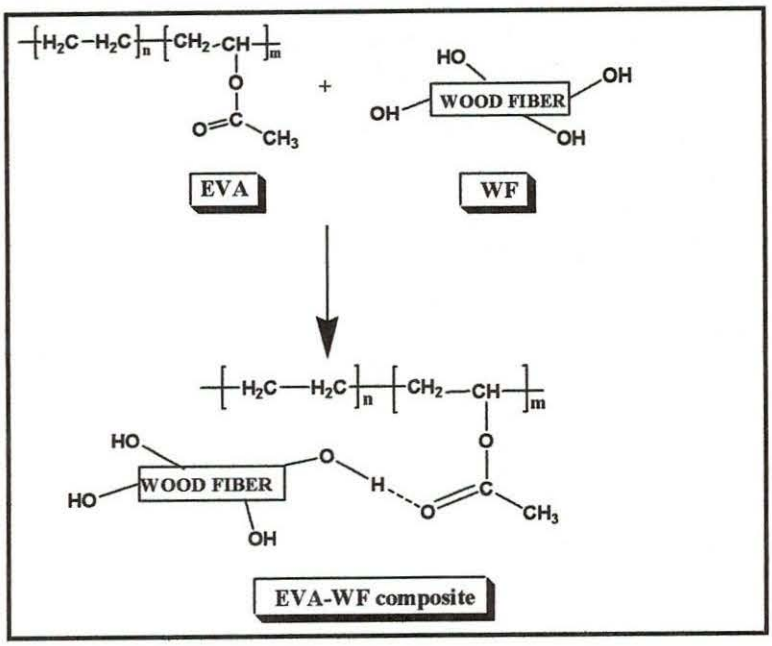

Figure 4.5 **Possible mechanism for EVA-WF interaction in the composite**

4.2.2 Compatibilized composites

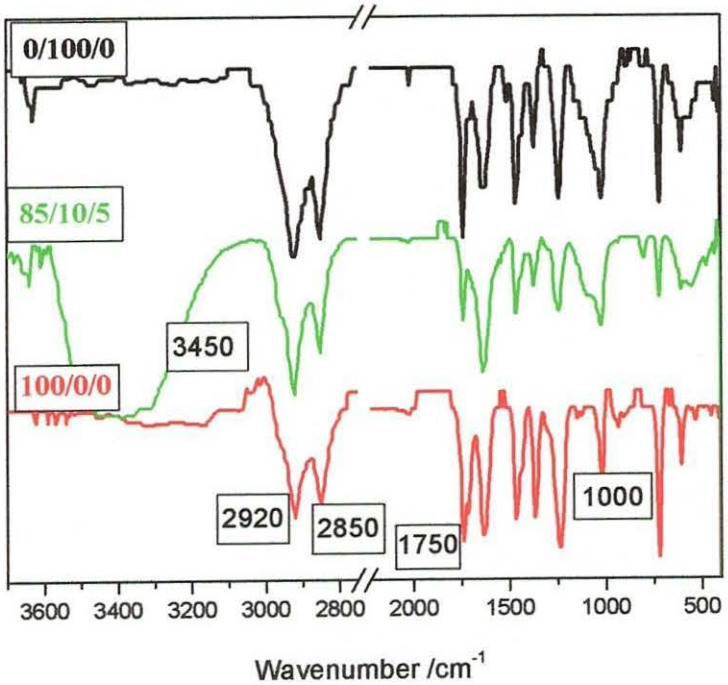

Figure 4.6 **IR spectra of pure EVA, pure EGMA and an EVA/EGMA-WF composite**

For EGMA, peaks are seen at 2850 and 2920 cm^{-1}, indicating C-H vibrations (Figure 4.6). Another pronounced peak at 1750 cm^{-1} for the –C=O and a very important peak at 1000 cm^{-1} representing an epoxy group are seen.

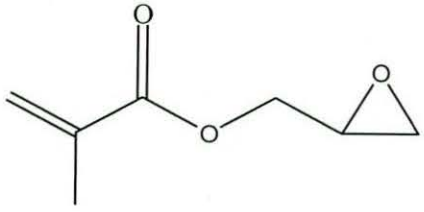

Figure 4.7 Structural representation of EGMA

The 85/10/5 w/w EVA/EGMA-WF composite shows a broad peak around 3450 cm^{-1} indicating the presence of OH groups. The characteristics peaks of EGMA and EVA are still seen in this composite. The peak at 1750 cm^{-1} is still visible, which shows that the final product contains of -C=O functional groups. The intensity of the peak at 1000 cm^{-1}, representing the epoxy group, has decreased in size compared to that of pure EGMA. This indicates that there is a possibility of a reaction between the epoxy group in EGMA and the OH group of wood fibre. Such a reaction is well known and extensively reported [1-4]

Chiou *et al* [1] investigated *in situ* compatibilized PP/liquid crystalline polymer blends (LCP), and reported that the epoxy functional group of the EGMA copolymer can react with the carboxylic acid and/or the hydroxyl end groups of the LCP.

Heino *et al* [2] used an ethylene-ethyl acrylate-glycidyl methacrylate (E-EA-GMA) terpolymer as a reactive compatibilizer for PP/LCP blends, resulting in improved impact strength, and they suggested that the reaction/interaction between PP and LCP was due to the epoxy group of (E-EA-GMA). Chiou and Chang [3] reported styrene-glycidyl methacrylate (SGMA) as an effective reactive compatibilizer for the blend polystyrene (PS)/LCP. The epoxy functional group in the SGMA reacts with the carboxylic acid or hydroxyl end groups during melt processing. Miller *et al* [4] used PP functionalized acrylic acid (PP-AA) as a compatibilizer for PP/LCP and, based on the observed compatibilization effect, concluded that there appears to be an interaction between the polar acrylic acid groups and the LCP rather than a true covalent bond.

It should be noted that the fact that the peak that represents the most reactive part of EGMA, which is the epoxy group, is found in the fingerprint region and at the same time EVA has the same characteristic peak. It therefore is challenging to conclude that indeed the reaction is taking place *via* the epoxy group. The fact that there is a decrease in this peak

intensity indicates there is a possible reaction taking place between EGMA and WF. The peak at 1750 cm^{-1} does not disappear completely because the resulting composite still contains of the -C=O functional group. The proposed mechanism (Figure 4.8) suggests the possibility of this reaction/interaction taking place.

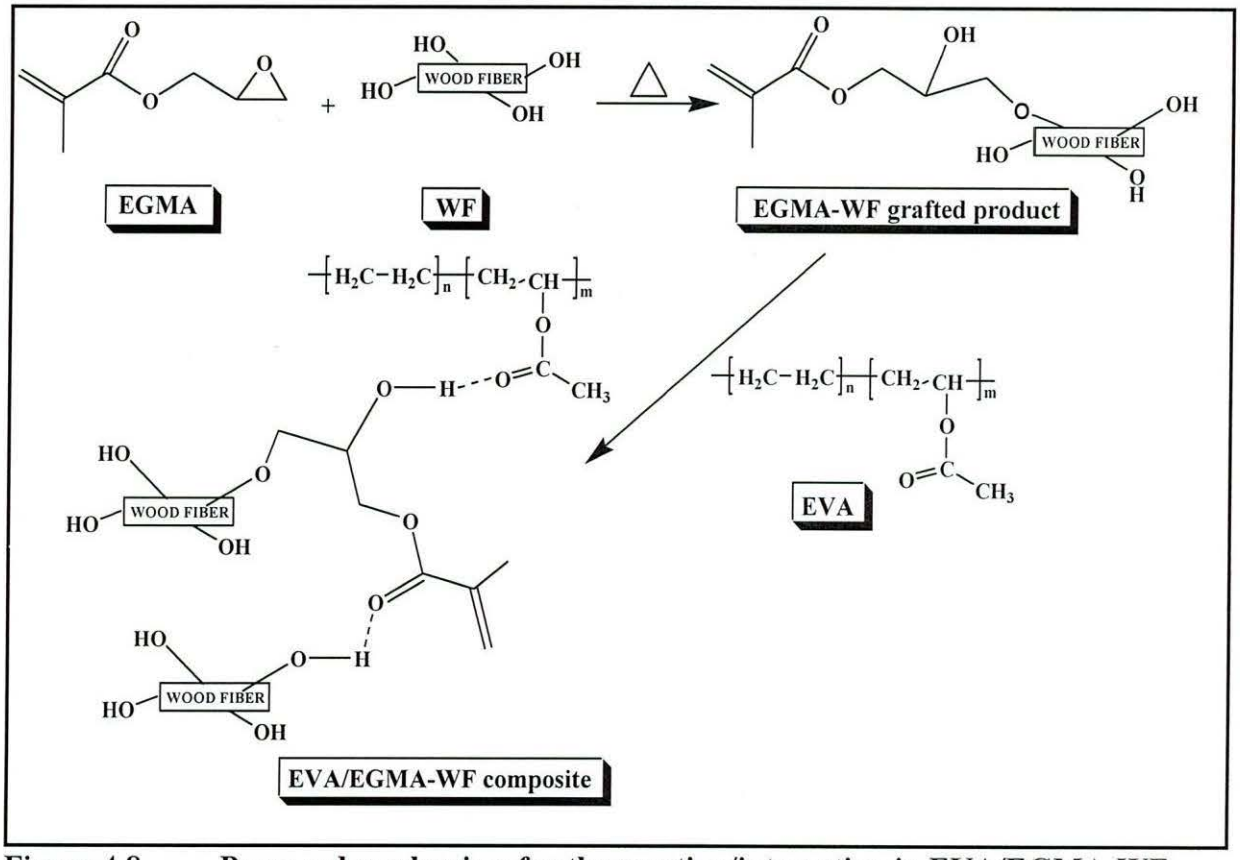

Figure 4.8 Proposed mechanism for the reaction/interaction in EVA/EGMA-WF composites

Chiou *et al* [1, 3] used infra red analysis to monitor qualitatively the reaction between EGMA and the end groups of LCP. The peak at 988 cm^{-1}, which is assigned to the epoxy ring, is used for this purpose. It was reported that the sizes of the epoxy peaks of the blends are significantly smaller than that of the pure EGMA, which is an indication of the reaction of the epoxy group. It is important to note that the epoxy group in EGMA prefers to react with a carboxyl group rather than with an aliphatic –OH group, due to the difference in acidity. The proposed mechanism, however, suggests that EGMA will react with the –OH on WF because there is no carboxyl group available in these composites.

Comparing the effect of compatibilizer, it is clear from Figure 4.6 that for compatibilized composites, the OH peak intensity at 3450 cm^{-1} is greatly reduced compared to

the uncompatibilized OH peak in Figure 4.4. This is not only because of the EGMA-WF reaction as the mechanism suggests, but also because of another competitive reaction, epoxy hydrolysis, which is likely to occur to a certain extent, because epoxy-containing compounds or polymers are known to act as acid or water scavengers in many condensation–type polymers in the melt, thus reducing the number of OH groups in the composite [1].

4.3 Differential scanning calorimetry (DSC)

4.3.1 Uncompatibilized composites

The effects of wood fibre content on uncompatibilized composites are shown in Figures 4.9 and 4.10. The composites were synthesized using 0-150 μm and 151-300 μm wood fibre particles. The curves show a single endothermic peak around 95 °C, the temperature at which EVA melts. The melting temperature was not influenced, within experimental error, by the wood fibre content in the samples. No increase or decrease in melting temperature indicates that WF has little influence on the lamellar thickness of EVA.

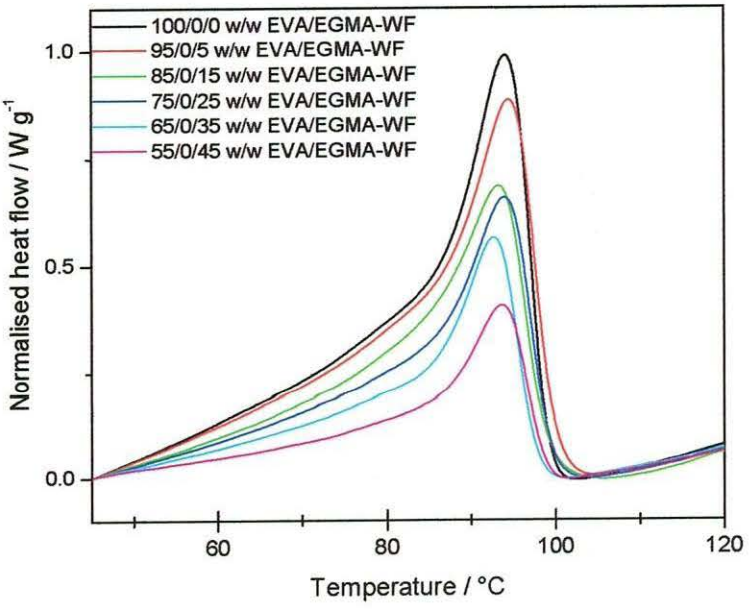

Figure 4.9 DSC heating curves of pure EVA and uncompatibilized EVA-WF (0-150 μm) composites at different WF ratios

Pure EVA has the highest melting enthalpy (ΔH_m), and generally, there is a decrease in melting enthalpies as more wood fibre is present in the samples. This is because wood fibre does not melt, and the EVA content decreases with increasing WF content. The experimental melting enthalpy of pure EVA is 24.9 Jg^{-1}, and it decreases to 23.3 Jg^{-1} when 5 % of wood fibre is present. The presence of 15, 25, 35 and 45 % of wood fibre further reduces of the enthalpy to 20.6, 18.4, 16.2, and 13.4 Jg^{-1} respectively (Table 4.1). The theoretically expected enthalpy values (taking into account the melting enthalpy of pure EVA and the original EVA/WF mixing ratios) are not very different from the experimental values (Table 4.1). The EVA part of the composite still crystallizes fairly normally, even though it is clear that the crystals are not as perfect as before as seen by the broadening of the peaks for samples containing more wood fibre (Figure 4.8 and 4.9). The formation of perfect crystals is hindered by the presence of the wood fibre particles that locate themselves along EVA as shown by the POM micrographs (Figure 4.1).

Table 4.1 Summary of DSC melting data for uncompatibilized EVA-WF composites

EVA/EGMA-WF (w/w)	$T_{o,m}$ / °C	$T_{p.m}$ / °C	ΔH_m^{obs} / J g^{-1}	ΔH_m^{exp} / J g^{-1}
100/0/0	85.7	94.7	24.9	
0-150 µm				
95/0/5	86.2	95.1	23.3	23.7
85/0/15	83.4	93.7	20.6	21.2
75/0/25	84.8	94.4	18.4	18.7
65/0/35	84.5	93.1	16.2	16.2
55/0/45	85.7	94.1	13.4	13.1
151-300 µm				
95/0/5	83.1	93.7	22.2	23.7
85/0/15	84.3	93.7	20.3	21.2
75/0/25	85.1	93.7	16.5	18.7
65/0/35	79.5	92.5	14.5	16.2
55/0/45	84.2	92.7	12.9	13.1

$T_{o,m}$- onset temp of melting, $T_{p.m}$-peak temp of melting ΔH_m^{obs} – experimentally observed melting enthalpy, ΔH_m^{exp} - theoretical expected melting enthalpy

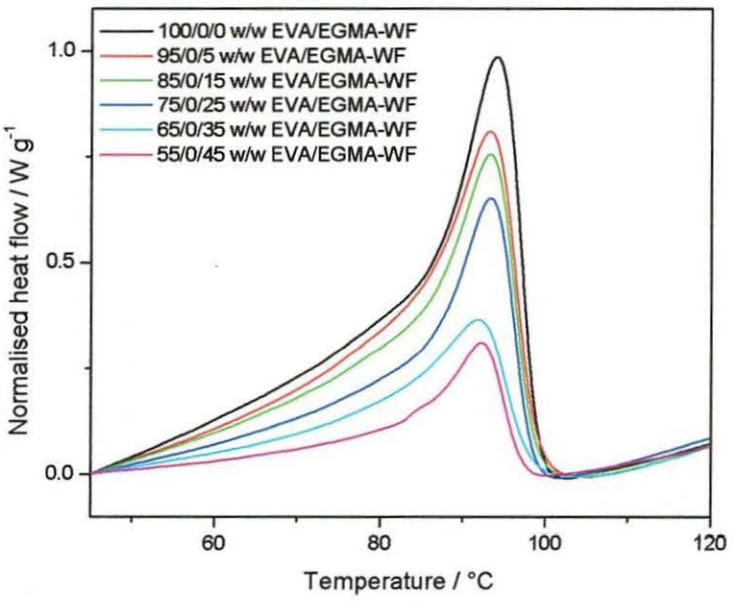

Figure 4.10 **DSC heating curves of pure EVA and uncompatibilized EVA-WF (151-300 μm) composites at different WF ratios**

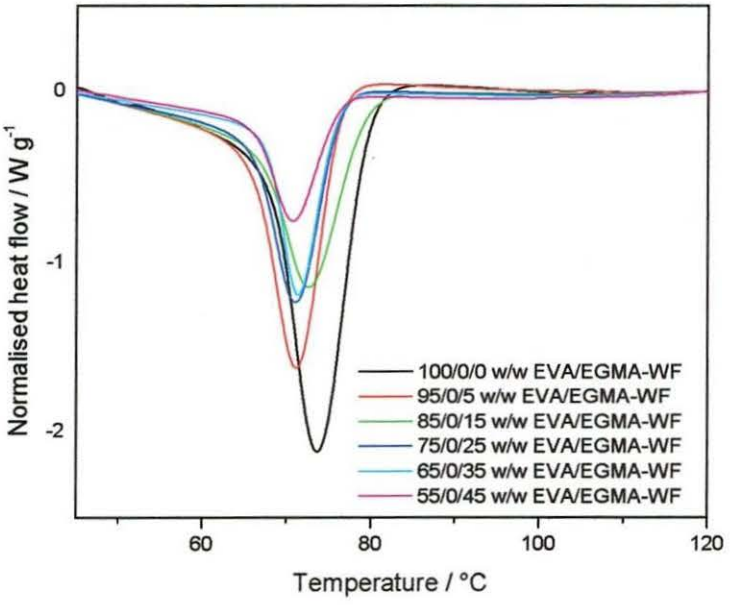

Figure 4.11 **DSC cooling curves of pure EVA and uncompatibilized EVA-WF (0-150 μm) composites at different WF ratios**

The DSC cooling curves of the uncompatibilized composites containing 0-150 μm WF particles are shown in Figure 4.11. Pure EVA crystallizes at a higher temperature than all the composites. The presence of 5 % wood fibre causes EVA to crystallize at a lower temperature, but the presence of more wood fibre shows a less significant difference in the crystallization temperature. WF will influence EVA crystallization in two ways. On the one hand it will restrict EVA chain mobility, and on the other hand it may act as nucleation points for EVA crystallization. A balance between these two effects eventually determines the crystallinity and crystallite structure of EVA in the presence of WF.

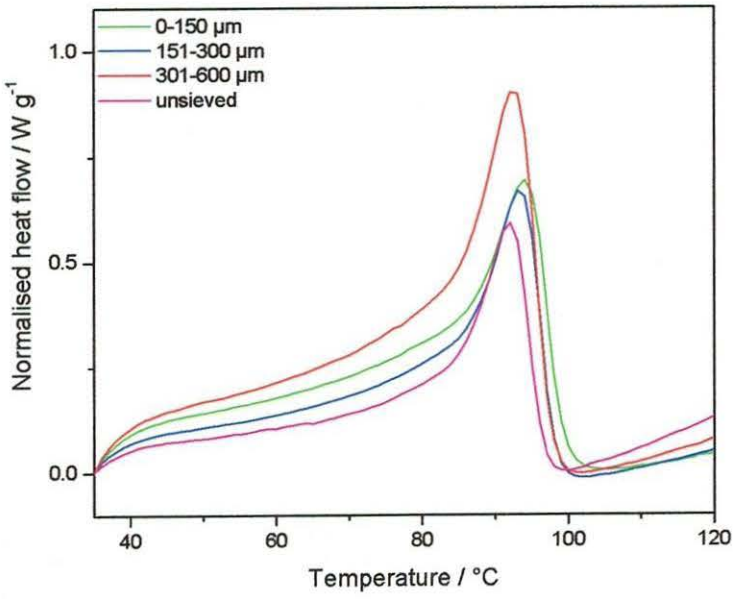

Figure 4.12 The effect of WF particle sizes on the DSC melting behaviour of 75/25 w/w EVA-WF composites

The effect wood fibre particle sizes (0-150, 151-300, 301-600 μm, unsieved) were investigated by using the 75/0/25 w/w EVA/EGMA-WF composites. Figure 4.12 shows the melting peaks of the composites prepared using 0-150, 151-300, 301-600 μm and unsieved particles, and their respective peak temperatures of melting are 94.4, 93.7, 93.1 and 92.4 °C. Taking into account experimental error, the effect of particle size is not that pronounced, all 70/0/25 w/w EVA/EGMA-WF composites melt at the same temperature irrespective of the particle size used.

4.3.2 5 % EGMA compatibilized composites

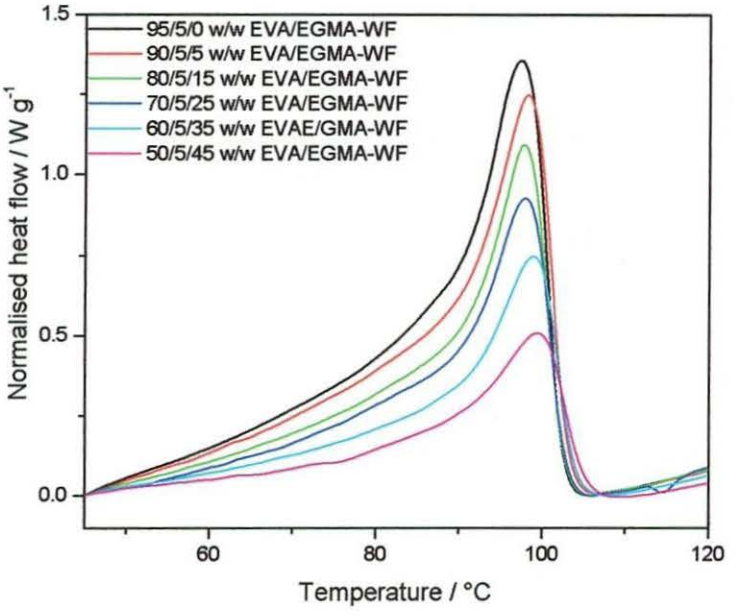

Figure 4 13 DSC heating curves of pure EVA and 5 % EGMA compatibilized EVA-WF (0-150 μm) composites

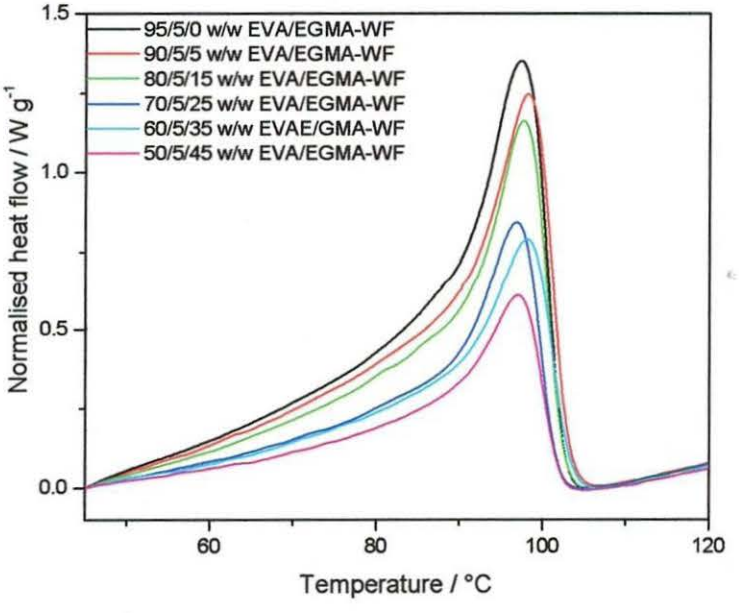

Figure 4.14 DSC heating curves of pure EVA and 5 % EGMA compatibilized EVA-WF (151-300 μm) composites

When 0-150 and 151-300 μm particles were used in the synthesis of 5 % EGMA compatibililized composites, a single endotherm is observed (Figures 4.13 and 4.14) indicating complete miscibility of EVA and EGMA. The EVA/EGMA blend has a melting temperature of 98.8°C. As wood fibre is introduced to the system there is a slight insignificant increase in melting temperature of the composite. There is a general decrease in the experimental enthalpy values with an increase in WF content (Table 4.2). The expected theoretical values are higher than experimental values indicating that the incorporation of WF has an effect on the crystallization behaviour of EVA/EGMA blend.

Table 4.2 Summary of DSC melting data of EVA/EGMA-WF (5 %) composites

EVA/EGMA-WF (w/w)	$T_{o,m}$ / °C	$T_{p.m}$ / °C	ΔH_m^{obs} / J g^{-1}	ΔH_m^{exp} / J g^{-1}
95/5/00	89.7	98.1	32.5	
0-150 μm				
90/5/5	89.3	99.1	31.7	30.7
80/5/15	90.3	98.1	27.7	27.3
70/5/25	89.4	97.8	22.8	23.9
60/5/35	89.9	99.4	19.9	20.5
50/5/45	88.5	100.6	16.7	17.1
151-300 μm				
90/5/5	89.7	98.7	27.9	30.8
80/5/15	90.6	98.6	26.2	27.3
70/5/25	89.5	97.4	19.2	23.9
60/5/35	90.8	98.7	14.7	20.5
50/5/45	89.1	97.7	12.7	17.1

$T_{o,m}$- onset temp of melting, $T_{p.m}$-peak temp of melting ΔH_m^{obs} – experimentally observed melting enthalpy, ΔH_m^{exp} - theoretical expected melting enthalpy

The crystals become less perfect as more wood fibre is added; this is shown by the broadening of the peaks. The DSC cooling curves of the 5 % EGMA compatibilized composites (0-150 μm WF) are shown in Figure 4.15. There is an insignificant difference between the crystallization peak temperatures of the different composites. Composites with and without WF crystallize around 77 °C. This shows the EGMA-WF grafted product does not substantially influence the crystallization behaviour of EVA.

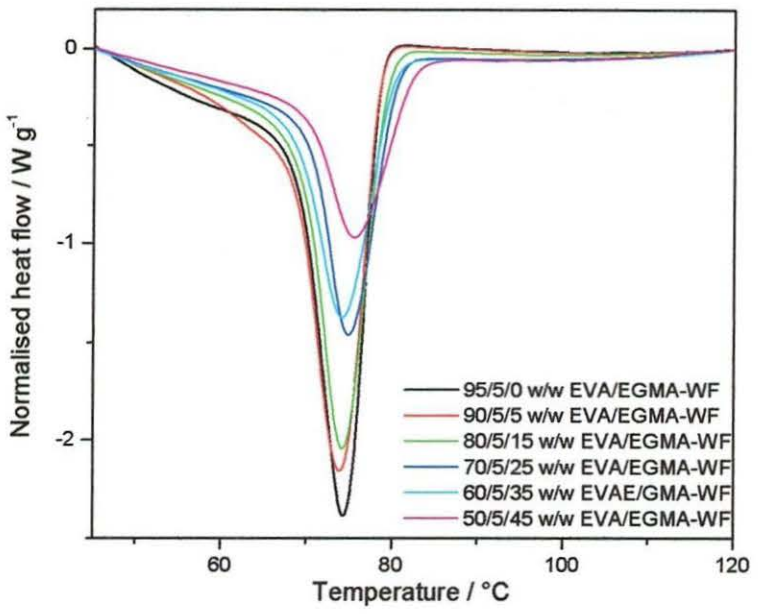

Figure 4.15 **DSC cooling curves of pure EVA and 5 % compatibilized EVA-WF (0-150 µm) composites**

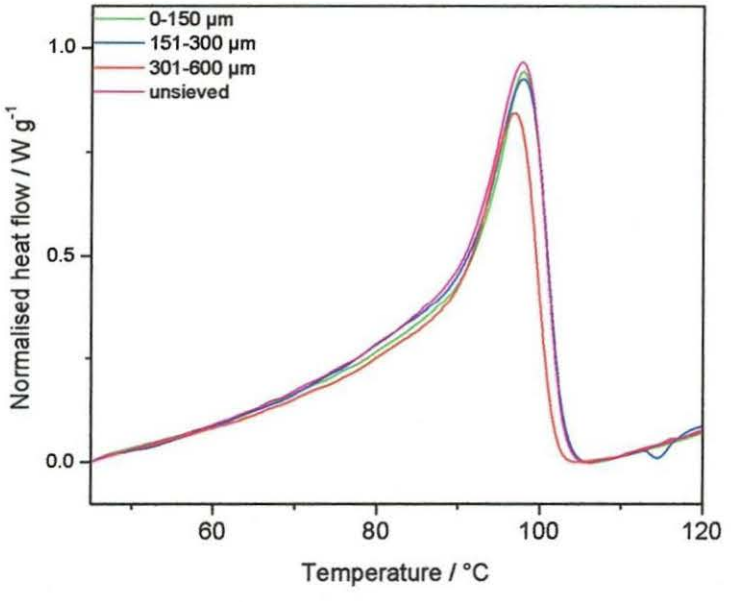

Figure 4.16 **The effect of wood fibre particle size on the DSC melting behaviour of 70/5/25 w/w EVA/EGMA-WF composites**

The effect of wood fibre particle size on 70/5/25 w/w EVA/EGMA-WF composites is shown in Figure 4.16. The melting peak temperatures of the composites have similar melting temperature values.

4.3.3 10 % EGMA compatibilized compsites

Figures 4.17 and 4.18 show the DSC curves for samples where 10 % of EGMA was used as compatibilizer in composites containing 0-150 and 151-300 μm WF particle sizes, respectively. There is a general decrease in enthalpy with increasing wood fibre content. The theoretical enthalpy values are generally higher than the experimental values (Table 4.3). This indicates that WF is hindering the crystallization of EVA chains, which is probably the result of the interaction between the EVA/EGMA blend and WF. This behaviour was not seen in uncompatibilized and 5 % compatibilized composites because of lower availability of the active groups.

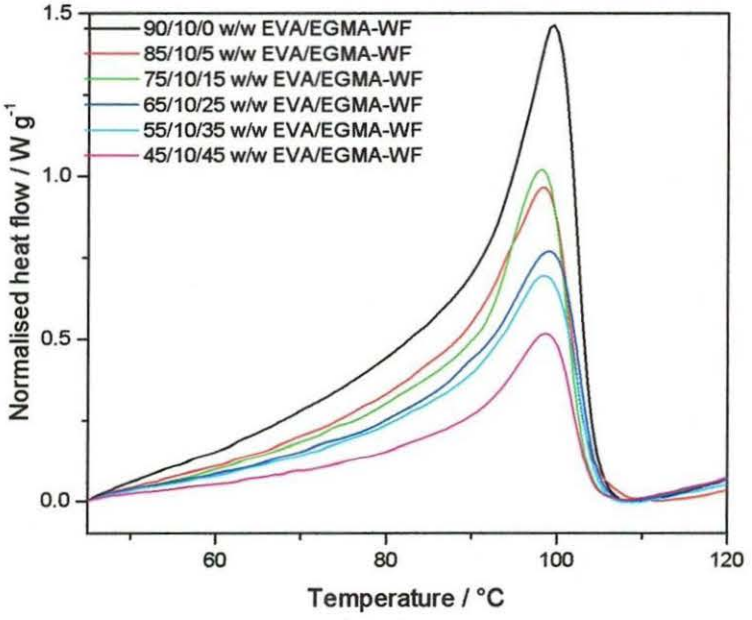

Figure 4.17 DSC heating curves of pure EVA and 10 % compatibilized EVA-WF (0-150 μm) composites

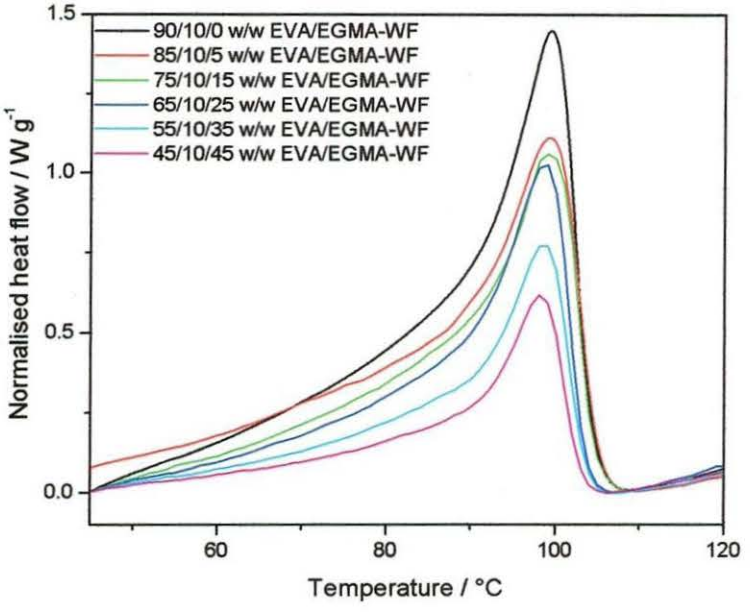

Figure 4.18 **DSC heating curves of pure EVA and 10 % compatibilized EVA-WF (151-300 μm) composites**

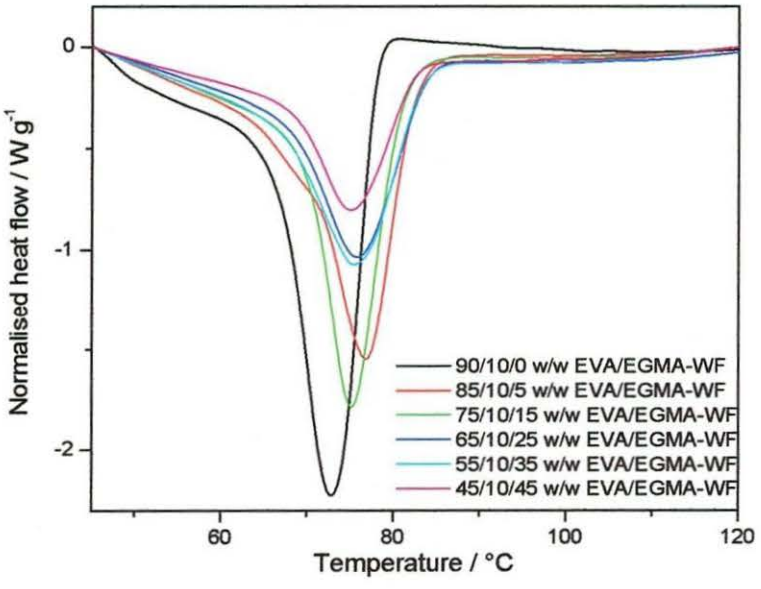

Figure 4.19 **DSC cooling curves of pure EVA and 10 % compatibilized EVA-WF (0-150 μm) composites**

The crystallization curves of the 10 % EGMA compatibilized composites are shown in Figure 4.19. The crystallization temperatures generally increase with increasing WF content, but remain fairly constant at higher contents. As the proposed mechanism suggests, EGMA react with WF providing an OH active group for EVA to interact with. This results in a better interaction between EVA and WF, which will reduce the mobility of the EVA chains, giving rise to higher crystallization temperatures. As more wood fibre is added, EGMA becomes saturated and can no longer accommodate WF, and thus there is not a substantial increase in crystallization temperatures at higher WF contents.

Table 4.3 Summary of DSC melting data of 10 % EGMA compatibilized EVA-WF composites

EVA/EGMA-WF (w/w)	$T_{o,m}$ / °C	$T_{p.m}$ / °C	ΔH_m^{obs} / J g^{-1}	ΔH_m^{exp} / J g^{-1}
90/10/0	89.6	98.7	33.8	
0-150 μm				
85/10/5	90.3	98.7	25.6	31.9
75/10/15	89.3	99.1	26.2	28.2
65/10/25	89.3	99.4	22.1	24.4
55/10/35	88.4	99.7	18.7	20.6
45/10/45	88.6	99.4	15.4	16.9
151-300 μm				
85/10/5	90.3	99.7	28.1	31.9
75/10/15	91.5	99.8	26.4	28.2
65/10/25	90.3	98.6	20.1	24.4
55/10/35	90.1	99.1	18.7	20.7
45/10/45	90.5	98.7	15.6	16.9

$T_{o,m}$- onset temp of melting, $T_{p.m}$-peak temp of melting ΔH_m^{obs} – experimentally observed melting enthalpy, ΔH_m^{exp} - theoretical expected melting enthalpy

Figure 4.20 shows the effect of WF particle size on the DSC melting behaviour of the 65/10/25 w/w EVA/EGMA-WF composites. Considering the experimental error, there is an

insignificant difference in the melting temperatures of the composites synthesized, irrespective of the wood fibre particle size used.

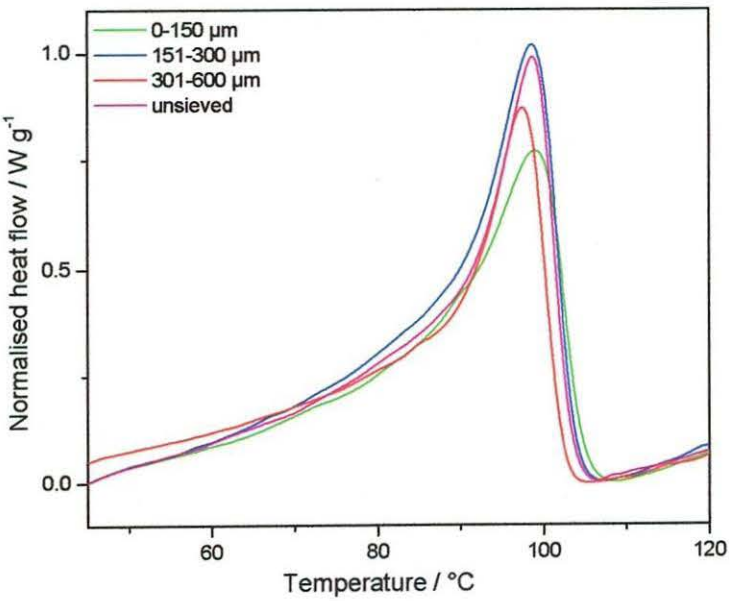

Figure 4.20 The effect of wood fibre particle size on the DSC melting behaviour of 65/10/25 w/w EVA/EGMA-WF composites

4.3.4 Thermal behaviour of EVA/EGMA blends

Figure 4.21 shows that pure EGMA and EVA have melting peaks in the same temperature range. According to the proposed mechanism there is no evidence of a reaction taking place between EVA and EGMA. According to Chiou *et al* [1] a reaction with EGMA is likely to occur with those polymers containing certain functional groups as chain ends or within the main chain, typical examples are –COOH (and/or -OH) of polyesters, phenolic –OH of PPO, and NH_2 of polyamides. Looking at the structure of EVA, none of these functional groups is present at the chain end or within the main chain, so that there is no probability of EVA and EGMA forming a reactive product during melt extrusion. The single melting peak for the blends, as well as the relative peak sizes, therefore shows that EVA and EGMA is miscible in the crystalline phase, and do not substantially influence each other's crystallization behaviour.

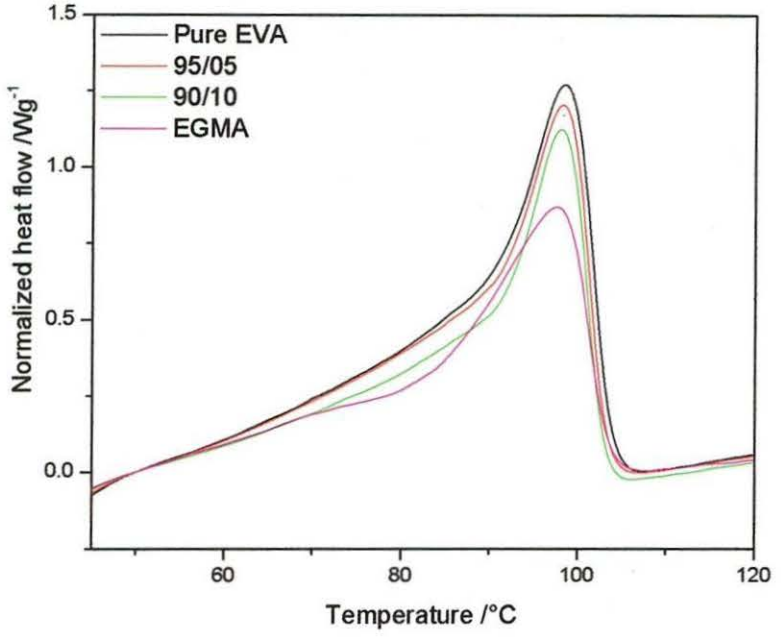

Figure 4.21 DSC curves of pure EVA, EGMA and EVA/EGMA blends

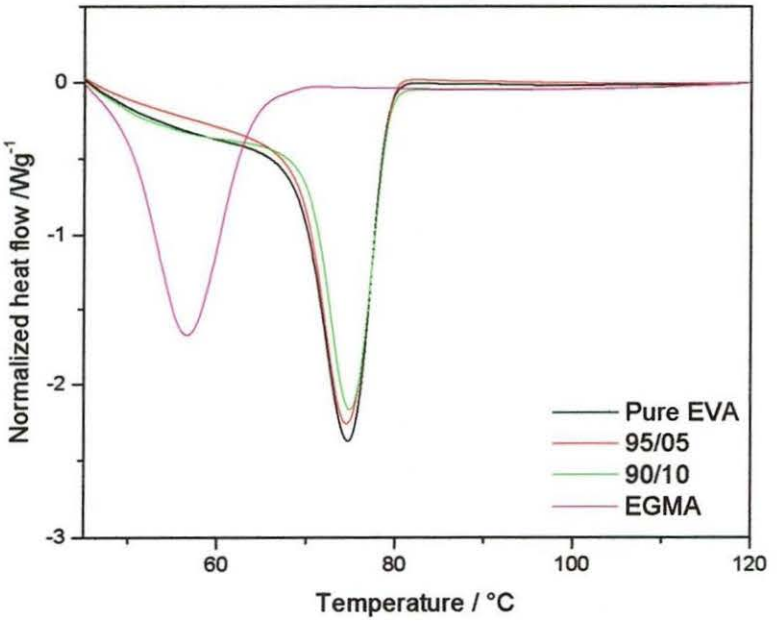

Figure 4.22 DSC cooling curves of pure EVA, EGMA and EVA/EGMA blends

Table 4.4 Summary of DSC melting data of pure EVA, EGMA and their blends

EVA/EGMA (w/w)	$T_{o,m}$ / °C	$T_{p.m}$ / °C	ΔH_m^{exp} / J g^{-1}
100/0	88.9	97.7	27.4
0/100	85.0	98.4	22.3
95/5	88.3	97.8	26.8
90/10	85.2	97.3	24.9

$T_{o,m}$- onset temp of melting, $T_{p.m}$-peak temp of melting

The decrease in enthalpy with increasing EGMA content is the result of the lower enthalpy of EGMA (Figure 4.21 and Table 4.4).

The crystallization behaviour of pure EGMA, EVA and their blends is shown in Figure 4.22. EGMA crystallizes at a much lower temperature then EVA or their blends. This is probably the result of much higher EGMA chain mobility, which is restricted when EGMA is blended with EVA, probably as a result of some interaction and not necessarily a reaction between EVA and EGMA.

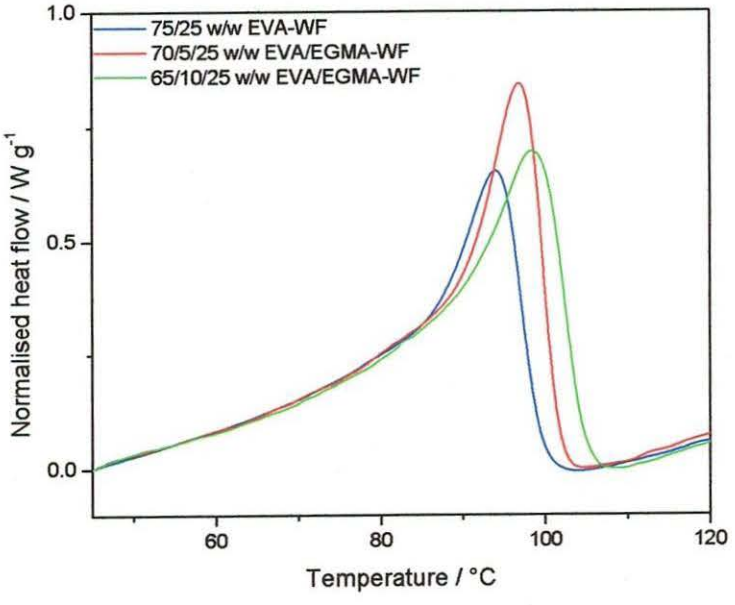

Figure 4.23 The effect of compatibilizer on the DSC melting behaviour of composites containing 25 % 0-150 μm wood fibre

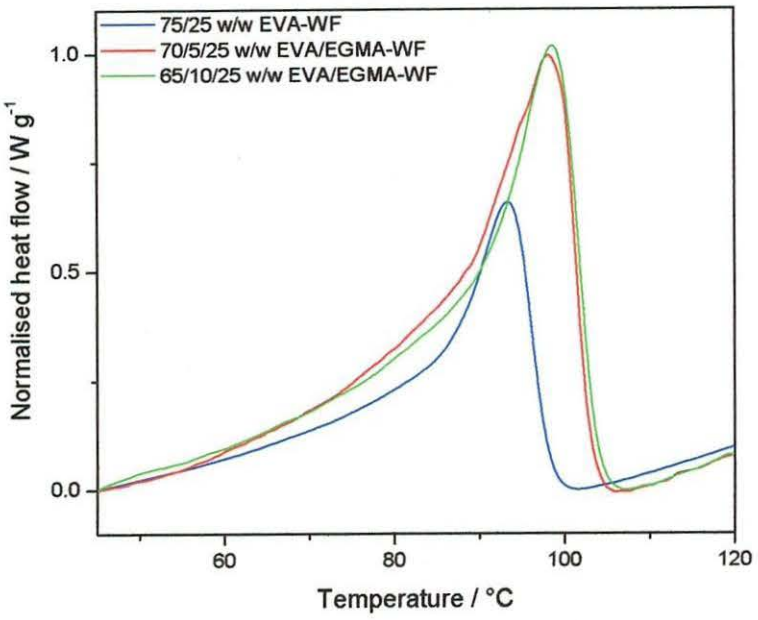

Figure 4.24 The effect of compatibilizer on the DSC melting behaviour of composites containing 25 % 151-300 μm wood fibre

Figures 4.23 and 4.24 show the effect of compatibilizer on the DSC melting behaviour of composites containing 25 % 0-150 and 151-300 μm wood fibre particles respectively. The compatibilized composites melt at higher temperatures than the uncompatibilized ones. This shows that in the presence of EGMA the WF more strongly interacts with the matrix, probably as a result of the wetting of WF particles through the formation of the EGMA-WF bonds. This will reduce EVA chain mobility, giving rise to higher melting points.

The effect of compatibilizer on the DSC crystallization behaviour of composites containing 25 % 0-150 μm WF is shown in Figure 4.25. In this case, compatibilized composites crystallize at higher temperatures than uncompatibilized composites. This was not the case in composites without WF (figure 4.21); EVA and EVA-EGMA blend had the same crystallization temperature. This shows the effectiveness of EGMA in compatibilizing WF and EVA thus giving composites that have a greater restriction of chain movement compared to uncompatibilized composites.

Table 4.5 Summary of DSC melting data showing the effect of compatibilizer on composites when 25 % WF is used

EVA/EGMA-WF (w/w)	$T_{o,m}$ / °C	$T_{p.m}$ / °C	ΔH_m^{obs} / J g^{-1}	ΔH_m^{exp} / J g^{-1}
0-150 µm				
75/0/25	84.8	94.4	18.4	18.7
70/5/25	89.4	97.8	22.8	23.9
65/10/25	89.3	99.4	22.1	24.4
151-300 µm				
75/0/25	85.1	93.7	17.5	18.7
70/5/25	89.5	97.4	19.2	23.9
65/10/25	90.3	98.6	20.1	24.4

$T_{o,m}$- onset temp of melting, $T_{p.m}$-peak temp of melting ΔH_m^{obs} – experimentally observed melting enthalpy, ΔH_m^{exp} - theoretical expected melting enthalpy

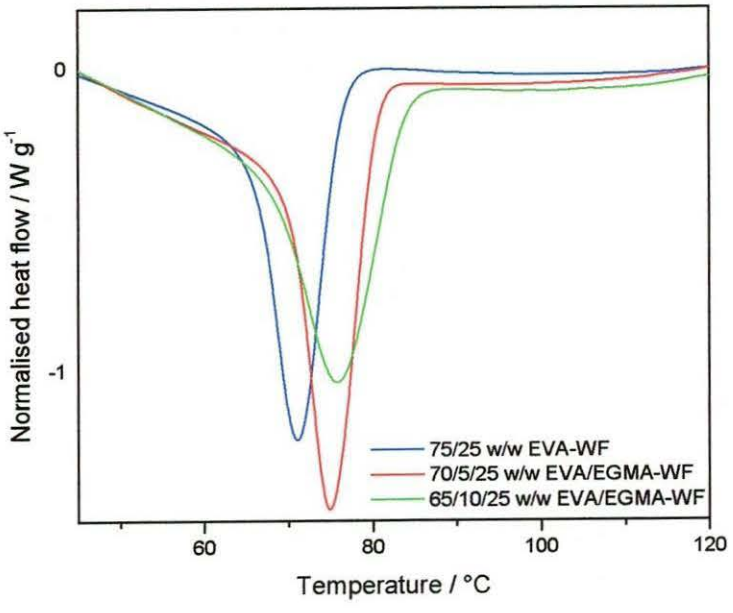

Figure 4.25 The effect of compatibilizer on the DSC crystallization behaviour of composites containing 25 % 0-150 µm wood fibre

4.4 Mechanical properties

4.4.1 Stress strain behaviour

The incompatibility of EVA and WF in the uncompatibilized composites is reflected in the stress–strain curves in Figures 4.26-4.28. These figures are the stress-strain curves for the EVA-WF composites prepared by using 0-150 μm WF particles without compatibilizer, and with 5 and 10 % EGMA respectively. Generally, the strength of a fibre-reinforced composite depends on the properties of the constituents and the interfacial interaction. Homogeneity of the overall composite has to be taken into account.

Pure EVA possesses a tensile strength of 10 MPa and an elongation at break of over 670 %. There is a significant decrease in stress and strain at break as WF is added to EVA, as can be seen in the stress-strain curves of the uncompatibilized composites in Figure 4.26. All the EVA-WF composites have lower values for both tensile strength and elongation at break, mainly because of the incompatibility between WF and EVA.

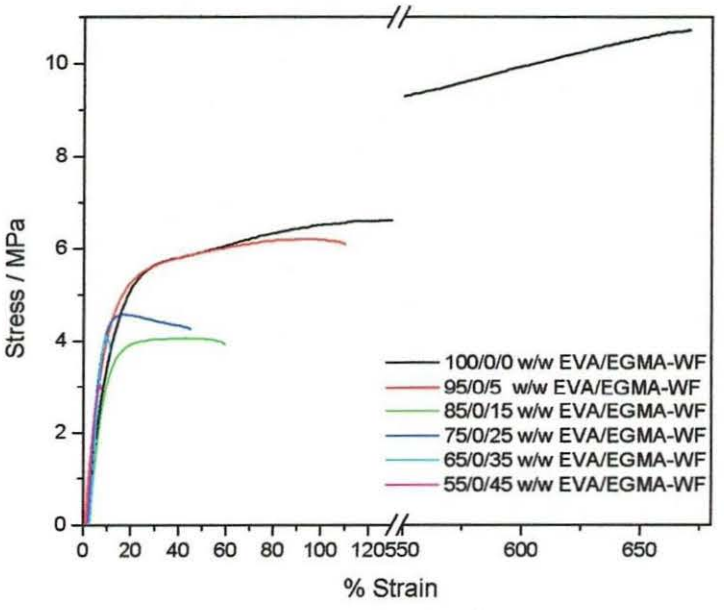

Figure 4.26 Stress-strain curves of EVA-WF uncompatibillized composites (0-150 μm WF)

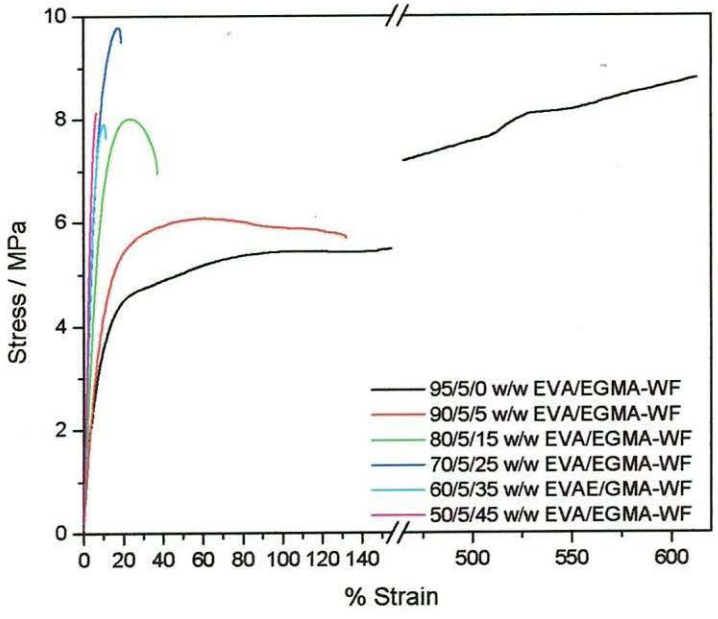

Figure 4.27 Stress-strain curves of EVA-WF 5 % EGMA compatibillized composites (0-150 μm WF)

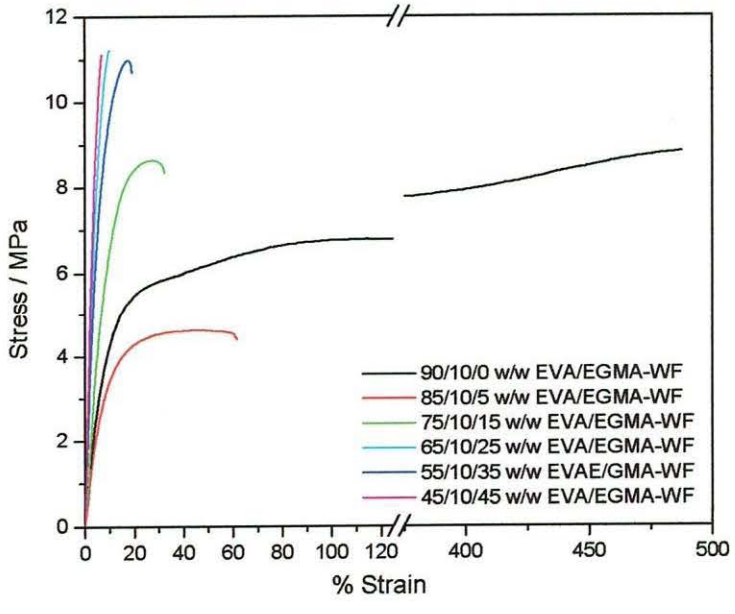

Figure 4.28 Stress-strain curves of EVA-WF 10 % EGMA compatibillized composites (0-150 μm WF)

Table 4.6 Mechanical properties of uncompatibilized and comptatibilized EVA-WF composites (0-150 and 151-300 μm)

EVA/EGMA-WF (w/w)	E ± sE/ MPa	ε_b ± sε_b/ %	σ_b ± sσ_b/ MPa
100/0	31.1 ±1.3	680 ± 7.6	10.8 ± 0.2
Uncompatibilized			
0-150 μm – 95/0/5	52.1 ± 2.2	231 ± 4.9	6.3 ± 0.3
85/0/15	76.3 ± 5.2	47.8 ± 3.9	5.1 ± 0.2
75/0/25	63.3 ± 3.2	44.7 ± 8.4	4.8 ± 0.2
65/0/35	96.6 ± 2.2	12.6 ± 2.1	4.1 ± 0.1
55/0/45	85.5 ± 2.3	5.23± 1.6	3.7 ± 0.1
151-300 μm – 95/0/5	37.3 ± 1.0	95.5 ± 5.7	4.6 ± 0.1
85/0/15	66.8 ± 1.9	49.2 ± 5.7	4.1 ± 0.5
75/0/25	91.1 ± 2.8	23.2 ± 1.7	3.9 ± 0.1
65/0/35	132.3 ± 1.3	8.5 ± 0.5	3.1 ± 0.5
55/0/45	107.5 ± 2.3	6.7 ± 0.3	2.7± 0.2
5% EGMA compatibilized			
95/5/0	34.4± 1.5	605 ± 21.5	9.1 ± 0.19
0-150 μm – 90/5/5	48.2 ± 1.3	125.6 ± 2.8	5.5 ± 0.1
80/5/15	93.1 ± 1.7	37.6 ± 1.4	7.1 ± 0.1
70/5/25	145.5 ± 3.3	17.3 ± 1.1	10.8 ± 0.3
60/5/35	142.6 ± 1.9	9.6 ± 0.2	7.7 ± 0.2
50/5/45	175.1 ± 5.1	5.5 ± 0.3	7.5 ± 0.4
151-300 μm – 90/5/5	34.8 ± 0.4	76.5 ± 4.4	4.9 ± 0.1
80/5/15	70.7 ± 1.87	28.6 ± 3.9	5.8 ± 0.2
70/5/25	103.2 ± 2.9	13.3 ± 1.2	6.9 ± 0.4
60/5/35	153.1 ± 1.6	8.9 ± 0.7	7.6 ± 0.6
50/5/45	161.2 ±5.9	9.2± 0.5	7.1 ±0.5
10 % EGMA compatibilized			
90/10/0	43.1± 2.2	511.8 ± 16.7	8.7 ± 0.1
0-150 μm – 85/10/5	45.2 ± 1.8	32.4 ± 2.7	4.3 ± 0.1
75/10/15	77.9 ± 4.8	32.4± 1.3	5.6 ± 0.1
65/10/25	137.4 ± 8.4	17.1 ± 2.4	8.6 ± 0.5
55/10/35	173.3 ± 10.0	11.3 ± 0.8	9.2 ± 0.5
45/10/45	228.1 ± 12.3	9.2 ± 0.5	10.4 ± 0.3
151-300 μm – 85/10/5	42.8 ± 3.65	46.8 ± 1.1	
75/10/15	68.9 ± 0.6	26.1 ± 1.6	4.1 ± 0.2
65/10/25	93.4 ± 2.8	17.2 ± 2.1	6.2 ± 0.1
55/10/35	129.3 ± 5.1	9.8 ± 0.6	5.7 ± 0.6
45/10/45	177.0 ± 2.9	7.8± 0.8	7.5 ± 0.4

E = tensile modulus; ε_b = elongation at break; σ_b = stress at break

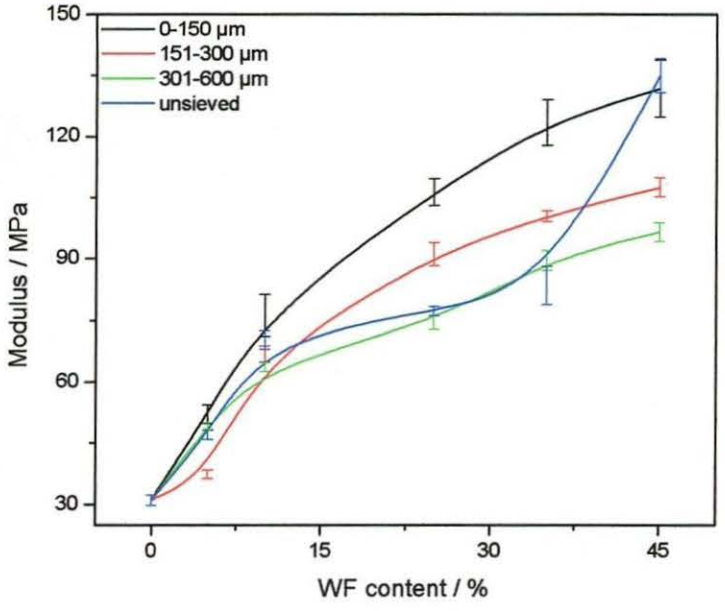

Figure 4.29 Modulus as function of WF content for samples containing different WF sizes in uncompatibilized composites

(ethylene-co-methacrylic acid) copolymer as an effective compatibilizer of LDPE-WF composites, and reported that the modulus increases gradually with increasing content of WF. Bledzki *et al* [10] and Salemane *et al* [5] studied PP-WF composites, and reported that the modulus of a PP-WF composite increased with increasing WF content. Balasuriya *et al* [11] studied the mechanical properties of wood flake – polyethylene composites, and reported that the modulus increases with increasing wood flake content. The increase in modulus is primarily influenced by the amount of filler loading, although the maximum values are dependent on the processing methods and flow behaviour of the matrix agent.

It is interesting to see that WF particle sizes have an influence on the modulus of the composite. As Figure 4.29 shows, the modulus decreases with increasing particle size. Smaller sized fillers gave higher modulus values than larger size fillers. This finding was also reported by Ismail *et al* [8]. This is because composites made from small particle size fillers show better filler dispersion and filler-matrix interaction than composites made form large particles. Interaction and interfacial adhesion is stronger in the case of small particle sizes than in the case of larger ones.

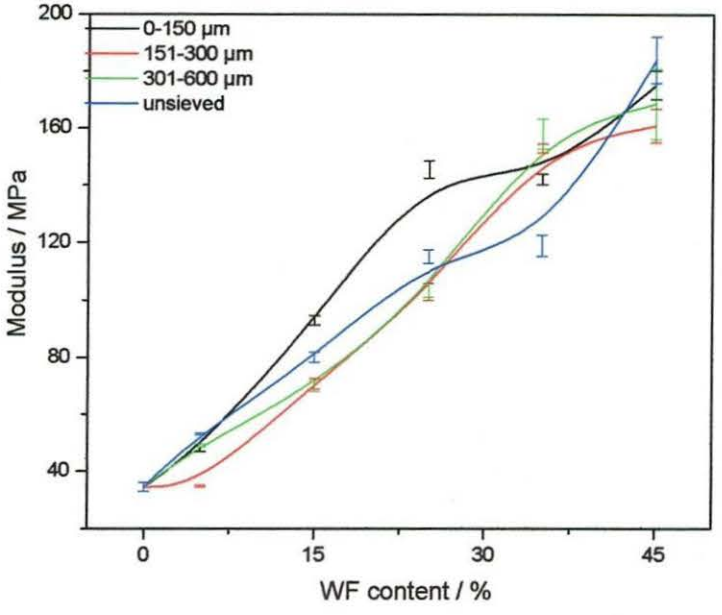

Figure 4.30 Modulus as function of WF content for samples containing different WF sizes in 5 % EGMA compatibilized composites

The presence of 5 % compatibilizer increases the modulus of the composites, as shown in Figure 4.30. In the presence of 5 % EGMA the maximum modulus is in the region of 200 MPa, compared to a maximum of about 150 MPa in the case of the uncompatibilized composites. Bonding between EVA and WF is stronger in the presence of EGMA, EGMA effectively link the two by forming a bond with WF on one hand while on the other hand it bonds to EVA. In uncompatibilized composites the bonding between EVA and WF is weak because of the large surface area of WF and its hydrophyllicity. This surface area is reduced the reaction between the epoxy group of EGMA and the OH group of WF resulting in a composite that is easily accessible to EVA. Chiou *et al* [1] reported that epoxy hydrolysis, is likely to occur, because epoxy containing compounds or polymers are known to act as acid or water scavengers in many condensation–type polymers in the melt, thus reducing OH groups of the composite [1].

The presence of 10 % EGMA in the composites gave rise to the highest moduli. 0-150 µm and unsieved WF particles give modulus values of approximately 250 MPa (Figure 4.31), compared to the 200 MPa that was reported for the 5 % compatibilized composites. Similar results were also obtained by other researchers.

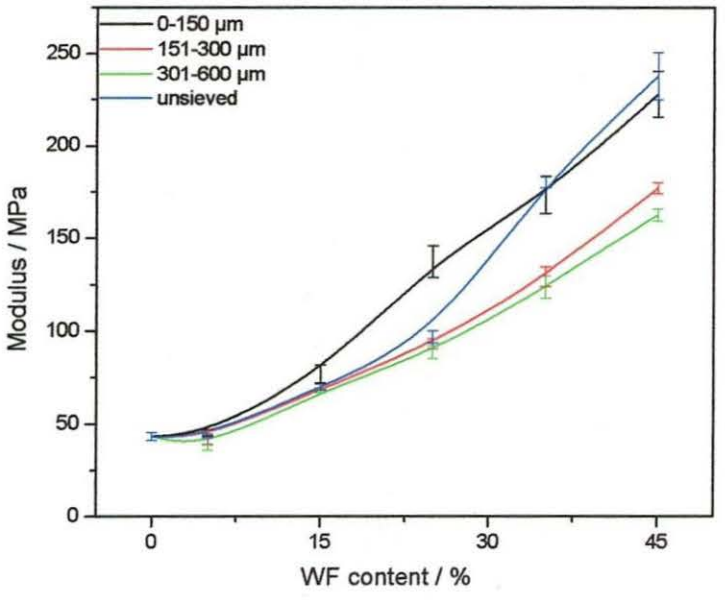

Figure 4.31 Modulus as function of WF content for samples containing different WF sizes in 10 % EGMA compatibilized composites

Elvy *et al* [12] reported that the addition of alkoxysilane coupling agents modifies the interface between dissimilar materials such as glass fibres and thermoplastics or thermosetting resins, and therefore increases its tensile properties. Salemane and Luyt [5] reported that the use of a compatibilizer can improve adhesion and thus enhance tensile properties of PP-WF composites. The composite properties changed with an increase in maleated polypropylene (MAPP) content. This improved filler-matrix interfacial adhesion is due to an esterification reaction between the hydroxyl groups of the cellulose filler and the anhydride functionalities of MAPP. This interaction overcome the incompatibility problem and increases the tensile and flexural strength of natural filler-polymer composites. Malunka and Luyt [6] reported that increasing sisal content as well as crosslinking and grafting gave rise to increased values of Young's modulus.

Figures 4.32 and 4.33 show the effect of compatibilizer on the modulus of EVA-WF composites for samples containing respectively 0-150 and 151-300 µm WF particles. In both cases, the influence of EGMA seems marginal at low WF content, while EGMA has a substantial influence at higher WF contents. This influence becomes stronger with increasing EGMA content because of the increased number of active groups when more EGMA is used.

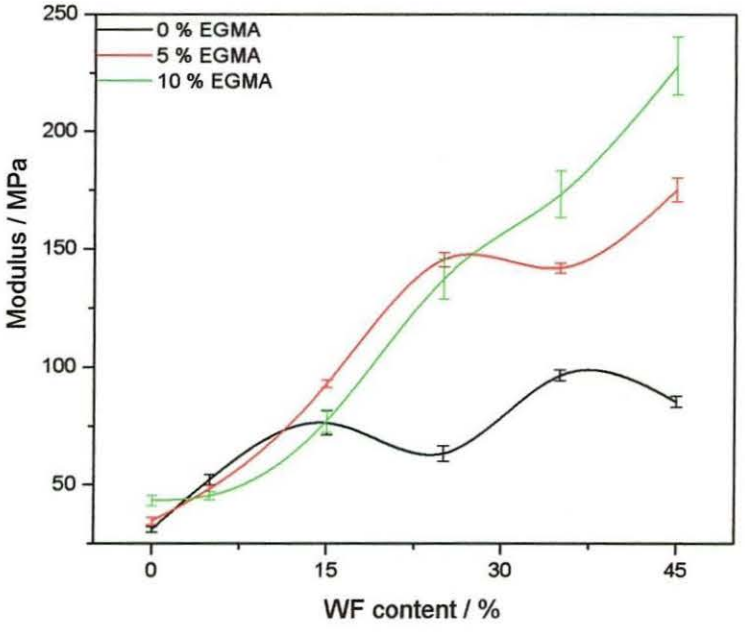

Figure 4.32 The effect of compatibilizer content on the modulus of EVA/EGMA-WF composites (0-150 μm WF)

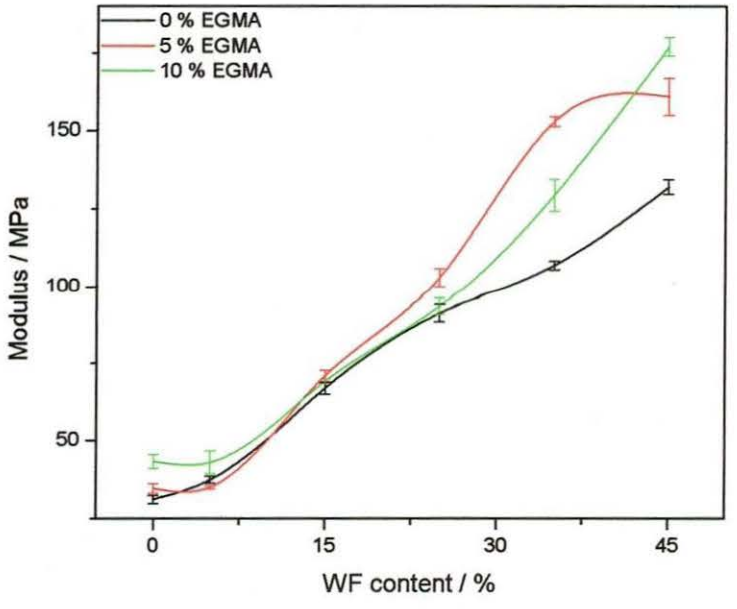

Figure 4.33 The effect of compatibilizer content on the modulus of EVA/EGMA-WF composites (151-300 μm WF)

4.4.3 Stress at break

The stress at break curves tells us a lot about the strength of the material. Composites, that can handle a lot of stress before breaking, have a high tensile strength. Figure 4.34 shows the stress at break curves of uncompatibilized EVA-WF composites. Pure EVA has the highest value of stress at break (11 MPa). The presence of 5 % WF in EVA causes a decrease in stress at break to about half that of pure EVA. An increase in WF content causes a further decrease in stress at break, indicating that the presence of WF has a substantial influence on the tensile strength of the composites. This is also the result of weak interaction between WF and EVA. This is because of the hydrophobic and the hydrophilic natures of EVA and WF respectively [7]. The inability of the filler to support stresses transferred from the polymer matrix, increases with an increase in filler loading. In the presence of WF chain movement in EVA is restricted, and thus its stress handling capacity is considerably reduced [13]. Georgopoulos *et al* [14] studied thermoplastic polymers reinforced with fibrous agricultural residue, and they reported a significant decrease in tensile stress upon filling the polymer matrix with natural fillers.

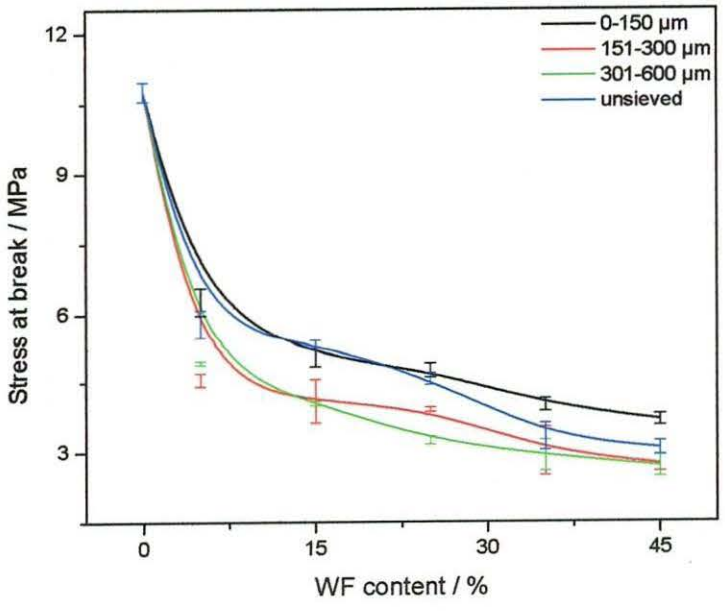

Figure 4.34 Stress at break as function of WF content for samples containing different WF sizes in uncompatibilized composites

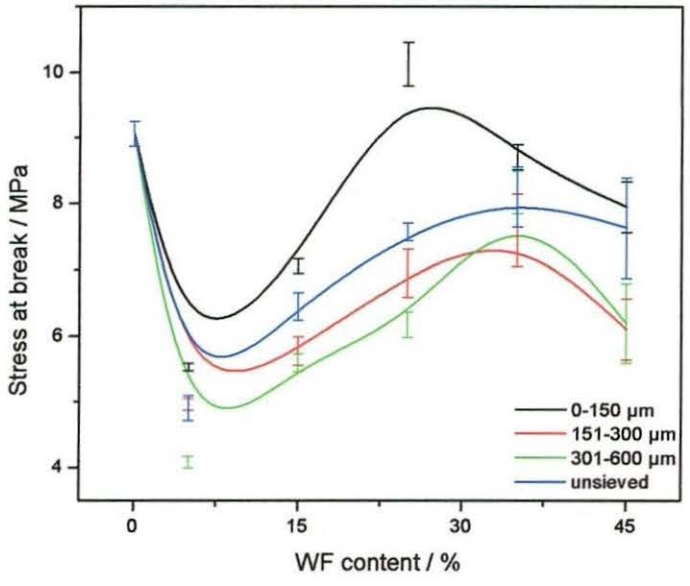

Figure 4.35 Stress at break as function of WF content for samples containing different WF sizes in 5 % EGMA compatibilized composites

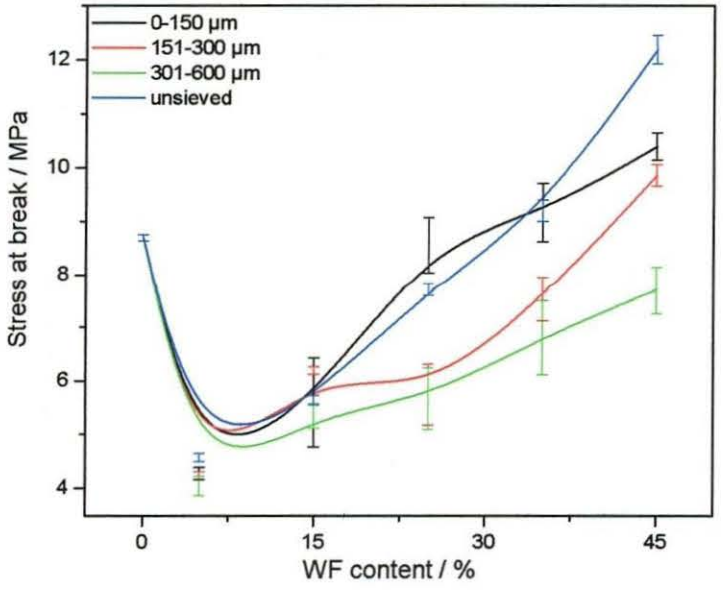

Figure 4.36 Stress at break as function of WF content for samples containing different WF sizes in 10 % EGMA compatibilized composites

It can be seen that small particle size composites exhibit higher tensile strength (Figure 4.34). The reason behind this is that there is better dispersion and filler/matrix interaction in the case of smaller particles [8]. Smaller particle composites can thus handle stress much better than larger particle composites. Similar findings were reported by Biggs [15] and Fuad *et al* [16]. All the 0-150 μm and unsieved WF composites have higher values of stress at break compared to the 151-300 and 301-600 μm composites. This confirms that the unsieved WF particles consist of mainly 0-150 μm particles. This is also clear from the water absorption results, which will be discussed further on.

The effect of the wood fibre particle sizes on the stress at break behaviour is shown in Figures 4.35 and 4.36 for 5 and 10 % EGMA, respectively. The 95/5 and 90/10 w/w EVA/EGMA blends have stress at break values of 9 and 8.5 MPa respectively, two units below the stress at break value of pure EVA. The presence of 5 % WF causes a further reduction in the stress at break to about 4 MPa, depending on the WF particle size used. It is interesting to see that the presence of 15, 25, 35 and 45 % wood fibre causes an increase in the stress at break of the composite. This is understandable since an increase in WF content means an increase in OH groups that react with EGMA, and subsequently EGMA-WF grafted product interact with EVA, thus increasing the stress at break in composites.

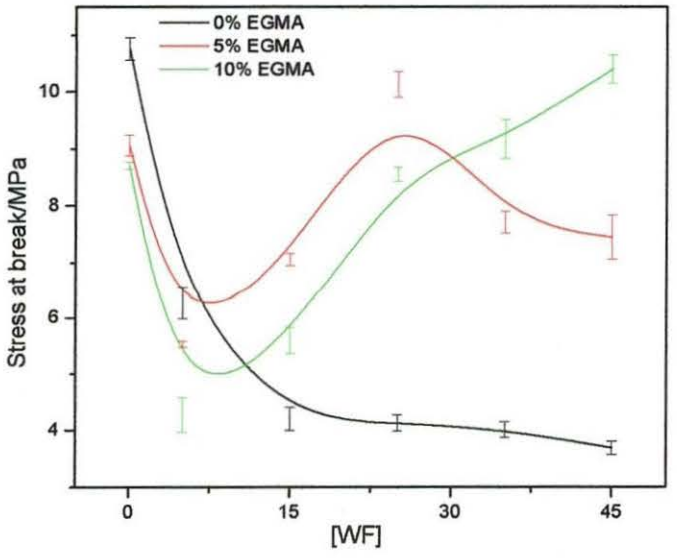

Figure 4.37 The effect of compatibilizer content on the stress at break of EVA/EGMA-WF composites (0-150 μm WF)

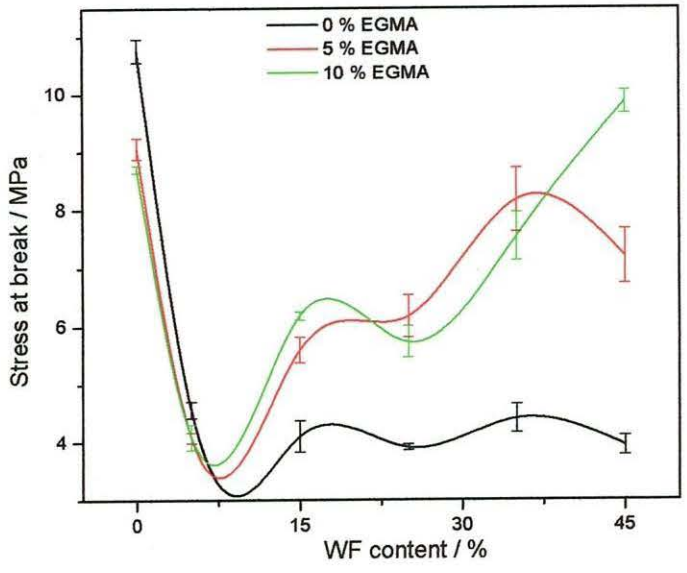

Figure 4.38 The effect of compatibilizer content on the stress at break of EVA/EGMA-WF composites (151-300 μm WF)

The effect of compatibilizer on the stress at break of 0-151 and 151-300 μm WF particle containing composites is shown in Figures 4.37 and 4.38. Pure EVA has a stress at break of 11 MPa. The presence of 5 and 10 % EGMA in the EVA causes a decrease in stress at beak to 9 and 8.5 MPa respectively. This is probably because EGMA has a lower stress at break than EVA. There is a continuous decrease in stress at break as more WF is present in the uncompatibilized composites, but this value increases with increasing WF content above 5 % when EGMA is used as compatibilizer. For 5 % EGMA the stress at break decreases again at high WF contents, but for 10 % EGMA there is a continuous increase, after the initial decrease. The initial decrease is probably the result of the small amount of WF, which is not enough to strongly interact with EGMA, but is enough to act as defect points. The decrease at high WF contents in the presence of 5 % EGMA is probably because there is not enough EGMA to completely cover the WF surfaces, giving rise to reduced interaction between EVA and WF because of insufficient wetting of the WF surfaces. A maximum stress at break of 10 MPa is achieved in the 45/10/45 w/w EVA/EGMA-WF composite.

4.4.4 Elongation at break

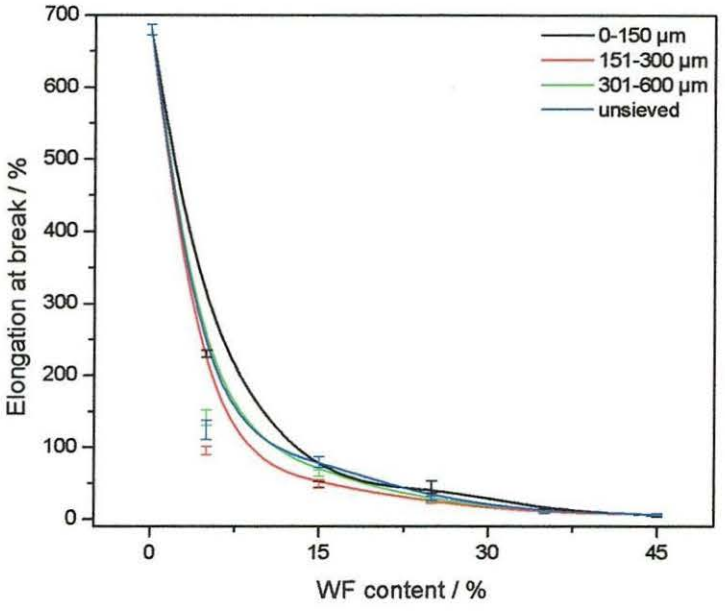

Figure 4.39 Elongation at break as function of WF content for samples containing different WF sizes in uncompatibilized composites

The elongation at break curves of uncompatibilized composites is shown in Figure 4.39. Pure EVA has the highest elongation of 680 %. The presence of WF in EVA leads to lower elongation at break values. The composite containing 15 % WF shows a very small elongation (below 100 %), while composites containing 25, 35 and 45 % WF have insignificantly low values. This decrease in elongation at break is the result of a restriction in the chain movement in EVA. As more WF is present, the stiffness and the brittleness of the composites increase gradually. Georgopoulos *et al* [14] reported a decrease in elongation at break; the composite seems to lose most of its flexibility, even at lower filler loading

It is interesting to note that the elongation of smaller filler containing composites is higher than that of the larger filler containing ones up to a filler content of 15 %. When more than 15 % wood filler is used, the elongations at break values of all the composites are more or less similar irrespective of the filler size. This trend may be attributed to two factors: (i) below 15 % there is a better dispersion of the small particles, because EVA reduces filler-filler interaction, and thus the sample can be elongated to a higher value.

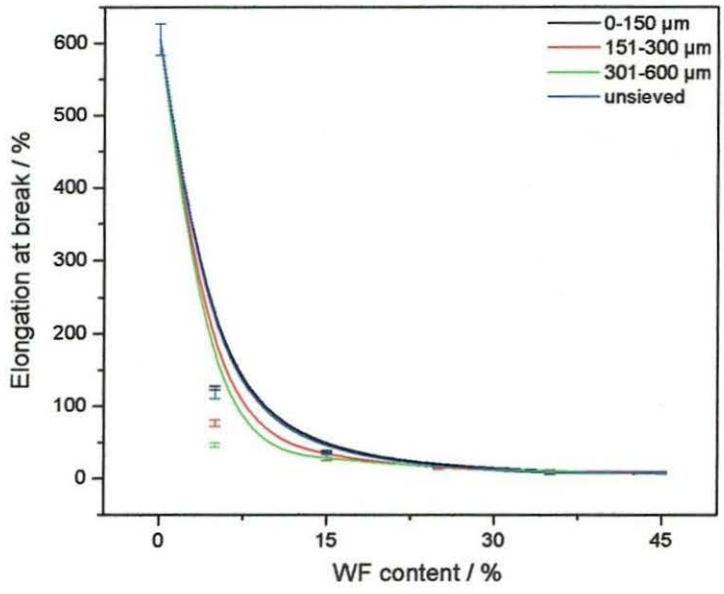

Figure 4.40 Elongation at break as function of WF content for samples containing different WF sizes in 5 % compatibilized composites

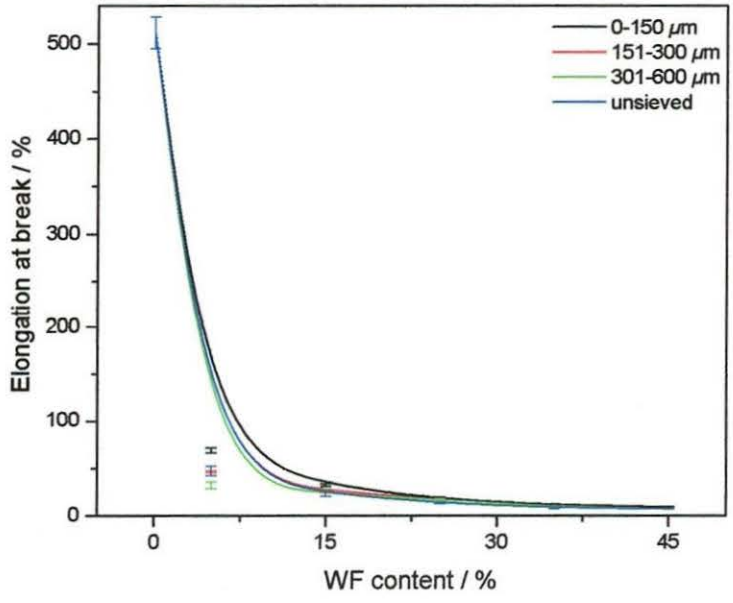

Figure 4.41 Elongation at break as function of WF content for samples containing different WF sizes in 10 % compatibilized composites

However, at the higher filler contents, the degree of filler-filler interaction becomes more prominent, even in the case of smaller particle composites, and as a result a reduction in elongation at break was seen, (ii) an increase in filler content will eventually result in the reduction of the deformability of the rigid interface between the filler and the polymer matrix. Balasuriya *et al* [11] reported that the ultimate elongation values at yield or break (no yield was observed for composites containing more than 30 wt % WF) for PE-WF composites show that ductility severely suffers from an increase in WF content. However, there was no significant difference in the elongation at break between different types of wood fibre composites.

Figures 4.40 and 4.41 show elongation at break as function of WF content when EGMA is used as a compatibilizer in EVA-WF composites. The 95/5 and 90/10 w/w EVA/EGMA blends show a lower elongation at break than pure EVA. This is because EGMA has a low elongation at break of 440 % than pure EVA of 680 %. There is a further decrease in elongation at break in the presence of 5 % WF. The presence of 15 % WF gives an elongation at break value of ~50 %. These values are lower than the elongation at break values in uncompatibilized composites. This indicates that the presence of EGMA gives rise to less deformation in the composites.

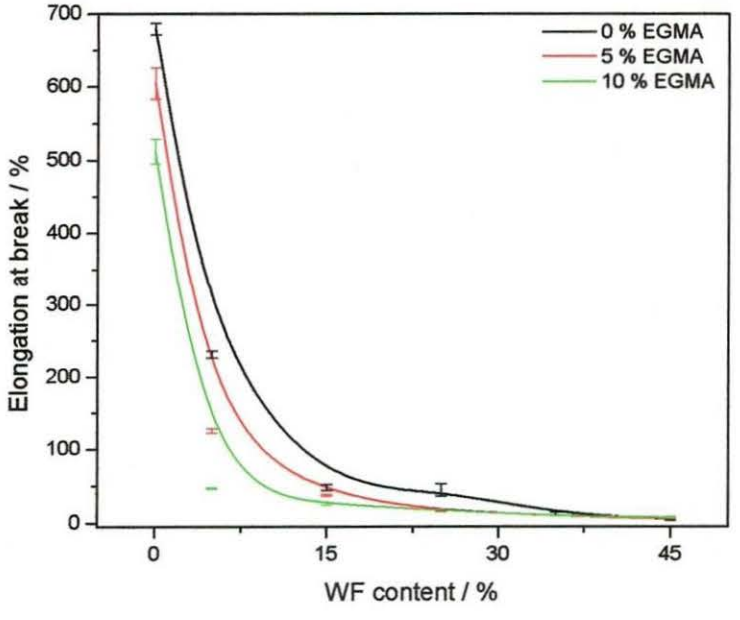

Figure 4.42 The effect of compatibilizer content on the elongation at break of EVA/EGMA-WF composites (0-150 μm WF)

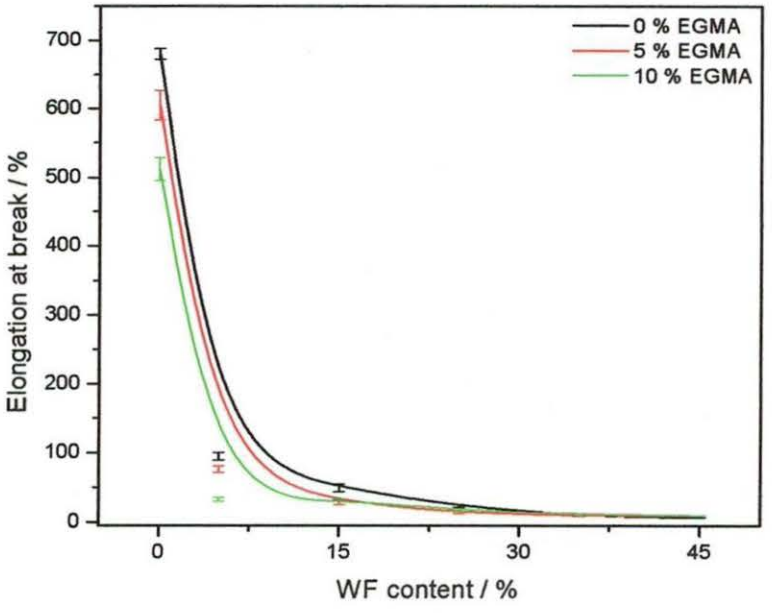

Figure 4.43 The effect of compatibilizer content on the elongation at break of EVA/EGMA-WF composites (151-300 μm WF)

The interaction and adhesion between the matrix and WF is stronger, giving rise to reduced chain mobility and more resistance to deformation. Elongation at break does not seem to depend much on WF particle size.

The effect of a compatibilizer on the elongation at break using 0-150 and 151-300 μm WF particles is shown in Figures 4.42 and 4.43. Pure EVA has an elongation of 680 %, and the presence of 5 and 10 % EGMA respectively in EVA causes a decrease in elongation at break to 600 and 500 % respectively. This shows the lack of a reaction between EVA and EGMA.

The presence of WF causes a sharp decrease in elongation at break, and the uncompatibilized composites have high values that the compatibilized ones. The 10 % EGMA compatibilized composites have the lowest elongation at break values. It is clear that composites with 35 and 45 % WF show an insignificant difference in elongation at break, irrespective of whether the composites are compatibilized or not.

4.5 Permeability

A polymer's barrier properties, i.e. polymer's ability to slow down or stop the passage of a gas through its structure, is of primary importance for packaging designers, especially for those working with food products that will be kept on a shelf for an extended time. Barrier properties are most commonly quantified by measuring polymer permeability, the rate at which a given gas passes through the polymer under a given set of conditions. Low permeability means that gases (O_2 and volatile flavour/odour components) and moisture have a difficult time passing through the packaging [17].

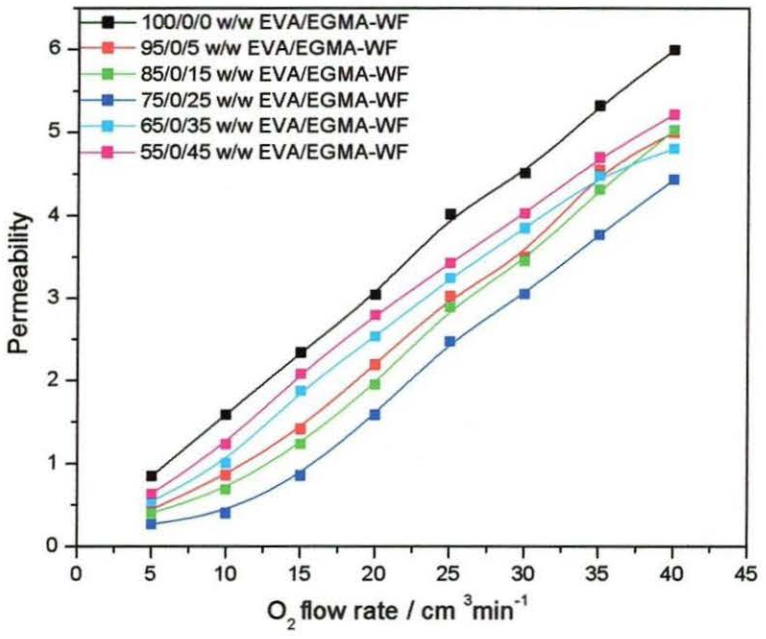

Figure 4.44 Effect of WF content on the permeability of EVA-WF composites at different O_2 flow rates (0-150 μm WF)

The effect of 0-150 μm WF content on the permeability of uncompatibilized EVA-WF composites is shown in Figure 4.44. The permeability of pure EVA is the highest with a value of 6 when O_2 is supplied at 45 cm^3 min^{-1}. This is because EVA is not 100 % crystalline; there are some amorphous parts that allow gas to pass through.

The presence of WF in EVA results in a decrease in permeability, and the lowest permeability values are obtained for the 75/0/25 w/w EVA/EGMA-WF composite. This shows that 5, 15 and 25 % WF accommodates amorphous EVA chains in their pores, giving

rise to lower O_2 permeability values. Higher permeability values (still lower than pure EVA) are seen when 35 and 45 % WF is used. The interfacial bonding between wood fibre and EVA is weak and the resultant composite will have voids and cracks; this will allow gas to pass through easily. WF itself exhibit high values of permeability because it is a highly porous material.

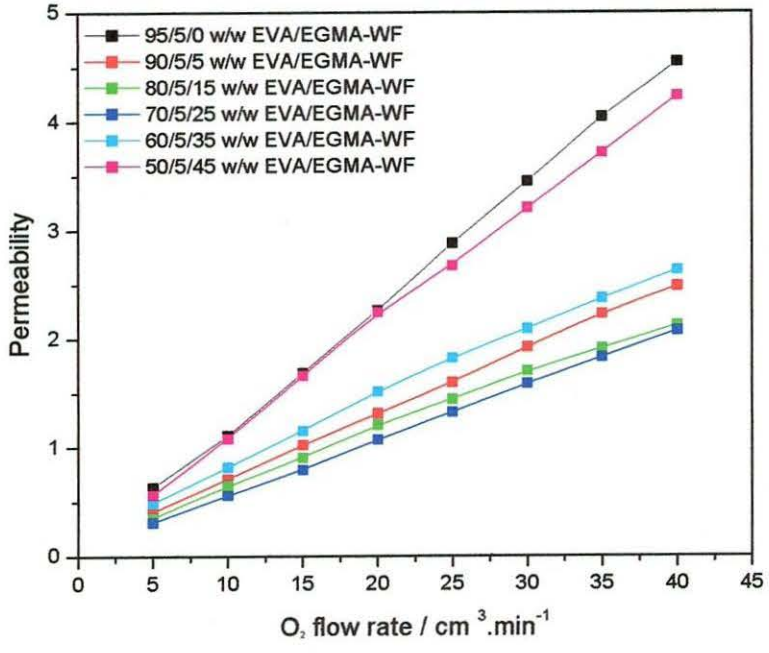

Figure 4.45 Effect of WF content on the permeability of EVA-WF composites, compatibilized with 5 % EGMA, at different O_2 flow rates (0-150 μm WF)

The effect of WF content on the gas permeability of 5 % EGMA containing composites is shown in Figure 4.45. The presence of EGMA compatibilizer causes a slight decrease in permeability compared to the samples where no compatibilizer was used. This is because of the interfacial adhesion that is promoted between WF and EVA, resulting in a less porous and less amorphous than pure EVA (see DSC discussion). The effect of WF content is the same as for uncompatibilized composites. 25 % addition of wood fibre exhibit least permeability values while 35 and 45 have higher values but still less than the composite without WF. The reason for that is that as more wood fibre is added, fibre to fibre interaction results due to the limitations in active groups in EGMA, which plays an important part in promoting adhesion between WF and EVA.

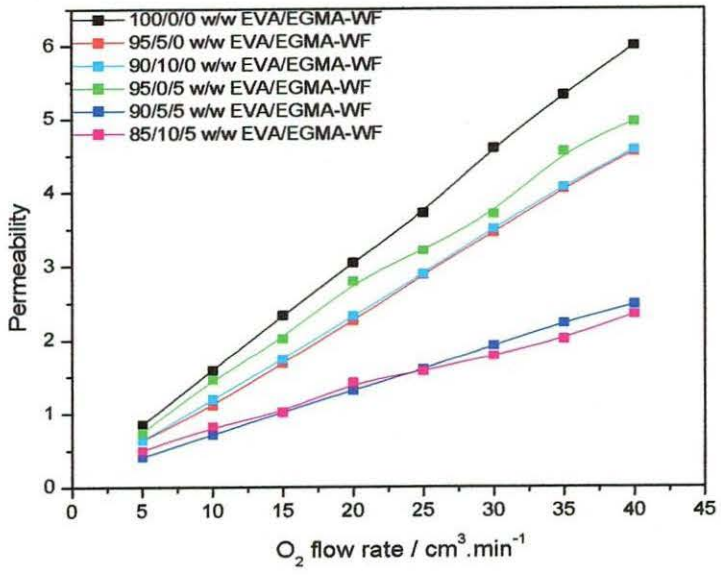

Figure 4.46 **Effect of compatibilizer and 5 % WF on the permeability of EVA/EGMA-WF composites**

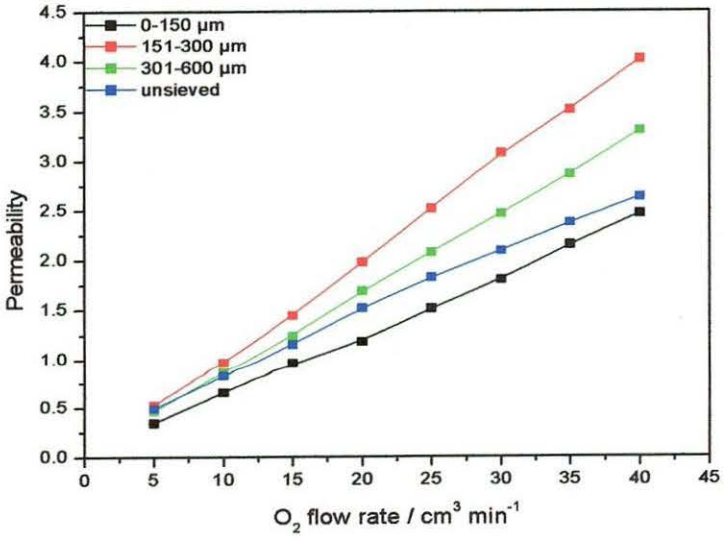

Figure 4.47 **The effect of WF particle size on the permeability of 70/5/25 w/w EVA/EGMA-WF composites**

The presence of EGMA causes a decrease in the permeability of pure EVA (Figure 4.46). Even though there seem to be no reaction taking place between EVA and EGMA, the fact that EVA is porous and amorphous polymer and addition of EGMA will fill the pores and decrease the amorphous part and the resulting copolymer is likely to have lower permeability values than pure EVA. The presence of EGMA and 5 % WF remarkably reduces the O_2 permeability of the samples. It is likely that the composite that is formed will be less amorphous, leaving very little space for the movement of O_2 molecules.

The effect of WF particle size on the permeability of EVA/EGMA-WF composites is shown in Figure 4.47. From this figure it is clear that wood fibre particle size has an effect on the permeability of the composites. The composites made from larger particles (151-300 and 301-600 μm) have higher permeability values compared to composites made from smaller particles (0-151 μm and unsieved). The reason for this is that small particle sizes form composite that are more intact and with less voids than when large particle sizes are used.

4.6 Thermogravimetric analysis (TGA)

4.6.1 Uncompatibilized composites

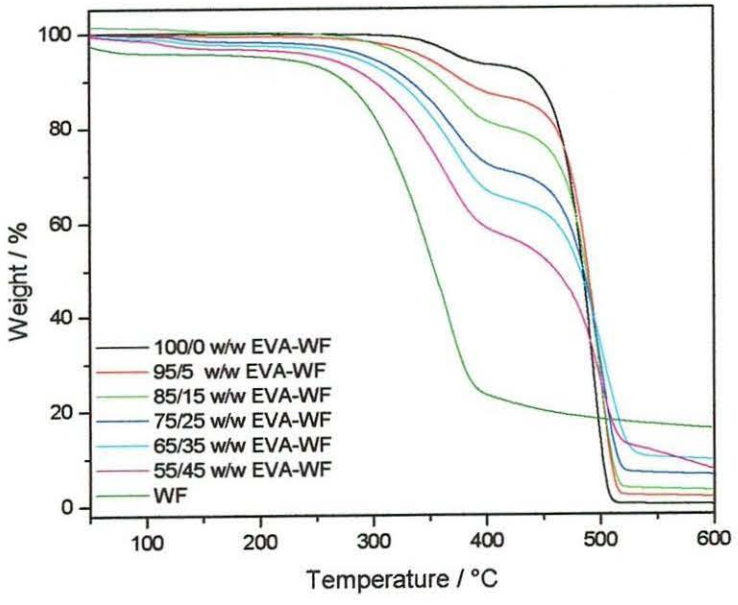

Figure 4.48 TGA curves of pure EVA, WF and EVA-WF composites (0-150 μm)

The TGA curves of the uncompatibilized composites are shown in Figures 4.48 and 4.51 for 0-151 and 151-300 μm particle sizes respectively. The WF curve shows one degradation step with an onset temperature around 200 °C. EVA is characterized by two degradation steps. The first degradation step, related to the removal of acetate groups, starts at ~331 °C. The second degradation step, due to the degradation of the polyethylene backbone in EVA, occurs at about 460 °C. These findings were also reported by Zanetti and Jansen [18, 19], and the first degradation step is shown in Figure 4.49.

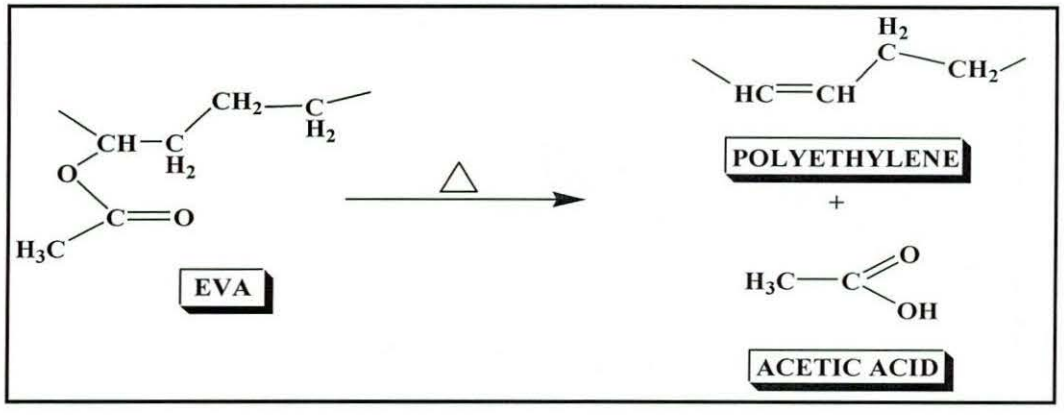

Figure 4.49 Structural presentations that shows EVA degradation

Table 4.7 Summary of TGA data for uncompatibilized composites

EVA/EGMA-WF (w/w)	150 μm		300 μm	
	1^{st} $T_{o,d}$ / °C	2^{nd} $T_{o,d}$ / °C	1^{st} $T_{o,d}$ / °C	2^{nd} $T_{o,d}$ / °C
100/0/0	360	460	360	460
95/0/5	332	474	325	471
85/0/15	314	470	308	477
75/0/25	307	476	298	471
65/0/35	268	480	252	478
55/0/45	243	458	238	458

$T_{o,d}$ - onset temperature of degradation

EVA-WF composites also show two degradation steps. The first degradation step is attributed to a combination of the decomposition of WF and the first step of the degradation of EVA, while the second step is attributed to the degradation of the EVA backbone. The onset temperatures of this step are higher than the observed onset temperature for pure WF. The onset temperatures of degradation of the composites decrease as more wood fibre is present and the intensity of the peaks increases as the wood fibre content increases (Figure 4.50). In the presence of 5 % WF the onset temperature is 332 °C. The presence of 15, 25, 35

and 45 % of wood fibre causes a decrease in onset temperatures to 314, 307, 268, 243 °C respectively (Table 4.7).

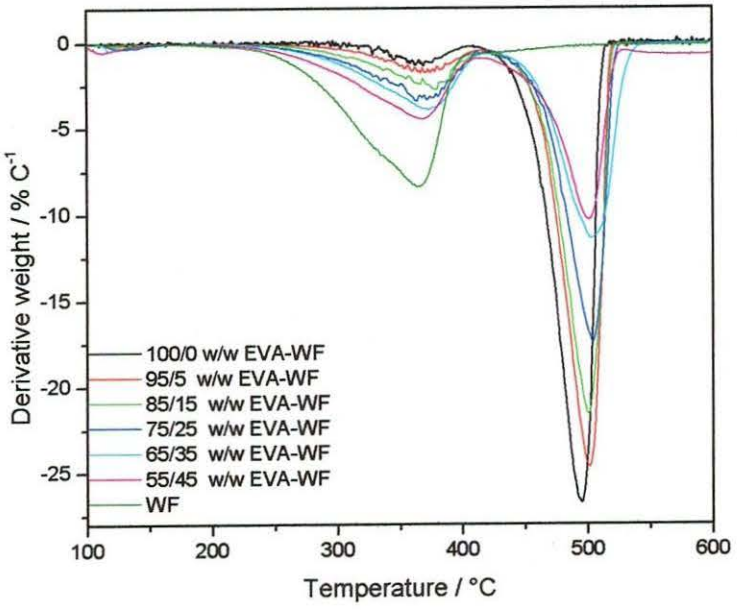

Figure 4.50 DTGA curves of pure EVA, WF and EVA-WF composites (0-150 μm)

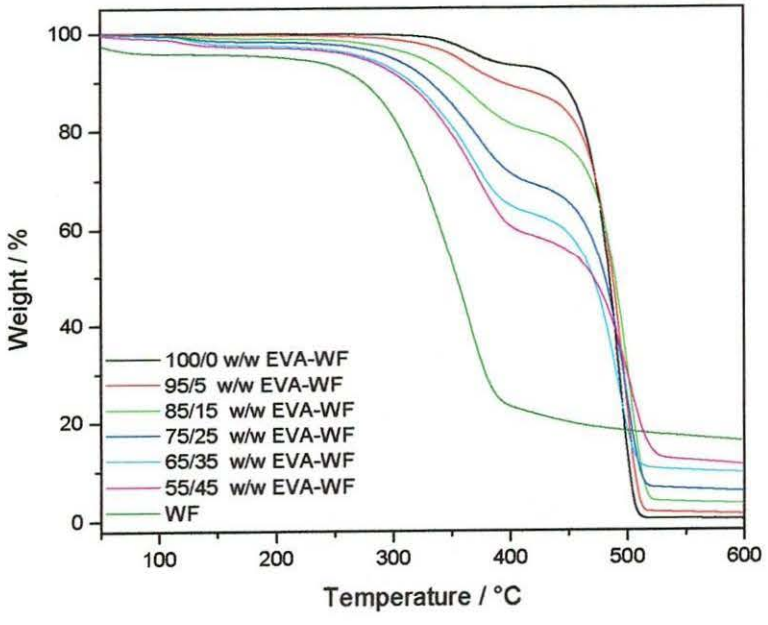

Figure 4.51 TGA curves of pure EVA, WF and EVA-WF composites (151-300 μm)

All these values are still higher than that of pure WF. The presence of WF causes an increase in the onset temperature of the second degradation step, as is shown in the derivative curves in Figure 4.50, because the presence of WF improves the thermal stability of EVA. It is also not easy to conclude whether the first degradation step is for WF or if it is related to the acetate groups on the EVA backbone, because their degradation occurs in the same temperature range. Jansen *et al* [19] investigated the effect of compatibilizer and curing systems on the thermal degradation of natural rubber/EVA copolymer blends and reported that the first degradation step related to acetic acid disappears, and the peak witnessed can be attributed to natural rubber indicating that EVA was stabilized in the process.

Pure EVA does not have any residue left after degradation, while the highest residual weight percentage (16 %) is obtained with pure WF. The presence of 5, 15, 25, 35, and 45 % EVA-WF gives residual weight percentages of 1, 3, 5, 9 and 11 % respectively. If WF alone was responsible for the formation of the residue, 0.8, 2.4, 4.0, 5.6 and 7.2 % residue would have been expected when 5, 15, 25, 35 and 45 % WF were used respectively. The reason for this is not clear at this point in time.

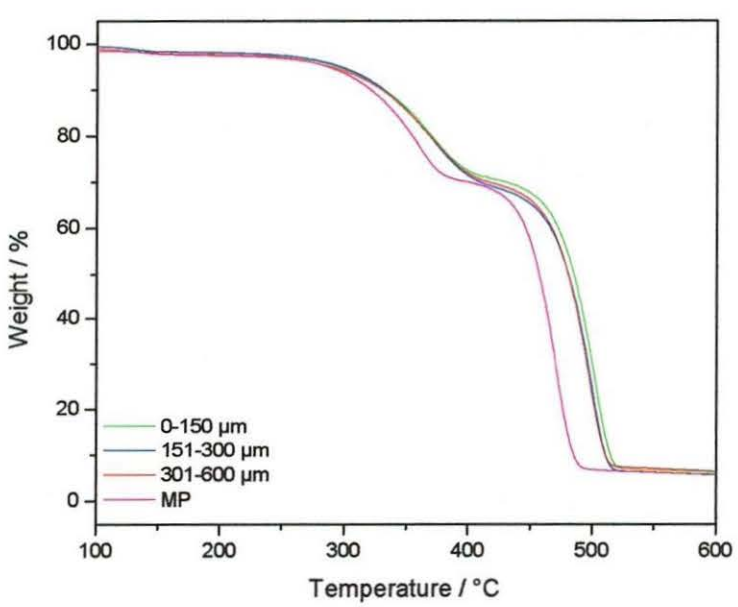

Figure 4.52 The effect of WF particle sizes on the degradation of 75/25 w/w EVA-WF composites

The effect of WF particle size on the degradation of 75/25 w/w EVA-WF composites is shown in Figure 4.52. All sieved (0-150, 151-300, 301-600 μm) WF composites degrade in a similar way, irrespective of the particle size used. The unsieved WF composite degrades at a lower temperature than the sieved WF ones. A possible reason for this observation is that the arrangements of equally sized particles within the composite contribute to similar degradation a pattern, which is not the case with the unsieved particles, because the composite consists of a large WF particle size distribution and this may contribute to the heterogeneity in the composite and thus different degradation behaviour.

4.6.2 EGMA compatibilized composites

The thermal degradation behaviour of EGMA compatibilized composites is shown in Figures 4.53-4.58. EVA/EGMA blends degrade in two steps, just like pure EVA. The presence of EGMA causes a decrease in the first and second degradation temperatures, probably because of a lower thermal stability of the EGMA.

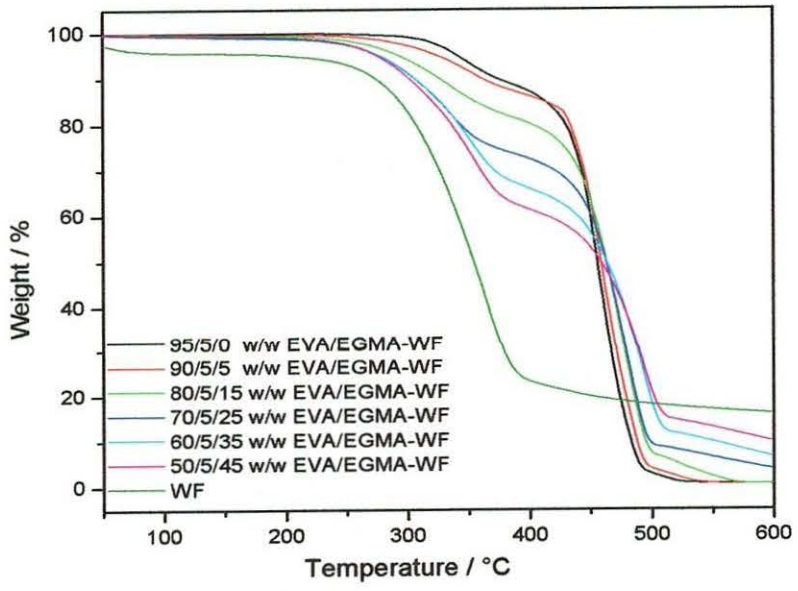

Figure 4.53 TGA curves of WF and 5 % compatibilized EVA-WF composites (0-150 μm)

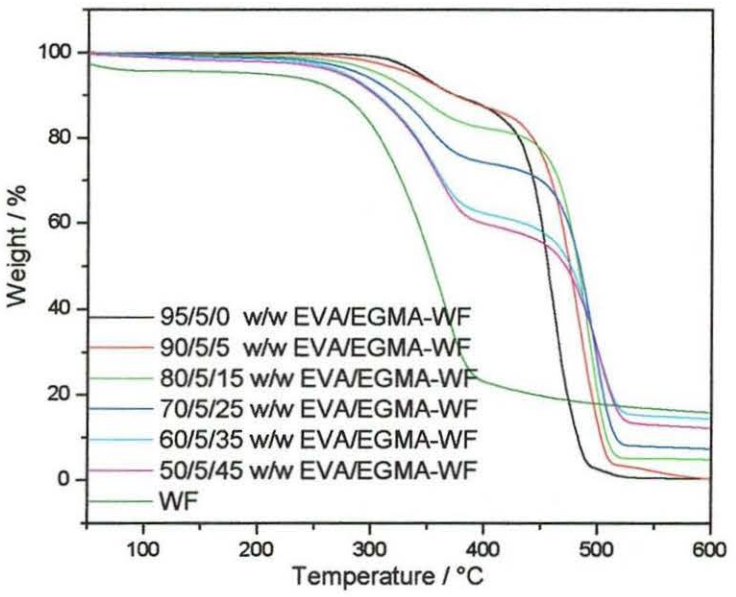

Figure 4.54 TGA curves of pure WF and 5 % compatibilized EVA-WF composites (151-300 μm)

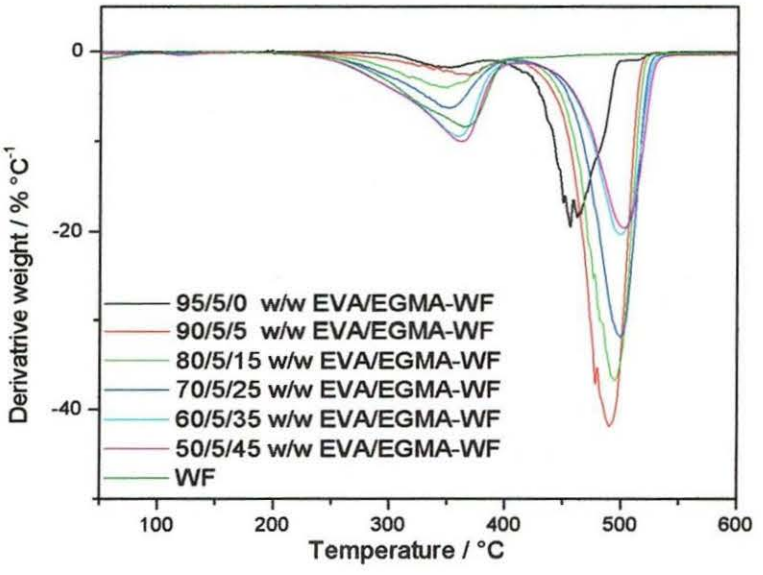

Figure 4.55 DTGA curves of pure WF and 5 % compatibilized EVA-WF composites (151-300 μm)

Table 4.8 Summary of TGA data for 5 % EGMA compatibilized composites

EVA/EGMA-WF (w/w)	150 µm		300 µm	
	1^{st} $T_{o,d}$ / °C	2^{nd} $T_{o,d}$ / °C	1^{st} $T_{o,d}$ / °C	2^{nd} $T_{o,d}$ / °C
95/5/0	320	432	320	432
90/5/5	295	465	309	438
85/5/15	278	471	289	444
70/5/25	268	473	285	441
60/5/35	246	476	248	455
50/5/45	235	482	210	463

$T_{o,d}$ - onset temperature of degradation

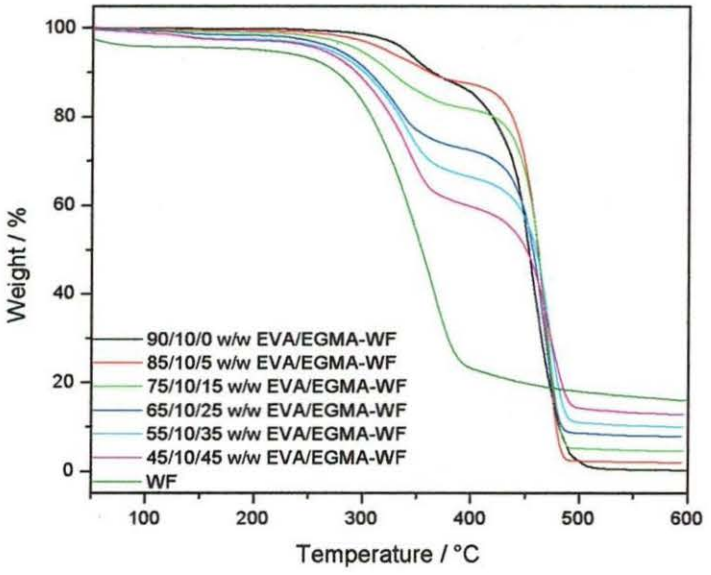

Figure 4.56 TGA curves of pure WF and 10 % EGMA compatibilized EVA-WF composites (0-150 µm)

Table 4.9 Summary of TGA data for 10 % EGMA compatibilized composites

EVA/EGMA-WF (w/w)	150 µm		300 µm	
	1^{st} $T_{o,d}$ / °C	2^{nd} $T_{o,d}$ / °C	1^{st} $T_{o,d}$ / °C	2^{nd} $T_{o,d}$ / °C
90/10/0	311	390	311	390
85/10/5	295	415	282	407
75/10/15	275	419	261	411
65/10/25	262	425	256	418
55//10/35	251	434	243	427
45/10/45	233	439	224	430

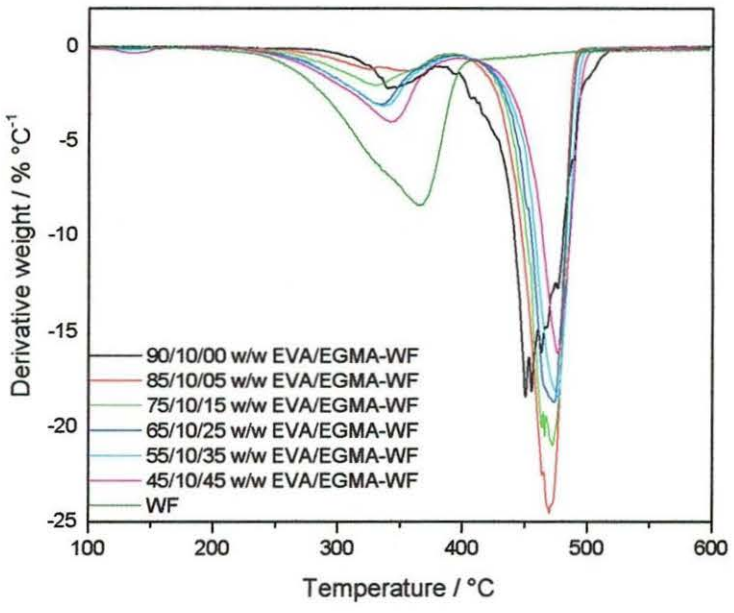

Figure 4.57 DTGA curves of pure WF and 10 % EGMA compatibilized EVA-WF composites (0-150 μm)

The 10 % EGMA compatibilized composites are thermally less stable than the 5 % compatibilized composites. A possible explanation for this behaviour is that EGMA has lower onset temperatures of degradation than EVA, thus it is likely to decrease the degradation temperature of the composites. The presence of WF causes a decrease in the temperature of the first degradation peak, but an increase in that of the second degradation peak compared to the composite without WF (Tables 4.8 and 4.9).

The intensities of the differential peak of the first degradation step increases as more WF is present, while the intensities of the differential peak of the second degradation step proportionally decreases (Figure 4.57). This shows that the first and second degradation steps are proportional to the amounts of WF and EVA respectively in the composites.

The effect of particle size on degradation of the 65/10/25 w/w EVA/EGMA-WF composites is shown in Figure 4.59. The first and second degradation steps occur at the same temperatures, irrespective of WF particle size. It is clear that when 10 % EGMA is used, there is an insignificant difference in the degradation behaviour of the composites, irrespective of the particle sizes used. This shows that 10 % EGMA effectively promotes interfacial bonding in the composites, even when unsieved particles are used.

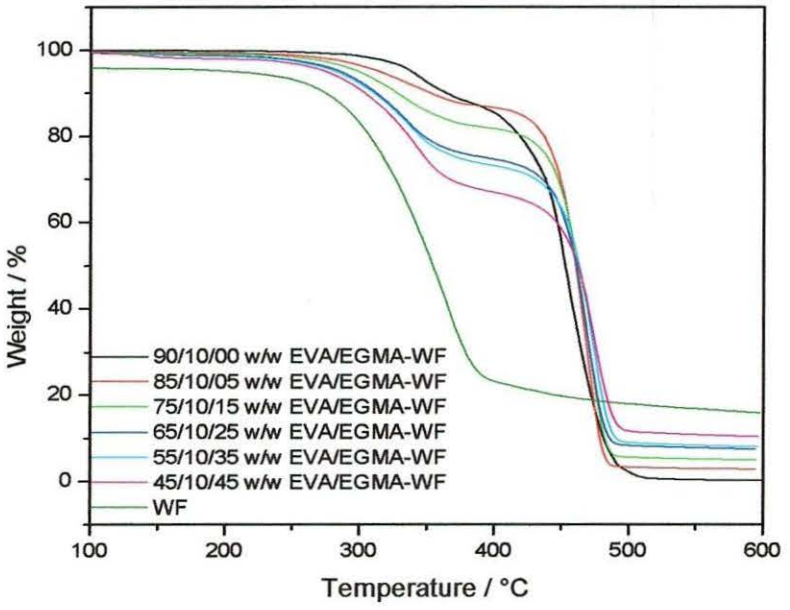

Figure 4.58 **TGA curves of pure WF and 10 % EGMA compatibilized EVA-WF composites (151-300 μm)**

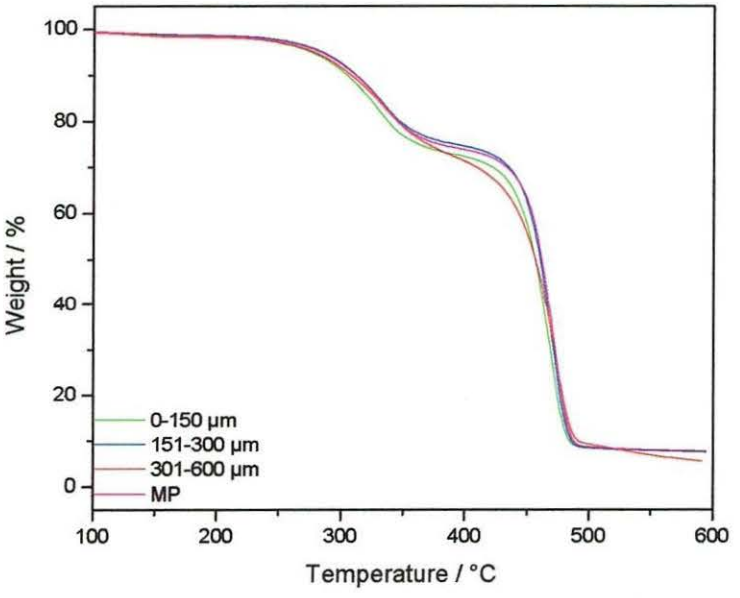

Figure 4.59 **The effect of WF particle size on the degradation of 65/10/25 w/w EVA/EGMA-WF composites**

4.6.3 Effect of compatibilizer content

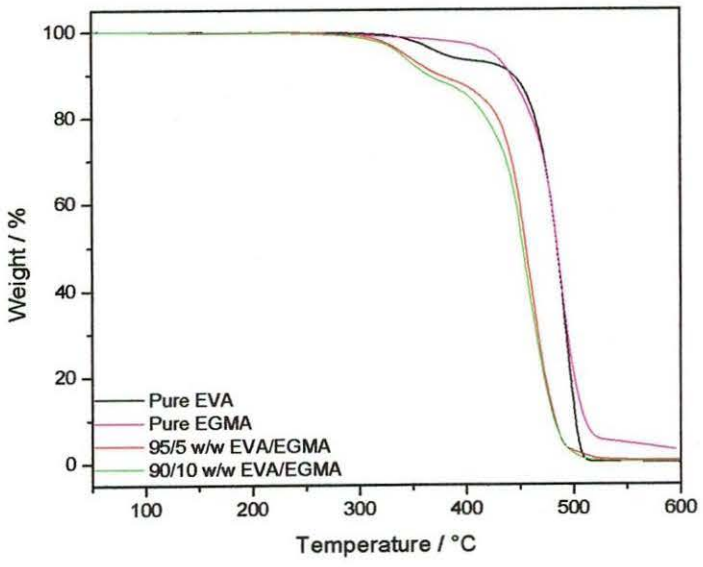

Figure 4.60 TGA curves of pure EVA, EGMA, 95/5/0 and 90/10/0 w/w EVA/EGMA-WF composites

The thermal stability of pure EGMA, pure EVA and EVA/EGMA blends is shown in Figure 4.60. EGMA has only one degradation step with an onset temperature of 400 °C. The EVA/EGMA blends have two degradation steps like pure EVA, with the onset of degradation for both peaks at lower temperatures pure EVA. The reason for this reduction in the degradation onset temperature is due to the presence of EGMA that start degrading at a lower temperature than EVA, thus affecting the degradation temperature of the EVA/EGMA blend negatively.

The thermal degradation behaviour of composites when 25 % of WF is used is shown in Figures 4.62 and 4.63. Both the first and second degradation steps in the uncompatibilized composites occur at higher temperatures than those of the compatibilized composites. The 5 % EGMA compatibilized composites have a better thermal stability than the 10 % EGMA compatibilized composites. This was expected because it has been shown that the presence of EGMA in EVA decreases the thermal stability of the matrix.

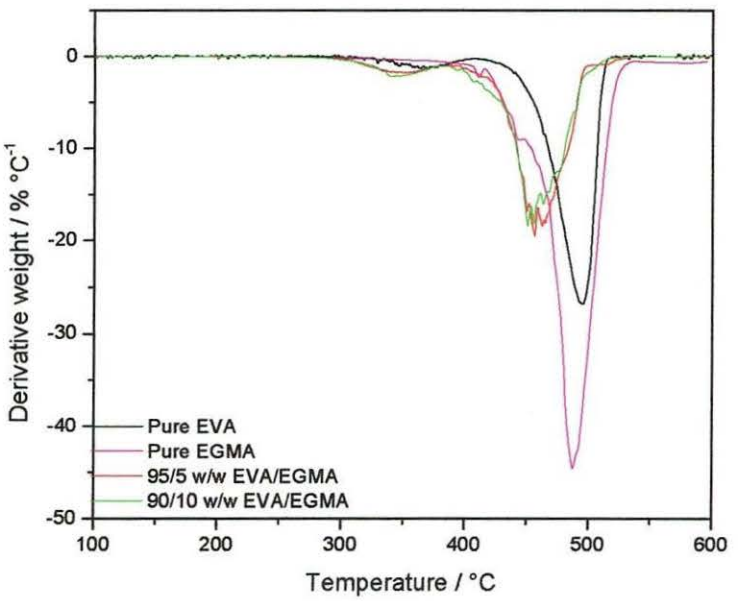

Figure 4.61 **DTGA curves of pure EVA, EGMA, 95/5/0 and 90/10/0 w/w EVA/EGMA-WF composites**

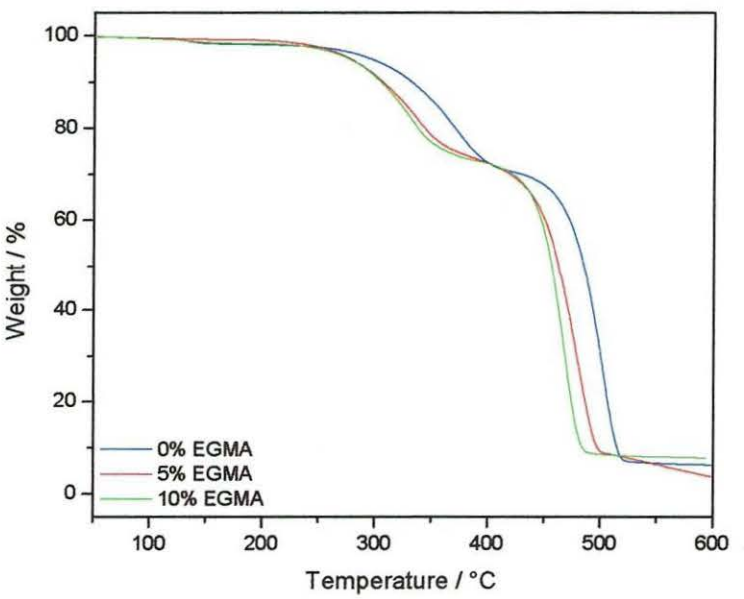

Figure 4.62 **The effect of compatibilizer on the degradation of composites with 25 % of 0-150 μm WF**

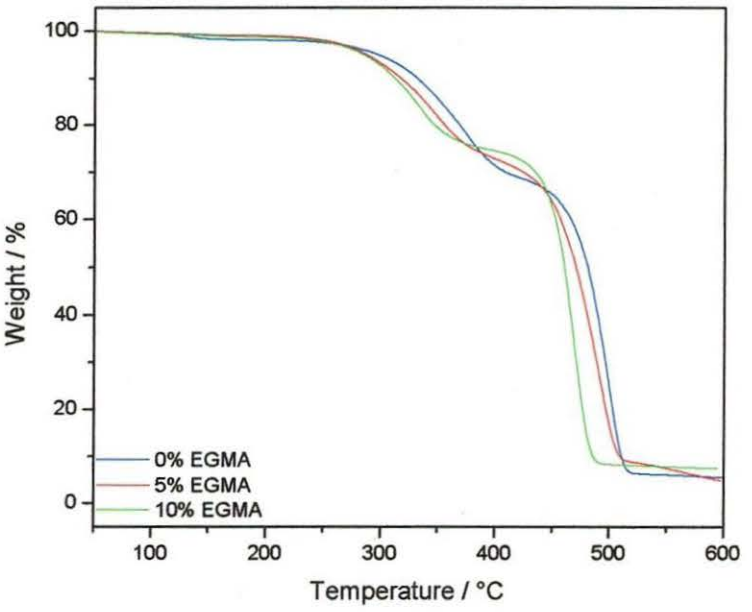

Figure 4.63 The effect of compatibilizer on the degradation of composites with 25 % of 151-300 μm WF

It therefore seems as if WF does not have a marked influence on the onset temperature of the second decomposition step in the absence of EGMA, while the decomposition temperature of this step increases with increasing WF content when EGMA is present, although it is still lower than that of the samples containing no EGMA. The observed behaviour in the absence of EGMA is probably the result of the relatively weak interaction between EVA and WF, while the behaviour in the presence of EGMA is in line with the postulated reaction between EGMA and WF and resultant stronger interaction with EVA. The reduced stability of the samples containing EGMA is the result of the low thermal stability of EGMA.

4.7 Water absorption

4.7.1 Uncompatibilized composites

The rate at which water is absorbed by a composite depends on many variables including the fibre type, matrix, temperature, the difference in water distribution within the

composite, and the reaction between water and the matrix [10]. Cellulose fibres contain many hydroxyl groups and readily interact with water molecules by hydrogen bonding. The quantity of absorbed water depends on the following factors:

- Relative humidity of the surrounding atmosphere
- Purity of the cellulose
- Degree of crystallinity; all OH groups in the amorphous phase are accessible to a polar solution, unlike crystalline phases where only the surfaces are available for water absorption [20].

Generally, wood fibre reinforced polymers can take up a large amount of water, which causes a reduction in mechanical properties [21].

Figures 4.64 and 4.65 respectively show the water absorption curves for the 0-150 and 151-300 μm WF containing, uncompatibilized composites. It can be seen that pure EVA absorbs water insignificantly, which is due to its hydrophobic nature and the fact that polymers' water absorption occurs only at the surfaces [21]. The presence of WF gives rise to an increase in water absorption. This is because WF is hydrophilic in nature; the amount of WF corresponds to an increase in the number of OH groups and thus an increase in water absorption.

Table 4.10 Water absorption percentage values of uncompatibilized composites

EVA-WF (w/w)	0 h	3 h	24 h	48 h	72 h
0-150 μm					
100/0	0	0	0	0	1.1
95/5	0	0.2	0.5	0.6	2.8
85/15	0	0.8	1.8	2.1	4.0
75/25	0	2.1	4.1	5.2	6.1
65/35	0	2.7	6.6	9.8	11.3
55/45	0	5.8	11.3	15.7	18.5
151-300 μm					
95/5	0	0.2	0.4	0.8	1.0
85/15	0	1.4	1.8	2.5	3.3
75/25	0	2.8	4.2	5.5	7.4
65/35	0	3.0	5.3	7.3	8.2
55/45	0	6.5	10.4	15.0	17.8

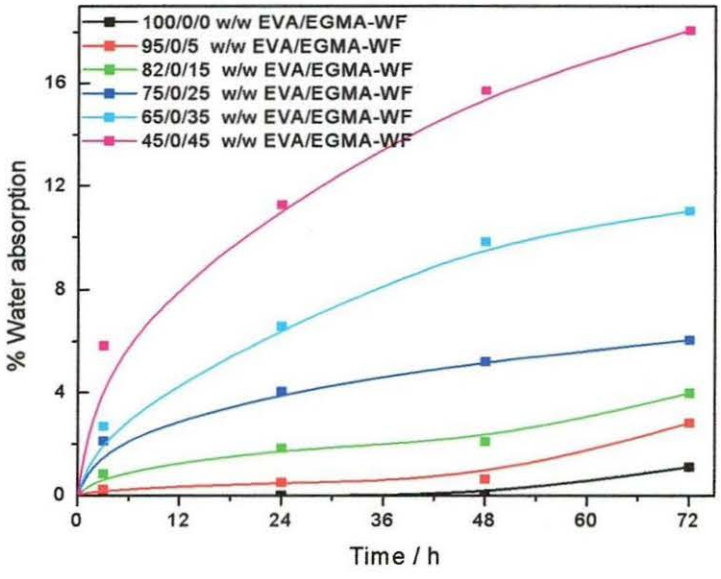

Figure 4.64 Effect of WF content on water absorption of uncompatibilized composites (0-150 μm WF)

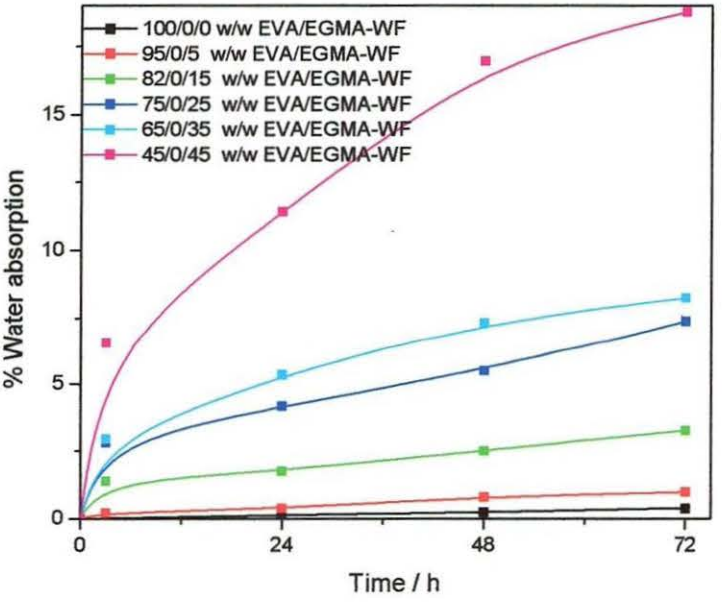

Figure 4.65 Effect of WF content on water absorption of uncompatibilized composites (151-300 μm WF)

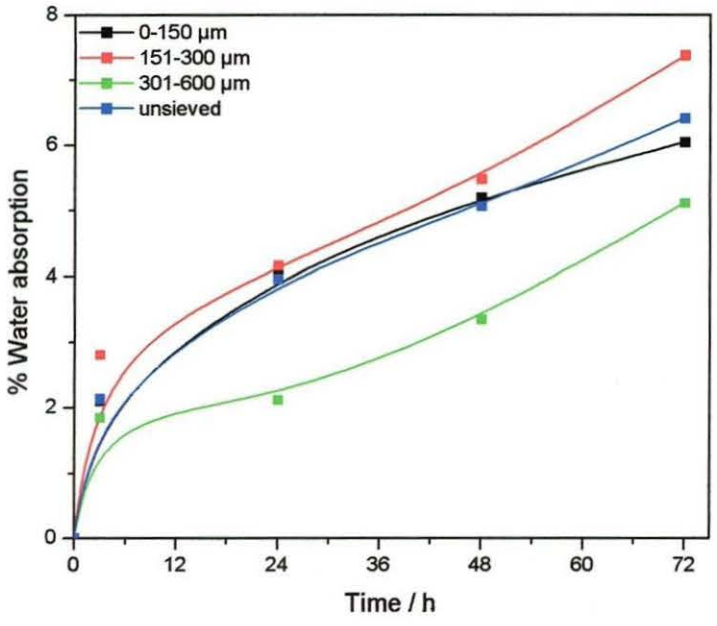

Figure 4.66 Effect of WF particle size on the water absorption of uncompatibilized composites at 25 % WF loading

Equilibrium values of water absorption are reached more quickly for composites with lower filler content, while the composites with higher filler content have not yet reached equilibrium after 72 hours exposure to water. In lower filled composites there are not so many OH groups available to form hydrogen bonds with water, some of the OH groups are used to bond to EVA as the mechanism suggest, and the remaining few are used to bond to water. Saturation is reached faster when all OH groups are used up. For higher WF filled composite, saturation is not easily reached because of the availability of more OH groups.

The effect of filler particle size on the water absorption of composites at 25 % filler loading is shown in Figure 4.66. It is observed that water absorption is higher in smaller particle size composites. This is because smaller particles have larger surface areas and consequently a higher availability of OH groups from the cellulose that would absorb more water. Ichazo *et al* [21] studied water absorption of PP-WF composites and reported that water absorption is always high in larger particle size composites, and mentioned this to be a contradiction as large surface areas are expected for small particles, and consequently a higher availability of OH groups. Again he emphasized that this can only be possible in cases where small particles agglomerate.

4.7.2 5 % EGMA compatibilized composites

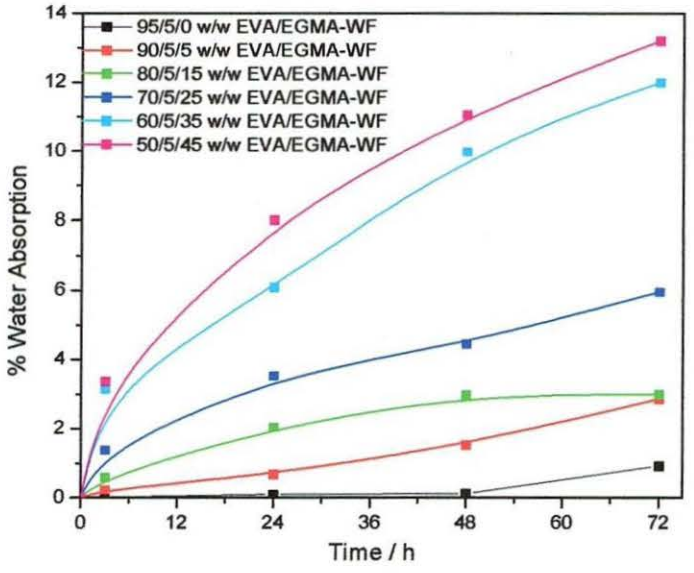

Figure 4.67 Effect of WF content on the water absorption of 5 % EGMA compatibilized composites (0-150 μm)

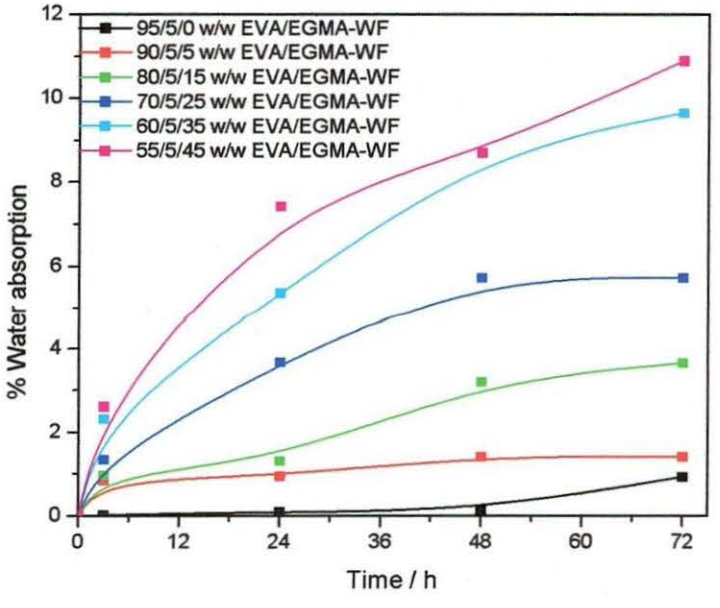

Figure 4.68 Effect of WF content on the water absorption of 5 % EGMA compatibilized composites (151-300 μm)

Figures 4.67 and 4.68 show the effect of 5 % compatibilizer on the water absorption of EVA-WF composites containing 0-150 and 151-300 μm WF respectively. The effect of filler content is the same as in uncompatibilized composites, i.e. water absorption increases as more WF is present because of an increase in the cellulose OH groups. Uncompatibilized composites absorbed up to 16 % of water, while 5 % compatibilized composites in comparison absorbed a maximum of 14 % water. It has been reported that the presence of a compatibilizer in the composite reduces the hydrophillicity of the fibres and therefore increases their compatibility with thermoplastic matrices [20]. The same phenomenon is experienced in this case, the mechanism suggest EGMA will reduce OH by bonding with wood fibre twice, using the epoxy and the carbonyl group. By so doing the surface energy and the hydrophyllicity of WF is greatly reduced and the OH group of the new composite will be used to interact with EVA.

Table 4.11 Water absorption percentage values of 5 % compatibilized composites

EVA/EGMA/WF (w/w)	0 h	3 h	24 h	48 h	72 h
0-150 μm					
95/5/0	0	0	0.1	0.1	0.9
90/5/5	0	0.2	0.5	1.5	2.8
80/5/15	0	0.6	2.0	3.0	3.0
70/5/25	0	1.4	3.5	4.5	5.0
60/5/35	0	3.1	6.1	9.9	12.0
50/5/45	0	3.4	8.0	11.1	13.2
151-300 μm					
90/5/5	0	0.8	0.9	1.4	1.4
80/5/15	0	1.0	1.3	3.2	3.7
70/5/25	0	1.3	3.6	5.7	5.7
60/5/35	0	2.3	5.4	8.7	9.6
50/5/45	0	2.6	7.4	8.7	10.9

The effect of particle size on 5 % EGMA compatibilized composites is shown in Figure 4.69. As in the previous case, the water absorption is the largest for the composites containing smaller WF particles. The 301-600 μm WF composite has maximum water absorption below 12 % after 72 hours, while the 0-150 μm WF composite has a maximum

absorption below 14 %. As mentioned before, smaller particles have larger surface areas and thus more exposed OH groups compared to larger particles.

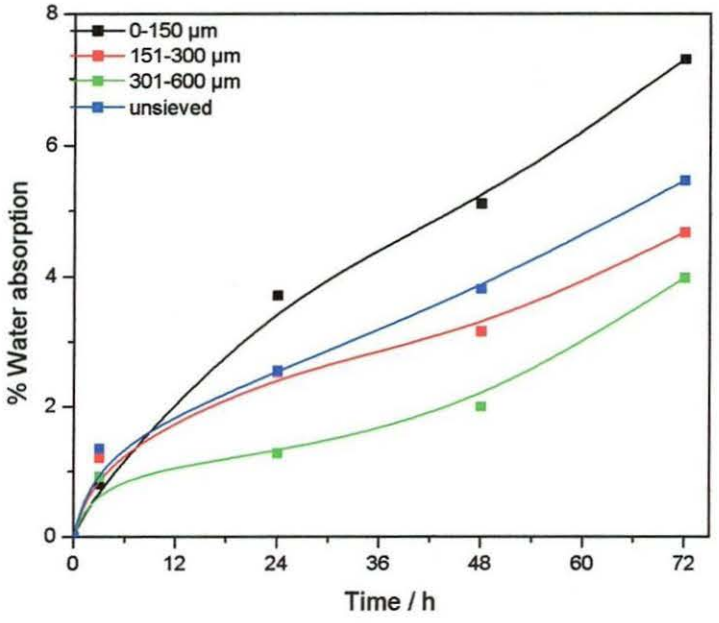

Figure 4.69 Effect of WF particle size on the water absorption of 5 % EGMA compatibilized composites at 25 % WF loading

4.7.3 10 % EGMA compatibilized composites

The effect of WF content on the water absorption of 10 % compatibilized composites is shown in Figures 4.70 and 4.71 for respectively 0-150 and 151-300 µm WF composites. 10 % compatibilized composite absorb the least water than the uncompatibilized and the 5% compatibilized composite. The reason for this is that the usage of more EGMA gives rise to the availability of epoxy groups will then interact with more OH groups of the WF. The trends for both filler content and particle size (Figure 4.72) are the same as in the previous cases, that is addition of more wood fibre equivalent to more water absorption and small wood fibre particle size absorb more that large particle sizes.

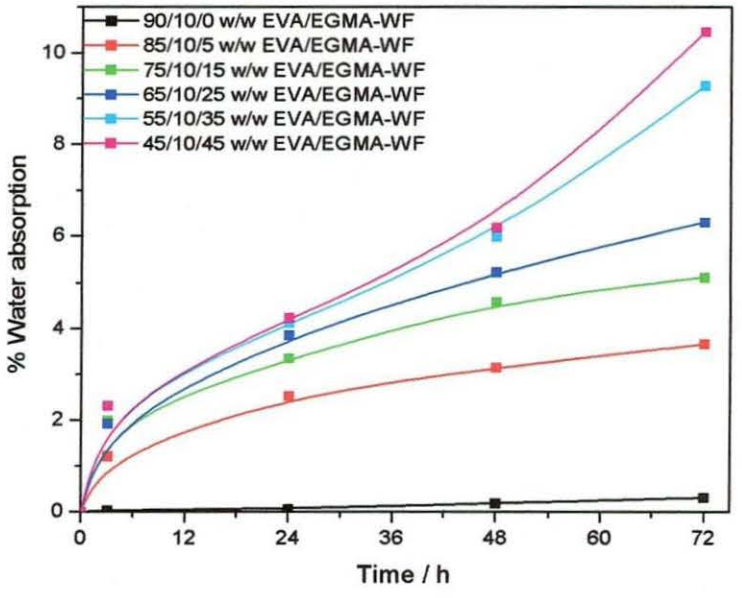

Figure 4.70 Effect of WF content on the water absorption of 10 % EGMA compatibilized composites (0-150 μm)

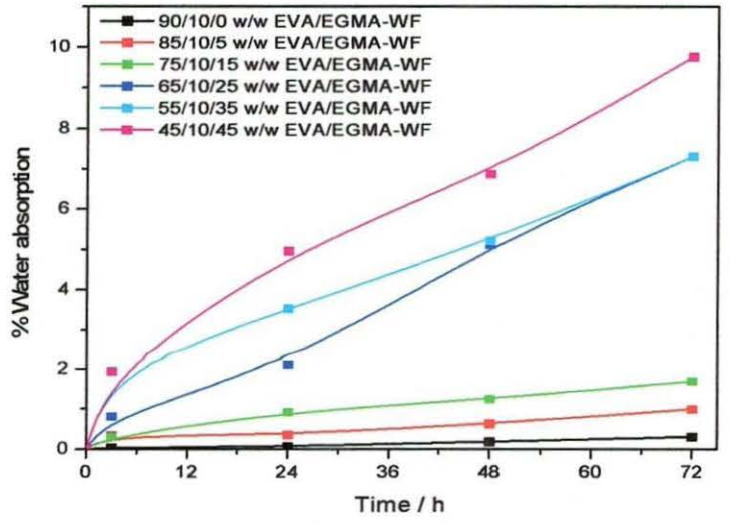

Figure 4.71 Effect of WF content on the water absorption of 10 % EGMA compatibilized composites (151-300 μm)

Table 4.12 Water absorption percentage values of 10 % compatibilized composites

EVA/EGMA/WF (w/w)	0 h	3 h	24 h	48 h	72 h
0-150 µm					
90/10/0	0	0	0.1	0.2	0.3
85/10/5	0	1.2	2.5	3.2	3.7
75/10/15	0	2.0	3.4	4.6	5.1
65/10/25	0	1.9	3.9	5.2	7.3
55//10/35	0	2.3	4.1	6.0	9.3
45/10/45	0	2.3	4.2	6.2	10.4
151-300 µm					
85/10/5	0	0.3	0.4	0.6	1.0
75/10/15	0	0.3	0.9	1.2	1.7
65/10/25	0	0.8	2.1	5.1	7.3
55//10/35	0	1.9	3.5	5.2	7.3
45/10/45	0	1.9	5.0	6.9	9.8

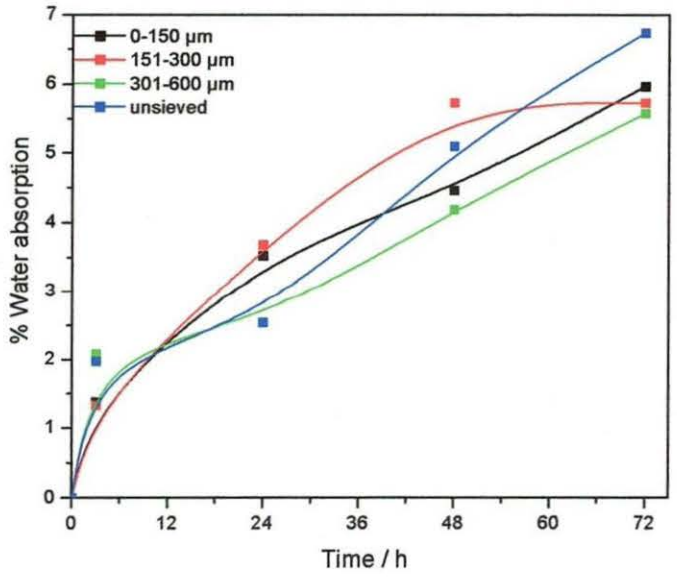

Figure 4.72 Effect of WF particle size on the water absorption of 10 % EGMA compatibilized composites at 25 % WF loading

4.7.4 Effect of compatibilizer content

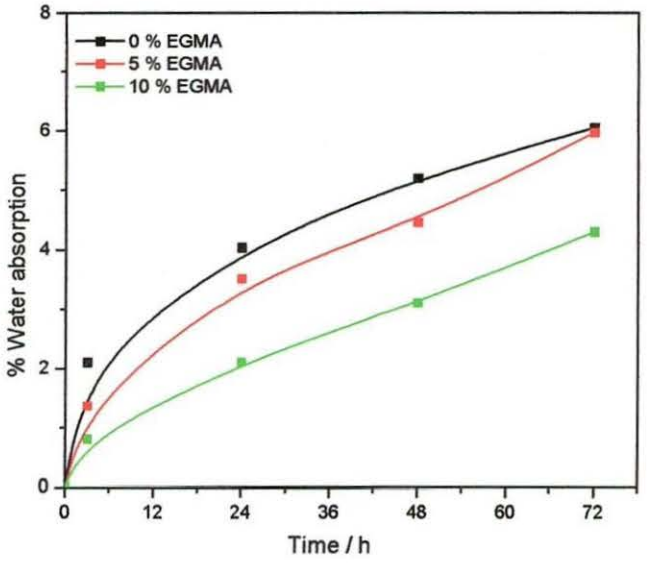

Figure 4.73 Effect of EGMA content on the water absorption of composites with 25 % WF (0-150 μm)

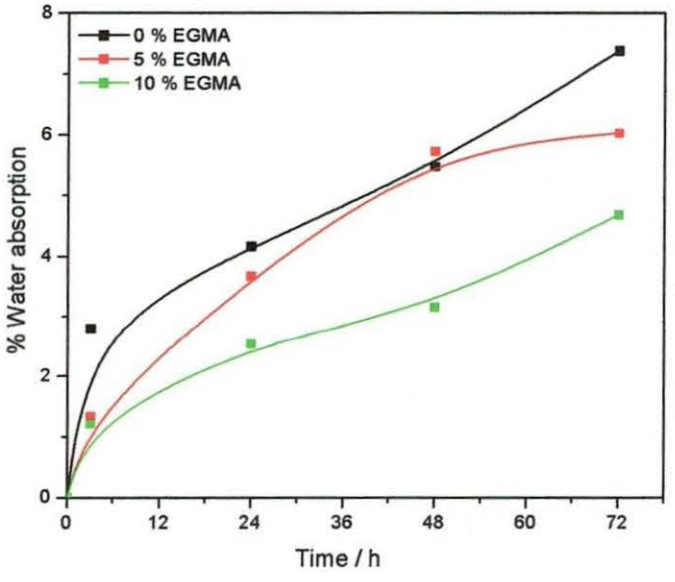

Figure 4.74 Effect of EGMA content on the water absorption of composites with 25 % WF (151-300 μm)

From previous graphs (Figure 4.65 and 4.68) it can be seen that the presence of EGMA in the absence of WF causes an increase in water absorption. Pure EVA has almost no water absorption, while 95/5 and 90/10 w/w EVA/EGMA blends show observable water absorption. The epoxy group on EGMA is known to act as a water scavenger [1], and therefore it should attract water, even when blended to EVA.

Even with the addition of 25 % wood fibre the trend still continues. Figure 4.73 and 4.74 shows that 75/0/25 w/w EVA/EGMA-WF composite absorbs more water than the compatibilized composites and the 10 % compatibilized composites absorbing more than the 5 % compatibilized composites. One reason for this is the availability of more active groups in EGMA that interact with OH thus reducing the hydrophillicity of the composite. Another reason is that epoxy containing polymers are water scavengers are likely to reduce the number of OH groups and hence less absorption.

References

1. Chiou YP, Chiou KC, Chang FC, *Polymer,* 37(18) (1996) 4099
2. Heino, MT, Seppala JV, *J. App. Polym. Sci.*, 48 (1993) 1677
3. Chiou YP, Chang DY, Chang FC, *Polymer,* 37(25) (1996) 5653
4. Miller MM, Cowie JMG, Tait JG, Brydon DL, Mather RR, *Polymer*, 36 (1995) 3107
5. Salemane MG, Luyt AS, *J. Appl. Polym. Sci.,* (In press)
6. Malunka ME, Luyt AS, Krump H, *J. Appl. Polym. Sci.*, 100(2) (2006) 1607
7. Lee SM, Cho D, Park WH, Lee SG, Han SO, Drzal LT, *Comp. Sci. Technol.,* 65 (2005) 647
8. Ismail H, Rozman HD, Jaffri RM, Ishak ZAM, *Eur. Polym. J.*, 33(10) (1997) 1627
9. Sedlackova M, Lacik I and Chodak I, *Macromol.Symp.*, 170 (2001) 157
10. Bledzki A, Faruk O, *Comp. Sci.Technol.*, 64 (2004) 693
11. Balasuriya PW, Ye L, Mai YW, *Composites A*, 32 (2001) 619
12. Elvy SB, Dennis GR, Teck L, *J. Mater. Process. Technol.,* 48 (1995) 365
13. Ismail H, Jaffri RM, *Polym. Test.*, 18 (1999) 381
14. Georgopoulos ST, Tarantili PA, Avgerinos E, Andreopoulos AG, Koukios AG, *Polym. Degrad. Stabil.,* 90 (2005) 303
15. Bigg DM, *Polym Comp.*, 8 (1987) 115
16. Fuad MYA, Ismail Z, Ishak, ZAM, Omar AK, *Eur. Polym. J.*, 31 (1995) 8

17. http://www.machinedesign.com/ASP/strArticleID/59141/strSite/MDSite/viewSelected Article.asp (14 March 2006)
18. Zanetti M, Camino G, Thomann R, Mulhaupt R, *Polymer,* 42 (2001) 4501
19. Jansen P, Soares BG, *Polym degrad.Stab* , 52 (1996) 95
20. Karmaker C, Hoffmann A, Hinrichsen G, *J. Appl. Polym. Sci.,* 54 (1994) 1803
21. Ichazo MN, Albano C, Gonzalez J, Perera R, Candal MV, *Comp. Struct.,* 54 (2001) 201

CHAPTER 5 (Conclusions)

The aim of this study was to prepare and characterize EVA-WF composites. The most important factors that were looked at were:

- effect of the wood fibre content (5, 15, 25, 35 and 45 %),
- effect of wood fibre particle size (0-151, 151-300, 301-600 μm and unsieved),
- effect of compatibilizer (EGMA),
- the effect of compatibilizer content (0, 5 and 10 % EGMA).

From the results and discussion it is obvious that the above factors play an important part in the morphological, mechanical, thermal, O_2 permeability and water absorption properties of the composites that are formed between EVA and WF.

Firstly, looking at the uncompatibilized composites and based on IR findings, it was proven that there is a possible interaction taking place between EVA and WF. The proposed mechanism suggests hydrogen bonding between the -C=O and OH groups of EVA and WF respectively. This is supported by a broad OH peak showing the incorporation of OH rich filler into EVA. It is important to note that the interfacial bonding between EVA and WF is very weak and thus the resultant composites have poor mechanical properties.

Addition of EGMA to the composite improved most investigated properties, because of the improved interaction between EVA and WF in the presence of EGMA. IR analysis shows that there is a reaction between the epoxy groups in EGMA and the –OH groups in WF, giving a grafted product which also provide –OH groups that can form hydrogen bonds with the –C=O groups of EVA. The reason why EVA interacts much more strongly with this grafted product than with WF particles is because of the wetting of the WF particles by the grafted EGMA. A possible mechanism for this reaction of EGMA and WF and then interaction with EVA has been proposed. The resulting composites have better morphological and mechanical properties than EVA and its uncompatibilized composites. It is interesting to mention that the uncompatibilized composites are more thermally stable than the compatibilized composites because of the presence of EGMA, which has a degradation onset temperature lower than EVA.

An increase in WF content causes an increase in thermal stability and mechanical properties of EVA-WF and EVA/EGMA-WF composites. An increase in WF content causes a decrease in O_2 permeability, 25 % WF showing the lowest O_2 permeability. O_2 permeability can be ranked as follows EVA > EVA-WF > EVA-EGMA > EVA/EGMA-WF indicating that pure EVA permeates O_2 more than all the composites. More water is absorbed with an

increase in WF content; this is expected because WF has more OH groups that can effectively bind to water molecules.

Small WP particles give rise to better properties than large particles, even in the absence of EGMA. It is clear from POM photos that that there is stronger interaction in EVA/EGMA-WF in the case of small particles than in the case of large particles. Tensile testing shows that composites made from 0-151 μm WF have better mechanical properties than those made from 300-600 μm WF. TGA confirms that small particle sized WF increases the thermal stability of EVA more than larger particles. O_2 permeability is less in composites made from small WF particles than when large particle sizes are used. However, small particle size composites absorb slightly more water than large particle size composites because of a larger surface area.

The amount of compatibilizer has an effect on the properties of the composites. The mechanical properties and morphology of the 10 % compatibilized composites are better than those o the 5 % compatibilized composites; this is to be expected, considering the fact that the using 10 % means availability of more active epoxy groups that will react with WF, creating -OH rich grafted product that will ultimately interact with EVA. Thermal stability is lower for composites containing 10 % EGMA than for composites containing 5 % EGMA; this is because EGMA is thermally less stable than EVA, and the quantity added is likely to negatively affect the composite stability. Permeability decreases with an increase in EGMA content. Water absorption decreases with increasing EGMA content, with uncompatibilized composites having the highest water absorption. This is explained as being the result of the EGMA ability to reduce surface area and hydrophylicity of wood fibre and by reacting with the hydroxyl groups in wood fibre.

For future work the aim is to:

- prove beyond reasonable doubt that the proposed mechanism is acceptable.
- to ensure that the addition of compatibilizer will improve the thermal stability of the composite.
- add other agents that will decrease water absorption as it seems to be the major challenge in this study.
- improve the mechanical properties and morphology of the composites further by determining the optimal conditions.

ACKNOWLEDGEMENTS

My sincere gratitude goes to the following important people who contributed to the success of this work:

- My supervisor, Prof AS Luyt, for believing in me and for his constant support and guidance. Your unselfish sharing of Polymer Science knowledge is highly appreciated.
- My husband, Tshepo, for allowing me to be away from him so that I can fulfill this dream, I cannot thank you enough.
- My father, my sisters (Sesi, Matshepo, Mpho, and Lebo) my brother Thabo, and all my handsome nephews (Thotloetso, Boikgethelo, Tekanyetso and Reamorata) my beautiful nieces (Obakeng, Palesa, Refiloe, Oreratile and Oagile) you are the wind beneath my wings; this is for each and every one of you.
- My wonderful friends, Andy, Kgomotso, especially Khosi, I couldn't have done it without you.
- My colleagues (Mpondi, Moipone, Rantoa, Buyi, Seadimo and Percy), your motivation and encouragement meant a lot to me.
- My assistant, Lulu, and research assistant, Puseletso, you are stars.
- UFS and NRF, for financial support

Most importantly, to Almighty God, for the strength, the courage and the wisdom He provided me to start and successfully finish this work. This is all possible because of His grace.